COMBINED HYDROGEN DIESEL COMBUSTION: AN EXPERIMENTAL INVESTIGATION INTO THE EFFECTS OF HYDROGEN ADDITION ON THE EXHAUST GAS EMISSIONS, PARTICULATE MATTER SIZE DISTRIBUTION AND CHEMICAL COMPOSITION

A Thesis submitted for the degree of Doctor of Philosophy

By

Lyn McWilliam

School of Engineering and Design,
Brunel University
United Kingdom

September 2008

ABSTRACT

This investigation examines the effects of load, speed, exhaust gas recirculation (EGR) level and hydrogen addition level on the exhaust gas emissions, particulate matter size distribution and chemical composition. The experiments were performed on a 2.0 litre, 4 cylinder, direct injection engine. EGR levels were then varied from 0% to 40%. Hydrogen induction was varied between 0 and 10% vol. of the inlet charge. In the case of using hydrogen and EGR, the hydrogen replaced air. The load was varied from 0 to 5.4 bar BMEP at two engine speeds, 1500 rpm and 2500 rpm.

For this investigation the carbon monoxide (CO), total unburnt hydrocarbons (THC), nitrogen oxides (NO_X) and the filter smoke number (FSN) were all measured. The in-cylinder pressure was also captured to allow the heat release rate to be calculated and, therefore, the combustion to be analysed. A gravimetric analysis of the particulate matter size distribution was conducted using a nano-MOUDI. Finally, a GC-MS was used to determine the chemical composition of the THC emissions.

The experimental data showed that although CO, FSN and THC increase with EGR, NO_X emissions decrease. Inversely, CO, FSN and THC emissions decrease with hydrogen, but NO_X increases. When hydrogen was introduced the peak cylinder pressure was increased, as was the maximum rate of in-cylinder pressure rise. The position of the peak cylinder pressure was delayed as hydrogen addition increased. This together with the obtained heat release patterns shows an increase in ignition delay, and a higher proportion of premixed combustion.

The experimental work showed that the particulate matter size distribution was not dramatically altered by the addition of EGR, but the main peak was slightly shifted towards the nucleation mode with the addition of hydrogen. Hydrogen addition does not appear to have a large effect on the chemical composition of the THC, but does dramatically decrease the emissions.

ACKNOWLEDGMENTS

I would like to thank, first and foremost, Dr Thanos Megaritis for all his help as supervisor, and Prof. Hua Zhao as second supervisor.

I would also like to thank all the technical staff at Brunel University for their help with endless problems, with special mention going to Andy and Ken in the engines lab, Keith in the materials lab, Clive for the electronic controls, Paul and Len in stores and John Langdon for all the ordering and support.

In addition I would like to thank the staff at the Hub for keeping me sane over the past three years.

NOMENCLATURE

BDC	Bottom Dead Centre
BMEP	Brake Mean Effective Pressure
BP	Brake Power
BTDC	Before Top Dead Centre
CAD	Crank Angle Degrees
CAI	Controlled Auto Ignition
CH_4	Methane
CI	Compression Ignition
CNG	Compressed Natural Gas
CO	Carbon monoxide
CoV	Coefficient of Variation
CV_H	Calorific Value
DME	Dimethyl ester
ECU	Electronic Control Unit
EGR	Exhaust Gas Recirculation
FSN	Filter Smoke Number
GC-MS	Gas Chromatography-Mass Spectrometry
GPPS	Glow Plug Pressure Sensor
GTL	Gas-To-Liquid
HCCI	Homogeneous Charge Compression Ignition

HRR	Heat Release Rate
ICU	Injection Control Unit
$l(\lambda)$	Intensity of light through sample cell
$l_0(\lambda)$	Intensity of light through empty cell
LPG	Liquefied Petroleum Gas
LTC	Low Temperature Combustion
MAF	Mass Air Flow
m_{CO}	Molar mass of CO
MFB	Mass Fraction Burnt
m_{fH}	Mass flow rate of hydrogen
m/z	Mass to charge ratio of an ion
N_{CO}	Number of moles of CO
NDIR	Non-dispersive Infra-red
NMHC/NMOG	Non-Methane Hydrocarbons/Organic Gas
NO	Nitrogen oxide
NO_X	Nitrogen oxides
O_2	Oxygen
P	In-cylinder pressure
PM	Particulate Matter
Rpm	Revolutions per minute
SCO	Specific Carbon monoxide
SFC	Specific Fuel Consumption
SI	Spark Ignition

SOF/VOF	Soluble/Volatile Organic Fraction
TDC	Top Dead Centre
THC	Total Unburnt Hydrocarbons
V	In-cylinder volume
VGT	Variable Geometry Turbine
$\alpha(\lambda)$	System dependant constant
Γ	Polytropic index
$\varepsilon(\lambda)CL$	Concentration of Sample gas
Θ	Crank Angle Degrees

CONTENTS

TABLE OF FIGURES

TABLE OF TABLES

TABLE OF EQUATIONS

CHAPTER 1

INTRODUCTION

1 CHAPTER 1 INTRODUCTION

1.1 Introduction

Since the invention of the internal combustion engine over a hundred years ago its impact has been immense. Engine applications range from small engines running handheld power tools, such as chain saws, up to static installations for power generation or marine applications. It started with the development of the Spark Ignition engine in 1876, by Nikolaus Agust Otto. The Compression Ignition (CI) engine, also known as the Diesel engine, was developed from the work of Akroyd Stuart and Rudolf Diesel. Stuart's engine was first produced in 1892 ran on a compression ratio of around 3, which was too low to ignite the fuel by compression alone. An external heat source was required to start the engine, but could be removed once in operation. Diesel's compression ratio was such that the fuel was spontaneously ignited after injection into the cylinder. This concept was finally achieved in 1893, and the prototype ran with a thermal efficiency of 26%. This was roughly double the efficiency of any contemporary power plant, and most research and development in the first place concentrated on improving the efficiency and performance of the engine [Stone (1992)].

Due to their higher efficiency when compared to spark ignition engines, diesel engines have found uses in static installations, such as power stations, and as prime movers in both heavy duty and light duty applications. This wide ranging application has meant the diversity of diesel engines has continually increased.

However, it has become apparent over the past 3 decades that the harmful effects of exhaust gas emissions, both in terms of the damage to the environment and to human health, is such that worldwide legislation has

been put in place. This has therefore meant that the developments on diesel engines have been driven by the need to improve the exhaust gas emissions. A number of different technologies have been implemented to achieve both better efficiency and lower emissions.

One such way of achieving both of these aims has been to turbo-charge diesel engines. This has widely been implemented in heavy duty and static installations, and now is penetrating the light duty market as well. With the introduction of variable geometry turbo-chargers, which limit the effects of "turbo-lag", turbo-chargers have become more attractive to the more transient running conditions required by light duty vehicles.

The implementation of high pressure fuel injection systems has also made huge advances in the control of emissions. Practically speaking the developments in the fuel systems have been high pressure fuel pumps, common rail fuel injection systems and improvements in the fuel injectors themselves. The implementation of piezo-electric fuel injectors allows for a shorter response time from the actuator, and therefore more control of the fuelling event. This great degree of control makes it possible to inject multiple times per cycle, supplying fuel to the combustion as it is required. With higher pressure fuel injection, comes better fuel atomization. This in turn improves the fuel/air mixing, and therefore promotes complete combustion. These both increase the fuel efficiency and the emissions as more complete combustion means more of the fuel is utilized, and there are less unburnt hydrocarbons and carbon monoxide being emitted due to incomplete combustion.

Another of the methods under investigation for improving the exhaust gas emissions of diesel engines is the implementation of dual fuelling. This

method introduces a high octane fuel to improve the performance of the engine by promoting premixed combustion. Examples of high octane fuels are methane, propane and hydrogen. The introduction of the secondary fuel can either be via the use of a secondary fuel tank, or by on-board diesel fuel reforming which produces the required gases.

The last idea has provided the jumping off point for this thesis, which will examine the effects of hydrogen induction on the diesel combustion event and how this effects the exhaust gas emissions. A speciation of the total unburnt hydrocarbons will also be conducted in order to assess the potential health risks associated with combined hydrogen/diesel combustion.

1.2 Objectives of the Project

The objectives of this project are to:

1. Investigate the relationship between the engine emissions and the combustion properties using measured in-cylinder pressure data for closed loop control of emissions.

2. Investigate the effects of combined diesel/hydrogen combustion on the combustion properties in order to establish appropriate control methods when compared to diesel combustion.

3. Investigate the effects of combined diesel/hydrogen combustion on the exhaust gas emissions in order to assess the impact of hydrogen addition.

4. Investigate the effects of combined diesel/hydrogen combustion on the particulate matter size distribution in comparison to diesel

combustion in order to assess the potential penetration ability into the body of the particulate matter produced.

5. Determine the speciation and potential health risks of the total unburnt hydrocarbons during diesel combustion, and compare with combined diesel/hydrogen combustion by implementing gas-chromatography-mass spectrometry.

6. Based on the results of the collected hydrogen data, suggest appropriate operating points to minimise the exhaust gas emissions.

1.3 Outline of Thesis

This introduction makes up the first chapter, and is immediately followed by a review of all the relevant literature. Chapter 2 is split into 10 main sections covering the various aspects of compressions ignition engines and their ancillaries, emissions, emissions control and methods of fuelling including alternative fuels. The final section of the chapter discusses gas chromatography and its potential applications with exhaust gas emissions speciation.

Chapter 3 describes the engine and experimental set-up. The key engine components required for the research and all the modification made to the engine are fully explored. Finally a description of all the instrumentation used and the positioning of all sensors on the engine and around the test cell are given.

The first results are presented in chapter 4, which looks at the effects of various parameters on the combustion properties and exhaust gas emissions. This chapter firstly covers the experimental work for the

injection timing and EGR investigation. The second section of this chapter examines the effects of injection timing and injection pressure in order to find an appropriate base point for starting the hydrogen investigation. The final section in this chapter looks at the effects of hydrogen addition on the combustion properties.

Chapter 5 looks at the effects of hydrogen on the exhaust gas emissions and the particulate matter size distribution by mass. This includes an investigation into the best substrate to capture the particulate matter and the set up of the dilution system used. The experimental test matrices for the emissions and particulate matter tests are shown, followed by the results and discussions for both sections. This chapter is finished off with a suggested optimum strategy for each operating point and the conclusions.

The last section of the investigation to be presented is the gas chromatography – mass spectrometry experimentation and is covered in chapter 6. The experimental work is split between a high molecular mass investigation and a low molecular mass investigation. There is a description of the differences between the experimental set-ups for the high and low molecular mass work. This is followed by a look at the chemical investigation that describes the various hydrocarbons that have been identified during this work. The next section is the experimental test matrix, followed by the results and discussions and the conclusions.

The final chapter, the seventh, summarises the general conclusions of the in-cylinder pressure data for closed loop control and the combined hydrogen and diesel combustion investigation. There are also some recommendations for future projects that could bring the potential of hydrogen addition closer to commercialisation.

CHAPTER 2

LITERATURE REVIEW

2 CHAPTER 2 LITERATURE REVIEW

2.1 Compression Ignition Engines

Compression ignition (CI) engines can operate in either 2 or 4 stroke modes, depending on the design. It is normal for automotive engines to be 4 stroke engines, so these will be the ones concentrated on. The 4-stroke process starts with the induction stroke, during which the inlet valve is open. As the piston travels down the cylinder, air is sucked into the cylinder. The next stroke is called the compression stroke. For this stroke both valves are closed, and as the piston travels up the cylinder the air is compressed. As the piston approaches top dead centre (TDC) the fuel is injected. During the power stroke, combustion occurs and the temperature and pressure increase. The piston is forced down the cylinder. Near bottom dead centre (BDC) the exhaust valve is opened and the exhaust gases are allowed to expand. The exhaust stroke completes the process. The piston is pushed back up the cylinder expelling the exhaust gases through the open exhaust valve. Near to TDC the exhaust valve closes and the inlet valve opens. The process then repeats [Stone (1992)].

Good running of a CI engine depends on good air fuel mixing. The fuel mixing is governed by the air motion and the fuel injection, both of which will be discussed in greater detail later in this chapter. The ideal system will have a high output, high efficiency, rapid combustion, a clean exhaust and be silent. Unfortunately achieving all of these aims is very difficult, and made more so by some of them being in conflict with one another. In particular the high output and clean exhaust is difficult to achieve because output is limited by the production of smoke [Stone (1992)].

When comparing CI engines to spark ignition (SI) engines, CI engines will always be more efficient. There are a number of reasons for this, the main ones being the compression ratio is higher, only air is present for the majority of the compression stroke and the air/fuel ratio is always weak in CI engines. SI engines are limited by the onset of knock, which is not a problem encountered by CI engines because the fuel is not compressed, but injected near the end of the compression stroke. Leading on from this, the power of a CI engine is controlled by the volume of fuel injected, as opposed to the throttling of the air in a SI engine. This again helps with the efficiency, because even at high fuel volumes the air/fuel ratio is weak of stoichiometric [Stone (1992)].

Looking at the disadvantages of CI engines in comparison the SI engines, there is a limit to the maximum speed of a diesel engine because of the slower combustion rate. Also, problems may be encountered with cold starting, and extra components, such as glow plugs to heat the combustion chamber, have to be employed until the engine has reached its optimum operating temperature. The combustion chambers themselves are designed to reduce heat transfer. This will reduce the ignition delay and increase the exhaust gas temperature. This type of engine is called an adiabatic engine, but it should be noted that these engines do not eliminate heat losses, only reduce it. The higher exhaust temperatures can be used to run turbochargers, which will be discussed in more detail later [Stone (1992)].

2.1.1 HCCI/CAI Combustion

Homogeneous Charge Compression Ignition (HCCI) and Controlled Auto-Ignition (CAI) are two forms of internal combustion in which the fuel and air are completely mixed prior to auto-ignition. The difference is only that

homogeneous charge compression ignition is defined as a controlled auto-ignition of pre-mixed fuel and air with diesel type fuel, and controlled auto-ignition used petrol type fuels.

Ideal HCCI combustion is characterised by low-temperature, lean combustion which is initiated at various points throughout the cylinder. This results in no flame propagation and therefore a reduction in nitrogen oxide emissions. Due to the lean nature of the combustion, and the lack of flame propagation, HCCI combustion has the potential to simultaneously reduce total unburnt hydrocarbons and nitrogen oxide emissions, which is traditionally a problem in compression ignition engines. HCCI combustion is also more efficient than traditional compression ignition combustion. The problem with HCCI is the control of the ignition point. Petrol engines use a spark to ignite the mixture, and diesel engines use the injection of the fuel at high compression to achieve this. With HCCI combustion this auto-ignition point must be controlled without either a spark or late fuel injection and using only the charge mixture composition and the temperature history. This has lead to the development of various techniques including the use of high levels of exhaust gas circulation, variable valve actuation, variable induction temperature and variable compression ratio. The problem is that none of these methods allow for HCCI combustion to operate over a sufficient range of loads and speeds [Zhao (2003)].

2.2 Fuel Injection

The relationship between the fuel injection and the engine governs the output, such as the torque of the engine, the power, the emissions and the engine noise created. Because complete combustion reduces the emissions, the air/fuel ratio and the air movement in the cylinder must be carefully

controlled. The load generated by a diesel engine is controlled by the volume of fuel injected, not by throttling the air intake, so complete control over fuel injection is absolutely vital to the performance of a diesel engine [Stone (1992), Bosch (1999) and Heywood (1988)].

There are two basic types of injection in diesel engines, direct injection and indirect injection, which are described below [Stone (1992), Bosch (1999) and Heywood (1988)].

2.2.1 Indirect Injection Diesel Engines

In indirect injection diesel engine systems, fuel is injected into a hot pre-chamber. The pre-chamber is designed with a baffle in the centre which the single injector nozzle is directed towards. This encourages a good fuel/air mixture, which is called pre-combustion. When combustion starts, the air/fuel mixture is driven from the pre-chamber into the main chamber. This movement increases the temperature of the mixture. Depending on the design of the passage from the pre-chamber into the main combustion chamber, whirl can be induced in the fluid flow [Stone (1992), Bosch (1999) and Heywood (1988)].

Indirect injection systems have the advantage over direct injection systems of a shorter ignition delay, and they require a lower overall pressure of fuel injection. This in turn leads to lower loads on the engine, and little noise production. Indirect injection systems are cheaper to design and build, particularly because they negate the need for high pressure fuel lines [Stone (1992), Bosch (1999) and Heywood (1988)].

An optimized pre-chamber will reduce particle emissions by up to 40% over one which has not been investigated. During the warm up period, a

technique called post-glow, where by the glow plug is still used to heat the pre-chamber, lowers gas emissions and noise production until the engine has reached optimum operating temperature [Stone (1992), Bosch (1999) and Heywood (1988)].

2.2.2 Direct Injection Diesel Engines

In a direct injection system, the fuel is injected at high pressure directly into the combustion chamber. In this system, the fuel atomization, heating, evaporation and mixing must all happen quickly. To achieve this, high turbulence is required within the combustion chamber. This can be produced by the design of the combustion chamber, which can be shaped to encourage squish and/or swirl [Stone (1992), Bosch (1999) and Heywood (1988)].

There are two ways to distribute the fuel within the combustion chamber; the air-distribution method and the wall-distribution method. In the air-distribution method, the fuel is injected into the compressed air of the combustion chamber. Mixing is achieved by the movement of the air molecules and their interaction with the atomized fuel. As the fuel mixes, it evaporates. This method uses multi-hole nozzles at high pressure [Stone (1992), Bosch (1999) and Heywood (1988)].

When the fuel injection is directed against the combustion chamber wall, it is called the wall-distribution method. Because the wall of the combustion chamber is hot, the fuel evaporates. This method uses a single hole nozzle and injects fuel at relatively low pressure. It does, however, result in higher fuel consumption than the air-distribution method [Stone (1992), Bosch (1999) and Heywood (1988)].

Regardless of the fuel distribution method used, the system is more complex and expensive than using indirect fuel injection systems and requires a high-pressure injection system. The main type of high-pressure injection systems is disused below [Stone (1992), Bosch (1999) and Heywood (1988)].

2.2.3 Common Rail Fuel-Injection System

In this system the pressure generation in the fuel and the fuel injection system have been decoupled. High pressure fuel is accumulated in the rail. Each cylinder has an injector unit which is controlled by the ECU, and triggered by a solenoid valve. Various sensors are used to determine the correct fuel-injection. These include a crankshaft speed sensor, camshaft speed sensor, accelerator pedal sensor, rail pressure sensor, coolant sensor and an air mass flow meter. The main advantages of the common rail injection are that the fuel injection pressure does not fluctuate greatly during injection and there is no need for long high-pressure fuel lines [Bosch (1999)].

Due to improvements in the design and control of the common rail injection system, it can now be used effectively to reduce PM emissions. By the use of sophisticated ECUs, up to 5 split injections per cycle per cylinder can now be easily achieved to better control the combustion process [Beatrice (2002)].

2.3 Air Management

It is very important to be able to control the air intake to an engine. Because the volume of the air intake does not vary, keeping a constant intake temperature, and therefore density, is vital to the efficient running of a diesel engine [Power Transmission and Technology Manual].

Intake air must be clean, free from suspended particulates and as cool as possible, to increase the density. In order to achieve this, air can either be wet or dry filtered. In a wet filter, the air is bubbled through an oil basin to remove any impurities. The air is then directed through a fine screen to remove any residual oil. This type of filter system is mainly used for large, stationary engine cases. In a dry filter, materials such as paper, cloth or metal screens are used to trap dirt and particulates. In order for the air to be as cool as possible it is drawn from as far from the engine as possible. In automotive cases, this means from out with the engine bay. After the air has been filtered it then flows either into the intake manifold, or is compressed and possibly cooled and then into the inlet manifold. The manifold itself is designed to reduce engine noise created by air flow [Power Transmission and Technology Manual].

Diesel engines can be naturally aspirated, supercharged or turbocharged. Supercharging and turbo-charging increase the mass flow rate of the intake air for the given volume occupied. This means there is an increase in the maximum volume of fuel which can be burnt. Super- or turbo-charging is when a separate pump or compressor is used to raise the pressure of the inlet air. The difference between the two is that a supercharger uses power from the engine to drive the pump or compressor, whereas a turbo-charger uses the exhaust gas to drive a turbine to drive a compressor [Power Transmission and Technology Manual].

When air is compressed the temperature is raised. Because this lowers the density of the intake air for a set volume, many automotive manufacturers now use coolers. These coolers are referred to as intercoolers, but are in reality after-coolers, due to their position in the air intake chain. An intercooler is essentially a heat exchanger designed for high flow rates. In

most automotive cases, ambient air is used as the coolant. There are various methods of getting the air to flow over the cooler radiator, but the most common is via a bonnet scoop. Intercoolers can also use water as the coolant, which is then cooled by the car radiator as is normal. Water cooled air is only common is large engines, where the speed of the vehicle may not be sufficient to force enough ambient air over the cooler radiator [Power Transmission and Technology Manual].

2.4 Exhaust Gas Emissions

In the ideal case, the only exhaust emissions from a diesel engine will be the products of complete combustion – carbon dioxide and water. Unfortunately, however, engines do not run at ideal conditions. There are numerous unwanted by-products of incomplete combustion, and the high-pressure combustion process. In order to reduce the damage done to the environment, the emission of carbon monoxide, unburnt hydrocarbons, nitrogen oxides, particulates and smoke are all controlled in diesel engines [European Emissions Standards and Garvie (1976)].

2.4.1 Carbon Monoxide

Carbon monoxide is formed during the incomplete combustion of hydrocarbons in diesel engines. It is an undesirable product because it is poisonous. CO has a 200 times higher affinity to haemoglobin than O_2, and so replaces oxygen in the blood stream when it is inhaled. This prevents the blood transporting oxygen, and leads to asphyxiation [Atkins (2002) and Zumdahl (1995)].

2.4.2 Nitrogen Oxides

Nitrogen oxides covers both nitrogen oxide (NO) and nitrogen dioxide (NO_2), collectively known as NO_X. NO_X is formed during the combustion process, without taking part in the reaction. NO_X is formed by the oxygenation of atmospheric nitrogen because of the elevated temperatures and pressures experienced in the combustion chamber [Heywood (1988)]. NO can combine with water to produce nitric acid. This is the primary form of acid rain. NO and NO_2 both contribute to the depletion of the ozone layer, which protects the Earth from harmful ultraviolet wavelengths of radiation [Atkins (2002) and Zumdahl (1995)].

NO_2 itself can be a deadly poison. Concentrations as low as 100ppm are considered dangerous, where as concentrations of 200ppm can be lethal, even at short exposures. NO_2 causes a build up of fluid in the lungs, which prevents the supply of oxygen to the blood stream [Atkins (2002) and Zumdahl (1995)].

2.4.3 Non-Methane Hydrocarbons/Organic Gases

There are various types of compounds which fall into the category of Non-Methane Hydrocarbons (NMHC) or Non-Methane Organic Gases (NMOG). These include aldehydes, ketones, alcohols and other pollutants which are not hydrocarbons, such as ammonia [European Emissions Standards]. All of these compounds can be formed by the incomplete combustion of the original diesel fuel, and possible later combinations with other molecules present in the combustion chamber, such as NO_X.

The simplest alkanal, or aldehyde, is formaldehyde. Formaldehyde is a carcinogen. Even small concentrations (as low as 0.1 mg/kg in air) can cause severe irritation of the eyes and nose [Atkins (2002) and Zumdahl (1995)].

Ketones have a similar chemical structure to alkanals. The simplest form of the ketones is acetone which causes irritation to the skin. Very high concentrations, when inhaled, can result in unconsciousness [Atkins (2002) and Zumdahl (1995)].

Aromatic compounds are any compounds which include a benzene ring. Inhaling benzene, even in small concentrations can cause drowsiness, dizziness, an increased heart rate, headaches, tremors, confusion and unconsciousness. In sufficient doses it can result in death. If benzene is ingested the results could be vomiting, drowsiness, dizziness, stomach irritation, convulsions, an increased heart rate and even death. Long term exposure to low concentrations damages the bone marrow and can decrease the red blood cell count, which affects the immune system and the bloods' ability to clot effectively. Because all aromatic compounds contain benzene, they all have similar effects [Atkins (2002) and Zumdahl (1995)].

The final compound which is classed in this section of legislation is ammonia. Ammonia itself is not harmful to mammals. However, fish and amphibians do not have the ability to break down or use any ammonia absorbed. This being the case, even very small concentrations of ammonia can be toxic to aquatic animals. For this reason ammonia is also one of the controlled emissions [Atkins (2002) and Zumdahl (1995)].

2.4.4 Particulate Emissions

Diesel particulate matter is of increasing concern, in terms of the damage it may do to an engine by way of coking, and the adverse effect it has on the environment, specifically the damage to human health. Diesel particulate matter is defined by the USEPA as the mass collected on a filter from the exhaust that has been diluted and cooled to below 52°C. The dilution and cooling process of diesel exhaust determines the nucleation, condensation and adsorption of the Soluble Organic Fraction (SOF) (also known as the Volatile Organic Fraction (VOF)) into the three classifications of diesel PM. Firstly, the nuclei mode of particulates is those under 50 nm in apparent aerodynamic diameter. These particulates consist of volatile organic and sulphur compounds which form during the dilution and cooling process. Secondly, the accumulation mode (also known as the soot mode) particulates are sized between 50 nm and 1 μm. The accumulation mode particulates consist of carbonaceous agglomerates, usually with adsorbed SOF. Finally, the coarse mode of particulates is in the size range between 10 and 1 μm. Coarse mode particulates are large clusters of accumulation mode particulates. By mass, the nuclei mode usually contains between 1 and 20%, and the coarse mode being between 5 and 20%. The accumulation mode accounts for the difference, and is always the highest proportion. However, and this is where the health implications stem from, the nuclei mode can account for up to 90% of the particulates by number [Kittelson (1998) and Burtscher (2001)]. Changes in operating conditions, the fuel and the exhaust gas dilution will all affect the mass of nuclei particles produced. When low sulphur fuel is used, 80% of all PM mass is accounted for by the accumulation mode and carbonaceous particles [Kamimoto (2004)].

There are many problems associated with particulate matter collection, one of which is particulate matter bounce. Particulate bounce depends on the impaction surface, the type and thickness of the coating material, the type of particulates, particulate loading, sampling conditions and the design of the impaction substrate. It is always desirable to use uncoated substrates where possible and essential when the particulate matter is to be chemically analysed. Temperature and humidity can affect the filters as well as the captured particulates [Chang (1999)]. The problem of collection must be overcome in order to conduct an effective investigation of the particulate matter produced.

Nag *et al* (2001) have investigated the possibility of oxygenated fuels being used to reduce the PM emissions from a diesel engine. It was found that this would reduce soot particles, without adversely effecting the formation of NO_X. One of the advantages found from higher injection pressures is better air/fuel mixing. This means a shorter combustion time, which in turn increases the temperature in the combustion chamber. This will slightly increase the production of NO_X during combustion; however, the production of PM emissions is significantly reduced. Oxygenate additives include ethanol, esters and ethers.

Recent biological investigations in cell cultures, as well as in rats, suggest that diesel particulates are capable of causing severe damage [Oh (2006) and Danielsen (2008)]. A single dose of diesel PM given orally to rats caused severe respiratory problems. This affected not only the lungs, but the liver as well. Furthermore, it has been estimated by the Scientific Committee on Food (2002) that between 12 and 18% of exposure to non-smoking humans to polycyclic hydrocarbons comes from the ingestion of vegetables contaminated with atmospheric particles. By comparison, the estimated

dosage from inhaled air pollution is only approximately 6%. The apparent aerodynamic diameter is critical in determining whether or not the respiratory filtering system can effectively remove these particles from our inhaled air. It follows that the size of the PM is as important as the concentration, possibly more so.

2.4.5 Legislation

Due to all of the above problems with unwanted products of incomplete combustion, there have been various legislative standards introduced to lower the emissions. At the moment Europe is working with Euro IV, which all new cars must comply with from October 2005. By October 2008, all new cars must comply with Euro V standards. Both of these standards for light-duty diesel engines - that is passenger cars - are described in Table 1 [European Emissions Standards].

Level	CO	NMHC	NO_x	PM
Euro IV	4.0	0.55	3.5	0.03
Euro V	4.0	0.55	2.0	0.03

Table 1 : Emissions standards for Europe, all values in g/kWh

USA regulations are slightly different. At the moment they are working to Tier 2 legislation, which has 8 different bins. These bins have varying levels of restrictions, which the car manufacturer must state which their cars can conform to. Contrary to the European way of legislating each type of engine based on the fuel consumed, in the USA all cars must conform to the same regulations. The Tier 2 emissions standards are given in Table 2 [USA Emissions Standards].

Bin	50 000 miles					120 000 miles				
	NMOG	CO	NO_x	PM	HCHO	NMOG	CO	NO_x	PM	HCHO
8	0.1	3.4	0.14	-	0.015	0.125	4.2	0.20	0.02	0.018
7	0.075	3.4	0.11	-	0.015	0.090	4.2	0.15	0.02	0.018
6	0.075	3.4	0.08	-	0.015	0.090	4.2	0.10	0.01	0.018
5	0.075	3.4	0.05	-	0.015	0.090	4.2	0.07	0.01	0.018
4	-	-	-	-	-	0.070	2.1	0.04	0.01	0.011
3	-	-	-	-	-	0.055	2.1	0.03	0.01	0.011
2	-	-	-	-	-	0.010	2.1	0.02	0.01	0.004
1	-	-	-	-	-	0.000	0.0	0.00	0.00	0.000

Table 2 : Emissions standards for the USA, all values in g/mile

Both the European governments and the USA government have introduced tax penalties for not achieving the target standards [European and USA Emissions Standards].

2.5 Exhaust After-treatment

There are three main ways of treating exhaust gases for harmful emissions. These are catalytic converters, thermal reactors and particle traps or filters [Heywood (1988)]. These will be covered in some detail in the following sections. A novel way to control emissions, which is still in the development stages, is the plasma after-treatment unit [Non-Thermal Plasma Exhaust After-treatment].

2.5.1 Catalytic Converters

Catalytic converters can either be oxidation catalysts, reduction catalysts or a combination of the two, which is known as a three-way catalyst. Oxidation catalysts can treat carbon monoxide (CO) and unburnt hydrocarbons (THC), by forcing complete combustion. Noble metals are the most suitable for oxidation, because they are active over a wide range of temperatures, and are less prone to fouling than base metals. The most commonly used oxidation catalyst is platinum. Because this is a very expensive metal, it is suspended in a substrate, such as aluminium oxide. Oxidation catalysts are ineffective below around 250 – 300°C. The light-off temperature is defined as the temperature at which the catalyst becomes more than 50% effective [Heywood (1988)].

Reduction catalysts are used to remove nitrogen oxide, NO using the CO, THC and H_2 in the exhaust. This is done by the following reactions.

$$NO + CO \rightarrow \tfrac{1}{2} N_2 + CO_2$$
$$2NO + 5CO + 3H_2O \rightarrow 2NH_3 + 5CO_2$$
$$2NO + CO \rightarrow N_2O + CO_2$$
$$NO + H_2 \rightarrow \tfrac{1}{2} N_2 + H_2O$$
$$2NO + 5H_2 \rightarrow 2NH_3 + 2H_2O$$
$$2NO + H_2 \rightarrow N_2O + H_2O$$

Unfortunately, there are still undesirable compounds, such as ammonia, in the products. At present there is no known catalyst which will reduce NO to O_2 and N_2, which will operate under engine exhaust conditions [Heywood (1988) and Majewski].

Three-way catalysts are used only when the normal operating condition for an engine is close to the stoichiometric ratio. Rhodium is the best catalyst for NO reduction, due to it being less inhibited by CO and sulphur compounds, and producing less ammonia than the more common platinum. Platinum is the most commonly used catalyst for THC and CO oxidation. If there is a sufficient concentration of rhodium present, the platinum will not take part in the reduction process [Twigg (2007) and Heywood (1988)].

In order for the catalysts to be as effective as possible, it is necessary for the surface area to be as large as possible. This is achieved by forming a honeycomb lattice, through which the exhaust gases are channelled. As a very rough guide, the volume of honeycomb required will be approximately half of the engine displaced volume [Twigg (2007) and Heywood, 1988].

2.5.2 Thermal Reactors

A thermal reactor is an enlarged exhaust manifold which is bolted directly onto the cylinder head. More air is added to the manifold, which promotes rapid mixing of the hot exhaust gases and the added air. The idea is that being on the cylinder head the reactor will retain enough heat to allow oxidation of THC and CO. The temperatures required for oxidation of THC and CO are 600^{o}C and 700^{o}C respectively. Unfortunately, most engines do not generate enough heat to support the oxidation reaction [Heywood, 1988].

2.5.3 Particulate Traps

A particulate trap is a temperature tolerant filter, designed to trap any particles in the exhaust gas. They are also known as diesel particulate traps [Yamane, 2005]. Once the particles have been trapped in the filter, they are

then oxidised. This solution is difficult to implement for a number of reasons. Any filter in the exhaust system significantly raises the system back pressure. As the filter collects particles, the pressure in the exhaust system steadily rises. This can then have a knock on effect on the EGR. Under normal operating conditions in automotive engines, the particles will not oxides, and when the particle do ignite, the oxidation must be closely controlled to prevent damage or destruction of the trap due to the high temperatures generated [Twigg (2007) and Heywood (1988)].

Particulate traps can be manufactured from ceramic monoliths, alumina-coated wire meshes, ceramic foam, ceramic fibre mat or woven silica fibre rope. However, particulate traps have been slow to be implemented due to the cost and problems associated with them, but are required by law in some areas, such as California [Twigg (2007) and Heywood (1988)].

2.5.4 Plasma After-treatment Units

A plasma after-treatment unit creates an ionized field within the exhaust by applying a pulsed electrical field. This field has sufficient power to break down most of the NO_X molecules in the field into their constituent ions. These O and N free radicals either react with the unaffected molecules or are converted into O_2 and N_2 by the catalyst [Non-Thermal Plasma Exhaust After-treatment].

When this plasma unit was tested in laboratory conditions, it was connected upstream of a catalytic converter and a particle filter. It was found to reduce NO_X emissions by 70% [Non-Thermal Plasma Exhaust After-treatment].

2.6 Exhaust Gas Recirculation

Exhaust gas recirculation (EGR) is a commonly employed method of reducing NO_X emissions in diesel engines. EGR reduces both the flame temperature and flame speed, which has a positive effect on the NO_X emissions. Ladommatos *et al* (2000) found that reducing the flame temperature by 225K reduces the NO_X formation by up to 80%. However, EGR can also decrease the efficiency of an engine and the lean combustion limit. Essentially EGR increases the residuals in the combustion chamber, either by replacement of inlet air by EGR or supplemental EGR [Stone (1992)].

EGR has three main ways of affecting an engine. It reduces the oxygen supplied to the combustion chamber, it increases the temperature of the inlet charge and the inlet charge mass flow rate is reduced due to the increase in temperature. Ladommatos *et al* (2000) found that the effect of the reduced oxygen mass fraction was to reduce NO_X formation, but to significantly increase the formation of PM emissions. Increasing the inlet charge temperature increases both NO_X and PM emissions. This can be negated by the use of cooled EGR. The reduction in inlet charge mass flow rate also increases PM emissions and decreases NO_X emissions.

EGR also provides CO_2 and water vapour to the combustion process and increases the specific heat of the inlet charge. Neither of these factors was seen to effect the emissions [Ladommatos, 2000].

McTaggart-Cowan *et al* (2004a) found that high EGR fraction induced ignition delay. This reduced and delayed the peak cylinder pressure. As the EGR fraction was increased, significant variations in combustion were

observed. This increased the emissions of THC and reduced fuel efficiency. Depending on the operating conditions, EGR fraction of between 15 and 20 % were found to reduce NO_X by more than 60% with no reduction in fuel efficiency or engine performance.

In a later study McTaggart-Cowan *et al* (2004b) found that EGR fraction of around 30% reduced the NO_X emissions by more than 90%, depending on operating conditions. On the flip side of this, there were substantial increases in THC and PM emissions. It was also found that various engine operating parameters, such as intake oxygen mass fraction, injection timing and engine speed, have an influence on the EGR reductions of NO_X. At high engine speeds greater increases of PM emissions were observed at low oxygen mass fractions. This is due to the shorter available time for complete combustion.

During this same study [McTaggart-Cowan (2004b)] an increase in inlet manifold pressure was investigated, with constant EGR. It was found that this reduced the emissions of PM and CO, with no effect on the fuel efficiency and only slightly increasing NO_X emissions, compared with the normal inlet pressure and EGR.

It is normal for petrol engines, or spark ignition engines, to use supplemental EGR, because they operate close to stoichiometric ratio, and this ratio is maintained by the throttling of the air intake. Diesel engines, or compression ignition engines, on the other hand normally use replacement EGR. Supplemental EGR in diesel engines reduces NO_X production, without effecting PM formation [Ladammatos (2000)]. Supplemental EGR in diesel engines does, however, increase the emissions of THC [McTaggart-Cowan (2004 a)].

Another method of reducing NO_X emissions is to use Selective NO_X Recirculation (SNR). By absorbing the NO_X in the exhaust stream and feeding it back into the air intake, the NO_X is broken down by a second pass through the engine. It was found that NO_X emissions could be reduced by 57% using this method of feeding NO_X back into the intake, however, a method for absorbing and depositing the NO_X back to the intake has not yet been developed [Tissera (2005)].

2.7 Alternative Fuels

Due to the increasing pressure from governments and World leaders to decrease the production of greenhouse gases, the research into alternative fuels has increased. Various alternatives which can be used in conventional internal combustion engines, as standard or with minor modifications, are going to be examined below.

Before describing the alternatives, it is necessary to first look at conventional diesel derived from petrochemical sources. Over the years petroleum companies have been trying to produce cleaner diesel by lowering the sulphur content, aromatics content, the distillation temperature and the density of the fuel. All of these fuel properties effect the particulate emissions adversely. Mineral diesel is mainly comprised of alkanes, formally known as paraffins, in the range of C5 to C11. However, some longer chain molecules may be included. When the diesel is made up of shorter chain molecules, the distillation temperature is lower and there is less chance of solid particles being produced by incomplete combustion of large molecules. There are three main sets of isomers of the alkanes used for diesel, n-alkane, isoalkane and cycloalkane (also known as n-paraffin, isoparaffin and cycloparaffin) [Nakakita (2005)]. These prefixes refer to the

shape of the molecule; n- means the molecule is a straight chain, iso- denotes the presence of two methyl groups at the end of a straight chain molecule and cyclo- denotes molecules with saturated rings [Schwarzenbach (2003)]. Nakakita *et al* (2005) found that at low to medium loads cycloalkanes produce the highest emissions, but at high loads the chemical structure had little effect. High concentrations of n-alkane do not produce as much PM as would be expected due to its high cetane number and corresponding short ignition delay and therefore short air/fuel mixing interval. By varying the composition of the fuel, it was found that the lowest emissions were produced with 55% isoalkane and 39% n-alkane. It was also found that aromatics produce the highest soot and PM emissions at medium to high loads.

2.7.1 Liquefied Petroleum Gas

Liquefied Petroleum Gas (LPG) is mainly a mixture of propane and isomers of butane. It has been found to have low PM emissions and low greenhouse gas emissions. The lower PM emissions is due to the short chain molecules not forming soot or large enough conglomerates on incomplete combustion, because the longest chain molecules are only C4. In Australia, Ford has started selling LPG cars, but these only account for ~10% of their petrol sales. LPG is limited at present by the cost of converting the engines to operate on LPG and the cost of the parts because of the, as yet, small production scale. LPG runs best on lean mixtures, and at its optimum set up, the brake thermal efficiency is 28% greater than for a petrol engine [Watson (2005)].

In tests where LPG was blended with diesel, it was found the lowest emissions were obtained for a 20:80 blend of LPG to diesel. This blend was

found to produce more NO_X than pure diesel, however. The blend had lower fuel consumption and the operating cost for the blend was reduced by 9.6% from that of the engine operating on pure diesel [Sethi (2004)].

2.7.2 Compressed Natural Gas

Compressed Natural Gas (CNG) is 80-98% methane (CH_4), depending on the source. The majority of the remainder of the composition is ethane (C_2H_6). CNG, like LPG, has the advantage of short chain molecules, and therefore little possibility of PM emissions being formed. CNG has low CO emissions and no sulphur emissions [Sasaki (2002)]. Tilagone *et al* (2005) found that CNG emitted 50% less THC than a conventional petrol engine and 23% less CO. This had been accredited to the higher hydrogen to carbon ratio, with for methane is four, and for CNG is very close to 4. The thermal efficiency of CNG was found to be around 25% higher than for petrol. This is due the much higher RON, which is greater than 120.

The disadvantages of CNG include the work required to compress the gas must be offset against the work produced by the engine. This makes the engine less efficient. CNG also has a very high self-ignition temperature, so spark or glow plugs are required to ignite the gas. A suggested solution to this is to produce a heat-insulated engine to limit the heat losses. This engine is to build of ceramic materials and allows the in-cylinder temperatures to rise to approximately 900K. This engine has high efficiency and low emissions [Sasaki (2002)].

As the sources of fossil fuels decrease, and become less accessible, other ways of producing methane may become more economically viable. One method is to use waste biomass, of which it is estimated the world produces

2 trillion tons of every year, and collect the methane which is emitted during the degrading process [Muraro (2005)].

2.7.3 Alcohols

Ethanol can be used in either petrol or diesel engines as blends or nearly pure. In petrol engines, E5 (5% ethanol in petrol) and E10 (10% ethanol in petrol) are already sold in many countries. E10 is known as gasohol in some countries. E10 has a higher octane rating than petrol, it burns slower and at a lower flame temperature. Due to the high oxygen content there is less incomplete combustion. No modifications are required to use E10 in modern petrol engines [International Energy Agency (2004)].

Brazil has been selling higher blends of ethanol and petrol, E22 and E26, for a number of years. Alcohols do degrade some plastics, rubber and various elastomers, and accelerate the corrosion of some metals, such as aluminium, zinc, brass and lead, so minor changes in materials are needed in petrol engines for these higher concentrations of ethanol. Slight changes in the tuning optimise the engine running [International Energy Agency (2004)].

Blends as high as E85 are being sold in the USA and Sweden. The cars which run on this blend have to have significant modification, and are fitted with ECUs which will optimise the engines timing etc. to burn various blends [International Energy Agency (2004)].

Higher blends than E85 cause problems for petrol engines. However, specially designed engines have been produced to run on hydrous ethanol (96% ethanol and 4% water). Brazil has been using this type of engine and fuelling system for a number of years, with no reported problems. The production of hydrous ethanol is cheaper than ethanol for blending, because

the water must be removed for blends. Because the boiling point of ethanol is so close to that of water, it is difficult to separate the last 4% of the water by distillation, and chemical methods must be employed. The compression ratio for ethanol engines can be increased compared to that of petrol engines, because ethanol has a very low cetane number and therefore, is not as prone to knocking [International Energy Agency (2004)].

Ethanol mixing with diesel is more difficult. Diesel and ethanol do not mix, they form an emulsion. One suggested solution to this problem is to use the ethanol as a dual fuel and atomise it in the air supply rather than mixing it with the diesel. Emulsions of less than 8% have been found to be comparable with straight low sulphur diesel in terms of performance [International Energy Agency (2004)].

Modified diesel engines can run on very high ethanol blends, up to E95. The ignition characteristics of the engine have to be altered, and additives are used in the ethanol to improve auto-ignition of ethanol and decrease ignition delay. However, because ethanol has only 60% of the energy contained in diesel, per unit volume, the fuel consumption increases to maintain performance [International Energy Agency (2004)].

Studies on the emissions produced from ethanol blends have found that, in petrol engines E10 reduces CO and PM emissions. However, there is an increase in NO_X and THC emissions. Similarly for diesel engines, E10 increases THC emissions, but lowers CO, PM and NO_X emissions. E95 trucks emit less PM and NO_X, but more CO and THC than diesel trucks [International Energy Agency (2004)].

Not all sources are in agreement with this. Brusstar *et al* (2002) found that all emissions are lower with methanol or ethanol engines. During this study it was also decided methanol is more efficient than ethanol. Using a low pressure injection system, means the cost of producing the engine is lower than that required for petrol or diesel.

2.7.4 Biodiesel

Biodiesel is the name given to diesel produced from renewable sources. The majority of biodiesel is produced from Fatty Acid Methyl Ester (FAME), the sources of which could be anything from vegetable oils, such as rapeseed, caster oil, soybeans or neem oil, to animal fats or used vegetable oil. The European Union has set a standard for any biodiesel produced from FAME (EN14214) [Verhaeven (2005)].

FAME is produced by transesterification of oils. Glycerol is a by-product and can be sold to cosmetics companies or pharmaceutical companies for use in their products. The reaction to produce FAME is shown in Figure 1.

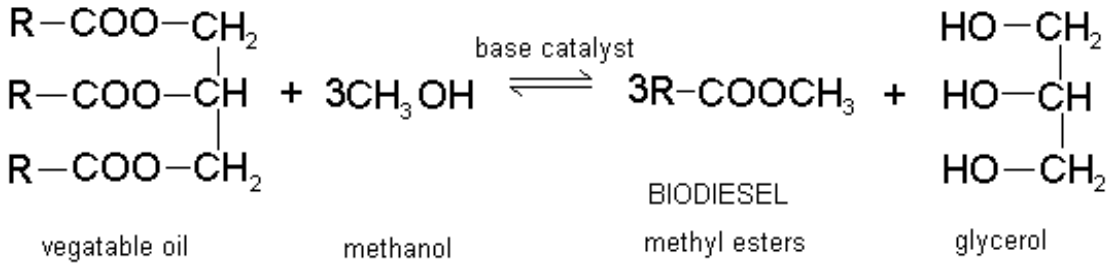

Figure 1 FAME production reaction (R is any long chain organic molecule)

Like with mineral diesel, the impact of using biodiesel on emissions depends on the engine and the chemical structure of the molecules. When tested in

Euro II engines, biodiesel was found to reduce PM emissions by 20% when compared with diesel. In Euro III, which has significantly lower emissions anyway, biodiesel still decreased the PM emissions by 12%. With the addition of glycerol derivatives PM emissions can be further lowered. The two main compounds used as additives are glycerol butyl acetal (GBA) and glycerol tertio butyl ether (GTBE) [Jaecker-Voirol (2005)].

Two studies [Xiaoming (2005) and Verhaeven (2005)] have found that a blend of mineral diesel and biodiesel produce lower emissions than that of either the pure mineral diesel or the pure biodiesel. At low blends, the NO_X emissions are not adversely effected, as they are at higher ratios and the fuel consumption is little effected. Because biodiesel is manufactured, it is easy to ensure no aromatics are contained in the final product. There is also no sulphur, and biodiesel is more biodegradable than mineral diesel [Xiaoming (2005) and Trapel (2005)].

Comparing pure biodiesel fuel consumption and power output with diesel, it has been found that biodiesel has slightly higher fuel consumption and slightly lower power output [Xiaoming (2005) and Nabi (2006)]. This is due to the lower energy content per unit volume of biodiesel. Blends, however, have comparable or better fuel consumption and power output than either pure biodiesel or pure diesel [Jaecker-Voirol (2005) and Trapel (2005)].

The main problem with biodiesel is that NO_X emissions increase with biodiesel in comparison to diesel [Xiaoming (2005), Nabi (2006), Kajitani (2002) and Trapel (2005)]. This can be countered by the use of water emulsions [Trapel (2005)], by after-treatment or by EGR [Kajitani (2002)].

2.7.5 Gas To Liquid

Gas To Liquid (GTL) is a manufactured diesel, produced by a refinery process, known as the Fischer-Tropsch process [Clark (2005)]. The equation for the basic reaction is given below.

$$CH_4 + \tfrac{1}{2}O_2 \rightarrow 2H_2 + CO$$
$$(n+1)H_2 + nCO \rightarrow C_nH_{2n+2} + nH_2O$$

The two main companies involved with the GTL production are Shell and Sasol, which is a South African company who developed the Fischer-Tropsch process to use coal as a feedstock to produce liquid fuels during the apartheid ban on trade. Shell produces GTL from natural gas [Clark (2005)].

Unlike biodiesel, pure GTL has significantly lower emissions than blends of diesel and GTL. However, it has been found that blends have lower emissions than would be expected, 50:50 GTL and diesel reduces emissions by more than 50% of the pure GTL reduction. One of the main advantages of GTL over biodiesel is that it reduces all emissions, including NO_X [Knottenbelt (2002), Clark (2005) and Schaberg (2005)].

2.8 Dual Fuelling

Due to the ever stricter emissions regulations, it is necessary to find new ways of reducing the environmental impact of automotive engines. One way which has been investigated is the use of dual fuelling [Lee (2003), Tsolakis (2004) and Tsolakis (2005a)]. The use of a high octane fuel to promote premixed combustion in a diesel engine can significantly improve the engine

performance, however, there are problems with engine knock and decreased ignition delays which need careful control.

2.8.1 Natural Gas

One of the high octane fuels considered for dual fuelling is natural gas, or methane. Natural gas can produce engine knock, but this can be controlled by precise control of the inlet temperature and natural gas volume. If natural gas is used to replace the pilot diesel injection, there will be an increase in ignition delay. With constant load and speed conditions, increasing the proportion of natural gas in comparison to diesel will result in a faster combustion and lower exhaust gas temperatures. The intake temperature, at which knock will occur, decreases with engine speed [Wannatong (2007)].

2.8.2 Propane

Yap et al (2005) has conducted studies on using propane as a secondary fuel to promote HCCI combustion. Propane has a high auto-ignition temperature, so requires high compression ratios or intake temperatures to achieve HCCI combustion. With a compression ratio of 15, residual gas trapping effectively raised the in-cylinder temperature sufficiently to not require intake air heating. It was also found that nitrogen oxides emissions were significantly reduced in comparison with petrol combustion [Yap (2005)].

2.8.3 Hydrogen

The use of hydrogen as a premixed high octane fuel, ignited by a main injection of diesel has been investigated as a combustion improver. Hydrogen can lead to lower particulate matter mass emissions, lower smoke emissions, lower CO and lower unburnt hydrocarbons. This, however, comes at the expense of the NO_X emissions, as is usually the case with diesel engines. Hydrogen inducted into the air supply will improve the brake thermal efficiency due to the higher calorific value of the hydrogen versus the diesel fuel and more complete combustion of all the available fuel, and increase the ignition delay. This increase in ignition delay means higher maximum cylinder pressures and rates of cylinder pressure rise. At low loads, hydrogen can produce misfire [Senthil Kumar (2003), Tsolakis (2005b), Tsolakis (2005c)].

Addition of hydrogen to diesel engines fuelled with alternative fuels has also been investigated. When hydrogen is inducted with the air, with dimethyl ester (DME) as the main fuel, the highest achievable load was found to be increased [Shudo (2006), Saravanan (2008b)]. Unfortunately, the auto-ignition point of hydrogen is not easily predictable. It does not vary logarithmically linearly like other high octane fuels, such as methane, meaning there are more control issues [Chen (2003)]. In combination with dimethyl ester (DME) as the main fuel, hydrogen inducted in to the engine air supply was found to increase the maximum achievable load. Using hydrogen as a secondary fuel does have a problem however.

Overall, there are clear advantages of using hydrogen in diesel engines, if the few drawbacks can be overcome. Previous results obtained using a single cylinder air-cooled naturally aspirated diesel engine with a low

pressure injection system (180 bar) have indicated the potential benefits of combining EGR with hydrogen addition in terms of improving the emissions of diesel engines [Tsolakis (2005c)].

A further advantage of increasing hydrogen fuelling in internal combustion engines that has been presented by Rakopoulos et al (2008) is increased second-law efficiency. This is achieved by the fundamentally different mechanisms of combustion between hydrogen burning, which combines two simple diatomic molecules, and hydrocarbon burning, which destroys relatively more complex molecules. Of course, increasing the use of hydrogen in internal combustion engines also has the distinct advantage of reducing the carbon available to produce green house gases, such as carbon monoxide and carbon dioxide. One hundred percent hydrogen fuelling in automotive engines would achieve local carbon free transportation.

Although hydrogen is the most common element in the Universe, it is very rarely found in its elemental form. The most prominent method of hydrogen production at the moment is hydrocarbon stripping. Any hydrocarbon can be used in this process, however efficiencies of up to 80% can be achieve with natural gas. This is an energy intensive process which also releases carbon dioxide. Centrally produced CO_2 can be captured and stored or mineralised to minimise the impact of emissions.

Hydrogen has a high lower heating value almost three times that of diesel, however the energy density is not favourable.

2.9 Gas Chromatography

The basic principle of a gas chromatograph is to separate out the various compounds present in a sample so that they can be identified. This is

achieved by eluting the sample through a column. The column has an internal coating, called the stationary phase, which acts as a resistor to the molecules passing. A carrier gas, called the mobile phase, is used to transport the sample through the column. Larger molecules are shown a higher resistance than small ones, and therefore take longer to elute. In order to speed up the process of elution, which for some large molecules could take days without assistance, the column is kept in an oven. The starting point for the oven temperature depends on the molecular mass of the sample, but it can then be ramped up to reduce the resistance of the column, and speed up the movement through the column. The most important property of this process is that, with the same temperature program and column, the elution time for a specific compound is fixed.

Gas Chromatography was first conceived in 1941 by A.J.P. Martin who published a paper on liquid chromatography in which he stated that using a gas carrier phase should be possible. It was not until 1951, however, that Martin's concept was brought to fruition. At this point the first paper on gas chromatography was published [James (1952)] describing the separation of fatty acids.

A modern gas chromatograph is made up of four units; the gas supply unit, the sampling unit, the column unit and the detector unit. The gas sampling unit controls the supply of the carrier gas. The carrier gas may vary depending on the detector chosen for the specific purpose. For example a flame ionisation detector needs a flammable gas such as hydrogen as the carrier, but a mass spectrometer needs an inert gas such as helium or argon.

The sampling unit controls the supply of the sample to be analysed. An automatic injector is contained within a thermostatically controlled

enclosure. The temperature of the injector must be accurately controlled in order to avoid condensation of the sample prior to injection. Automatic injectors range in complexity from a simple heated valve to complex transport and supply systems which automatically start the next test on completion of the first. The accuracy of a gas chromatograph is only as good as its injector system. If the sample is smeared onto the column, rather than injected as a solid slug, the results will also be smeared.

The third unit is an oven containing the column. This essentially the part which separates out the sample into the component parts, so needs to be accurately controlled. In order to reduce the total time for a test the column temperature is continuously raised throughout a test. This method is used in preference to increasing flow rates, because it allows the retention times to be dramatically reduced. This is due to the fact that retention times decrease exponentially with increasing temperature, rather than linearly with increasing flow rates.

The final part of a gas chromatography set up is the detector. There are a wide range of detectors which can be used in conjuncture with a gas chromatograph, and the choice will depend on the performance characteristics required for the particular test set up. In order to avoid condensation on the detector, or in the connecting conduit, the detector and the conduit must be heated. A temperature of at least 15^{o}C above the maximum oven temperature is recommended to avoid condensation problems. This necessarily means that the detector and the conduit require heaters and the control systems to thermostatically maintain them.

Given all of the above, it is clear that an accurate gas chromatograph requires careful control, and therefore a computer with software controls is the most appropriate method [Grob (1995)].

2.10 Motivation

Given the information presented in this chapter, it was decided that an investigation into the effect of dual fuelling on the exhaust gas emissions from a high speed direct injection diesel engine would be conducted. Specifically, a prototype diesel engine was modified to induct hydrogen. The exhaust gas emissions are of increasing concern, both in terms of the adverse effects on the environment and on human health. This being the case, it is necessary to examine not only the exhaust gas emissions, but the particulate matter size distribution and the chemical composition as well. This is required to determine the ability of the particulate matter to penetrate the respiratory system, and whether or not the chemicals will be harmful if they reach the mucus membranes.

CHAPTER 3

EXPERIMENTAL ENGINE AND INSTRUMENTATION

3 CHAPTER 3 EXPERIMENTAL ENGINE AND INSTRUMENTATION

3.1 Introduction

The engine used for this series of experiments is a modern high speed direct injection diesel. The engine was built by the Ford Motor Company as a prototype for the Duratorq series of engines, also known as the Puma engine. When the engine was donated to Brunel University's Internal Combustions Engine's Research Group it was installed in a test cell with a Schenk eddy-current dynamometer. This chapter describes the engine, its control and monitoring systems and the analysers used during the experimentation.

3.2 Ford "Puma" 2.0L HSDI Diesel Engine

A Ford pre-production prototype engine was used to conduct all the experiments presented in this work. The engine block is based on the 2.0 L Ford Duratorq engines which power Ford Transits and diesel Mondeos. The cylinder head is a production Ford Zetec head, with twin camshafts, and 4 valves per cylinder. A full list of the engine specifications are given in Appendix A. The engine has two main differences from the production engines.

The first difference is the air intake manifold. On the production models the intake manifold was designed to promote swirl, and in some models actually had a variable swirl port installed. This was not available on the test engine. The inlet manifold on the test engine has straight cylinder feeds.

The second difference was the pistons used. The production model of the 2.0L engine had a slightly different bowl design, and a compression ratio of 19:1. The test engine has a lower compression ratio of 18.2 due to the larger bowl volume.

The engine is fitted with a Garrett turbocharger. The Variable Geometry Turbine – 15 (VGT – 15) is design to balance the need for a small turbine housing at low engine speeds and the large "turbo – lag" which can be experienced if a turbocharger is designed for higher speed operation.

3.3 Fuels

3.3.1 Diesel Fuel

The diesel fuel used throughout testing is Ultra Low Sulphur Diesel supplied by Shell and stored in the diesel tanks at Brunel University. The tanks are large enough that one batch of fuel was used for all the tests, eliminating any possibility of discrepancies between fuel supplies. A full list of the diesel fuel properties are given in Appendix B.

3.3.2 Hydrogen Fuel

The hydrogen used was supplied from a compressed gas cylinder supplied by BOC Speciality Gases. The hydrogen was research grade, meaning that BOC certified the hydrogen purity at 99.9995%.

3.4 Engine Control and Operation

3.4.1 Engine Management System

For experimental investigations, complete control over the engine set-up is a necessity. To this end a system is required that gives direct access to the Electronic Control Unit (ECU) was implemented. A 486 PC running GrEDI v 2.298 was used to write, and modify, the engine maps. A schematic of the engine management system is shown in Figure 2.

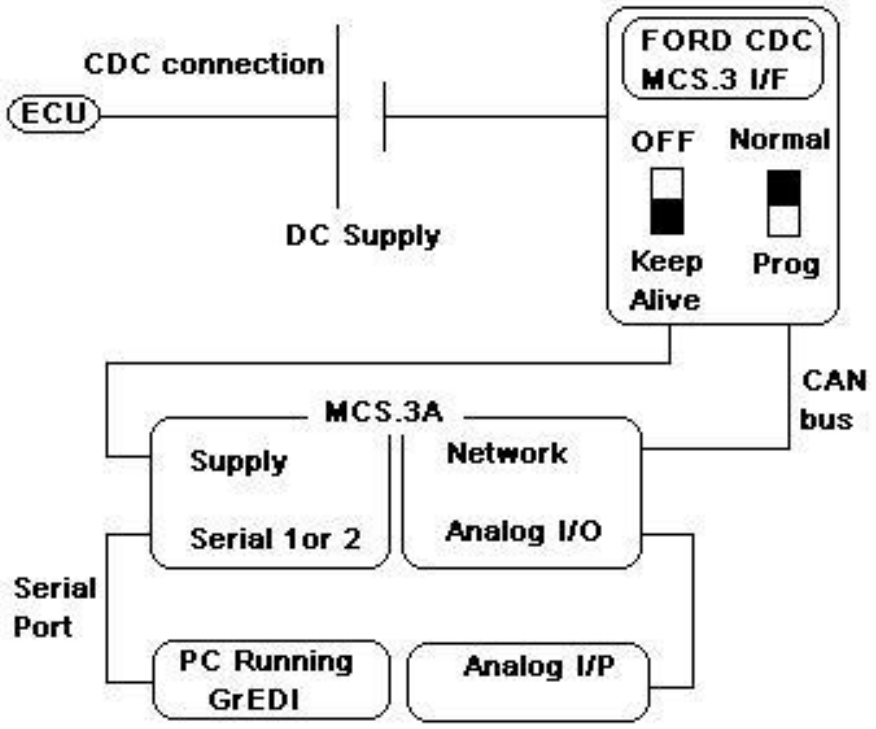

Figure 2 Engine management system showing the connection to GrEDI

GrEDI is an MS-DOS based program that allows direct manipulation of the ECU parameters. The engine maps can be set-up offline, i.e. when the engine is not running, and then modified online. Most of the engine

parameters, such as Exhaust Gas Recirculation (EGR) levels, injection timing, injection strategy, injection pressure and boost pressure, were controlled via GrEDI. The system had previously been modified to allow the fuel level to be controlled directly by the operator via a potentiometer box. The potentiometer is the direct analogue of the accelerator pedal in a car.

During normal operation in a vehicle, the ECU would monitor all the engine variables. GrEDI provides a read back facility which allows various temperatures, pressures, flow rates and voltages to be captured, which can be used to monitor the engine. All of the values required for experimental analysis were verified by secondary measurements.

3.4.2 Engine Water Cooling

In terms of experimentation, it is important to maintain a steady operating temperature for the engine. This is achieved by the use of a cooling circuit as shown in Figure 3. The engine coolant was cooled by the cold water from the reservoir tank on the roof of the lab flowing through the Bowman heat exchanger. The engine coolant was held at 75^{o}C, as would be the case in standard engine conditions. The cold water valve was opened by the thermostat control when the engine coolant reached 80^{o}C, increasing the cold water flow rate through the heat exchanger. The high flow rate of cold water through the heat exchanger was maintained by the thermostat until the engine coolant temperature dropped below 70^{o}C.

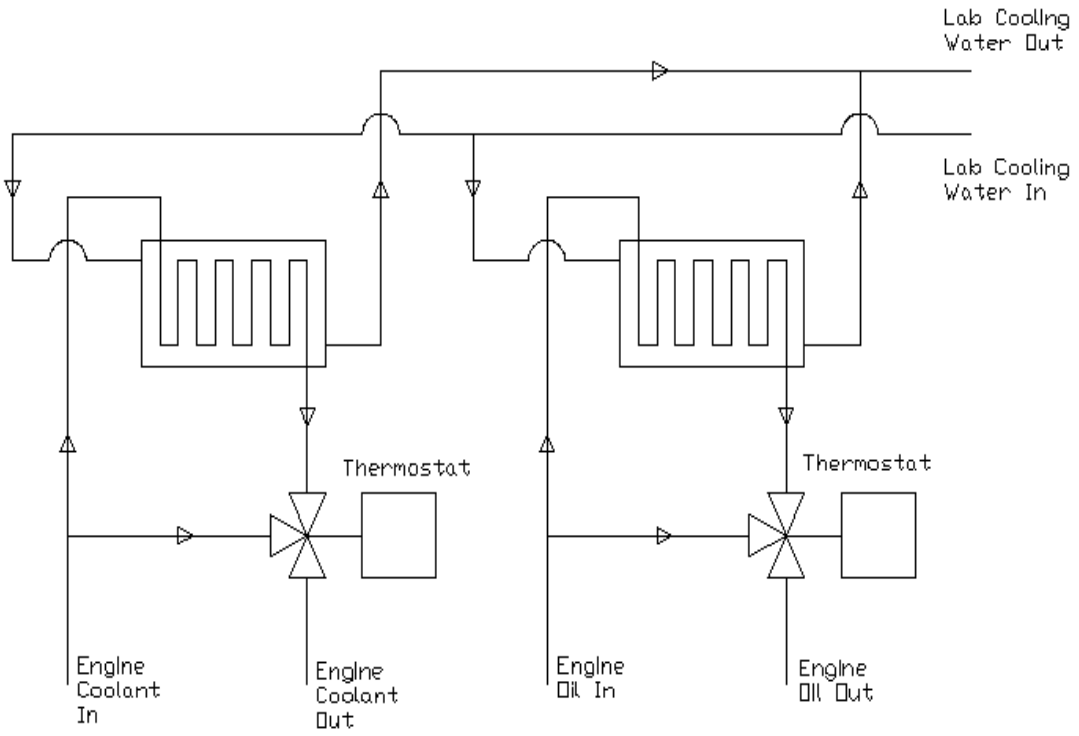

Figure 3 Engine fluids cooling schematic

3.4.3 Air Intake System

The air intake system before modification, apart for the air flow meter, was as used on the standard Duratorq engine. The inlet air is filtered through a paper filter in order to remove any particulate matter which could potentially enter the combustion chamber, and cause damage. The system then connects to the turbocharger, where the air is boosted to the required pressure. Due to the temperature increase boosting produces, an intercooler was fitted. As it is not possible to cool the intake air with a standard air cooled intercooler, a water cooler was used in the lab. The mixing point of the fresh intake air and the EGR is immediately prior to entering the intake manifold. A schematic of the air intake system is show in Figure 4.

However, when conducting experiments it is important to only change one variable at a time. That being the case, it was necessary to bypass the VGT in order to maintain a constant air intake pressure over the changing engine loads, speeds and EGR levels, all of which effect the volume of exhaust gas available to power the turbine. So as not to disrupt the exhaust gas flow, the bypass was made by simply disconnecting the compressor side of the VGT and linking the two pipes.

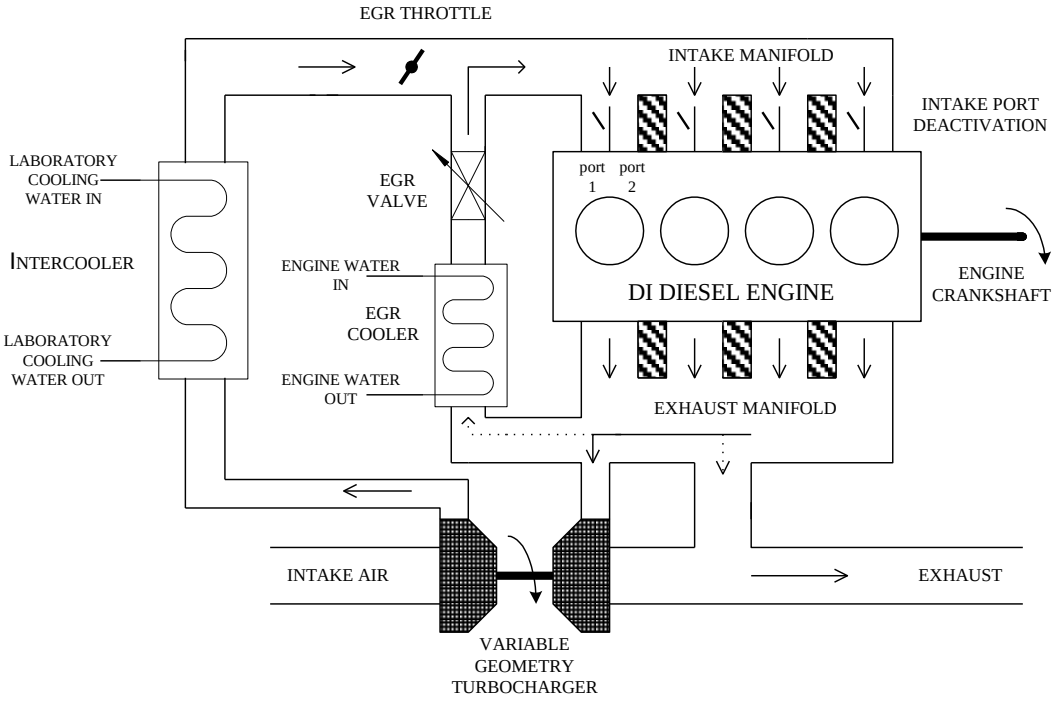

Figure 4 Schematic representation of the turbocharged, intercooled Ford Puma diesel engine [Ford M.C. (2001)]

3.4.4 Engine Lubricant and Oil Cooling

The engine oil used was 10W/40 Grade oil. The oil pump maintained a supply of oil to all the moving parts. The oil temperature was kept at no more than 100^{o}C, via the oil cooling circuit, shown in Figure 3. Oil pressure

was measured by the dynamometer pressure sensors, and maintained between 2.5 and 3 bar gauge.

3.4.5 Fuel Supply System

The engine is equipped with a modern high pressure common-rail injection system. The maximum achievable pressure in the rail is 1600 bar, but can also be run at very low pressures. The common rail system is capable of multiple injections per cycle.

The pressure in the common rail is maintained by the high-pressure fuel pump, and is controlled by the Injection Control Unit (ICU). The ICU is a sub-system of the ECU and controls the volume and timing of each fuel injection. The ICU uses inputs such as the fuel temperature in the fuel pump, the common rail pressure and engine parameters to interpret the correct timings of the injectors opening.

Each cylinder is supplied with fuel via a central injector supplied by Lucas (now Delphi). The injectors themselves are two stage high pressure injectors with six holes. The nominal diameter of each of the injector holes is 0.154mm, generating a spray angle of 154^{o}. These have been specifically designed to improve fuel atomization and therefore the combustion.

Excess fuel supplied to the common rail is filtered, cooled and fed back to the high pressure fuel pump.

3.4.6 Dynamometer

In order to control the speed and load put on the engine, the engine was mounted on a Schenck W130 eddy-current dynamometer. The engine

connection to the dynamometer was made via a rubber coupling to isolate the dynamometer from any high frequency vibrations from the engine. The dynamometer itself consists of a thin disc mounted on a shaft. The disc rotates inside a magnetic field normal to the rotation which creates a resistive torque. To control the load applied to the engine, which is equivalent to the torque applied to the coupling shaft, the magnetic field can either be increased or decreased from the dynamometer control panel. Any currents generated within the dynamometer rotor are short-circuited, creating considerable heat. The temperature of the dynamometer is controlled via a water cooling system, connected the to the laboratory cold water. A diagram of the dynamometer is shown in Figure 5.

The engine load was measured by a load cell connected to the casing of the dynamometer. This load cell together with a speed senor was used to accurately measure the speed and torque generated by the dynamometer. In order to remove any interference generated by the engine vibration, the signal was low pass filtered.

There are two main modes of engine control with this model of dynamometer: constant speed and constant torque. In the constant speed mode, the dynamometer maintains a constant rotational speed of the connecting shaft by increasing or decreasing the resistive torque as necessary depending on the force produced by the engine. The torque of the engine in this mode is therefore controlled by the level of fuelling. Similarly, in the constant torque mode, the dynamometer maintains a constant resistive torque, allowing the shaft, and therefore engine speed rise and fall depending on the fuelling level.

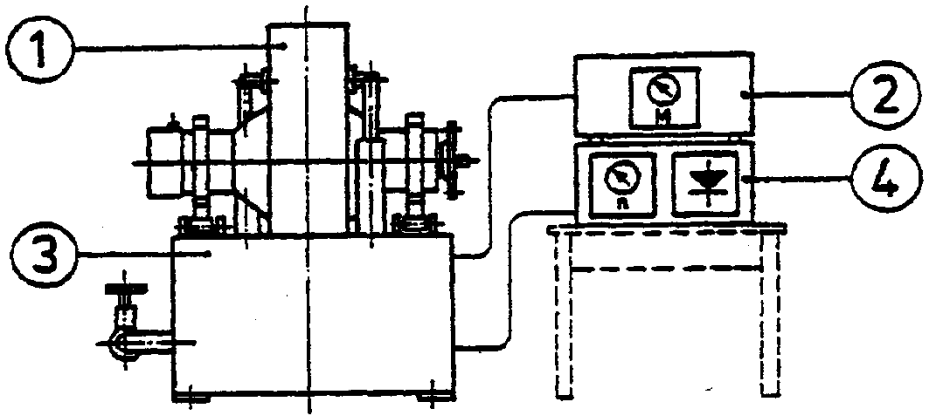

Figure 5 Eddy current dynamometer used for absorbing power developed by the engine; (1) dynamometer containing magnetic-field-producing-stators and eddy current rotating disk; (2) torque measuring unit, connected to the load-cell, which was mounted between (1) and (3) (load cell not shown); (3) dynamometer base made from a large concrete block surrounded by a metal frame; (4) simplified control unit for control of engine speed and torque [Schenk Users Manual (1983)].

3.5 Engine Properties Measurements

3.5.1 Fuel Flow Rate and Air Flow Rate Measurements

Prior to entering the standard engine air supply system, a rotary air flow meter is used to measure the air flow entering the engine. The frequency of the rotation is given on a digital display, and can then be used to calculate the Mass Air Flow (MAF).

An AVL fuel mass flow meter was used to measure the precise mass of fuel supplied to the engine. The meter uses a gravimetric system to determine the mass of fuel supplied to the engine over a set length of time. A torsion and beam spring balance measures the change of mass of fuel in a vessel over the pre-set time.

The complete measuring process starts with the filling of the measuring vessel. This is followed by a short steadying time, to allow the balance to come to rest. The mass of fuel in the vessel is then taken. Several measurements are then taken, at pre-determined time intervals, so that the residual mass can be used to calculate the consumed mass. The measuring vessel periodically refills, leading to a short cessation of measurement.

The accuracy of the AVL fuel flow meter is stated as 0.12% of the fuel measured by AVL.

3.5.2 Temperature and Pressure Measurements

For the experimental work to be correctly monitored, and key temperatures and pressures recorded where needed, a series of temperature and pressure sensors were fitted to the engine at various locations.

To measure the temperature a number of Standard K-type thermocouples were used. A K-type thermocouple uses the Seebeck effect, which states the voltage between 2 strips of metal is proportional to the temperature. The two metals in question in a K-type thermocouple are nickel-chromium and nickel-aluminium, arranged as shown in Figure 6. Although any two different metals can be used as a thermocouple, a number of standards are used because of their predictable output [Thermocouple Application Note].

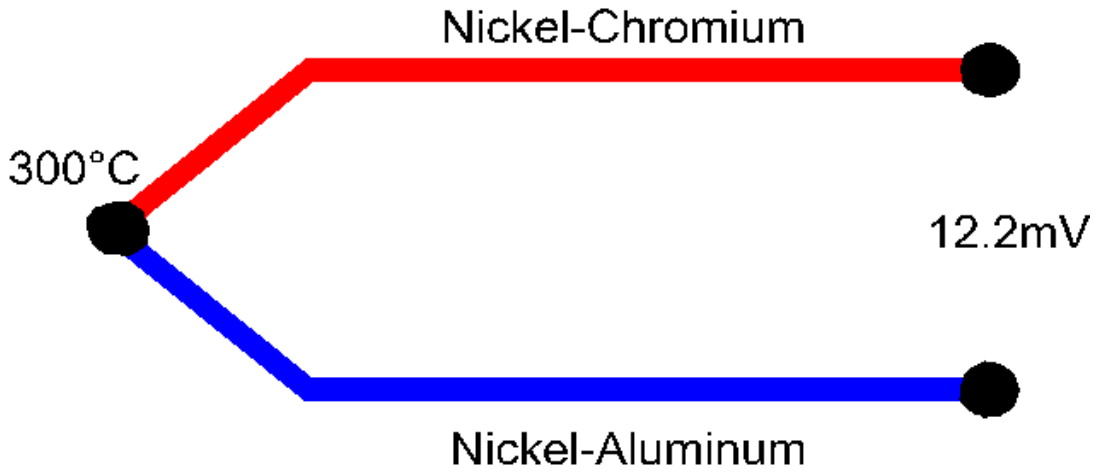

Figure 6 K-type thermocouple

The positions of all the thermocouples used on the engine are given in Table 3. The values from the thermocouples were calibrated by look up tables contained within the dynamometer control desk and displayed on the dynamometer digital read backs on the desk.

Temperature measurement	Position on the engine
Engine coolant in	Engine inlet water, before engine thermostat
Engine coolant out	On the outlet water line, after thermostat
Exhaust manifold	Exhaust manifold, prior to the turbine
Exhaust gas	Exhaust down pipe
Inter-cooler outlet air	After inter-cooler, before EGR/Air mixing
Oil	Oil sump
Air filter	Air filter, after flow meter
Inlet fuel	Inlet fuel line, prior to high pressure pump
EGR	After EGR cooler, before mixing with air
Compressor outlet air	After compressor, before inter-cooler
Atmospheric dry	Thermometer in test cell
Atmospheric wet	Thermometer in test cell

Table 3 Temperature sensors on the engine

Similarly, various pressures around the engine were monitored and recorder where necessary. Piezoelectric pressure transducers were used, and a full description of the operation is given in Section 3.5.4. In order to decrease the number of pressure transducers needed, a switch rack was installed so that 1 sensor could read back pressures from 8 different points around the engine. The positions of the pressure taps are give in Table 4.

Pressure measurement	Position on the engine
Compressor outlet air boost	After compressor, before the inter-cooler
Exhaust manifold	Exhaust manifold
Exhaust gas	Exhaust down pipe
Inter-cooler outlet air	After intercooler, before mixing with EGR
Oil	Oil pump
Air filter	Air filter, after flow meter
Inlet fuel	Fuel line after filter, before high pressure pump
Atmospheric	Open to test cell

Table 4 Pressure sensors on the engine

3.5.3 Shaft Encoder

In order to measure in-cylinder pressures at known crank angle positions, it is necessary to know the position of Top Dead Centre (TDC) and measure the rotation of the crank shaft. For this a GEL 244 pickup head and a 360-toothed gear wheel with separate TDC flag was used. The TDC pulse and the corresponding crank degree pulses were used together with the data acquisition system to log the pressure traces from cylinder 1.

To correctly calibrate the position of TDC, threaded adjustment rods controlled the position of the pickup head. TDC was found by delaying the fuel injection until after TDC and then matching up the peak cylinder pressure with the TDC flag from the toothed wheel.

The complete shaft encoded fitted to the engine is shown in Figure 7.

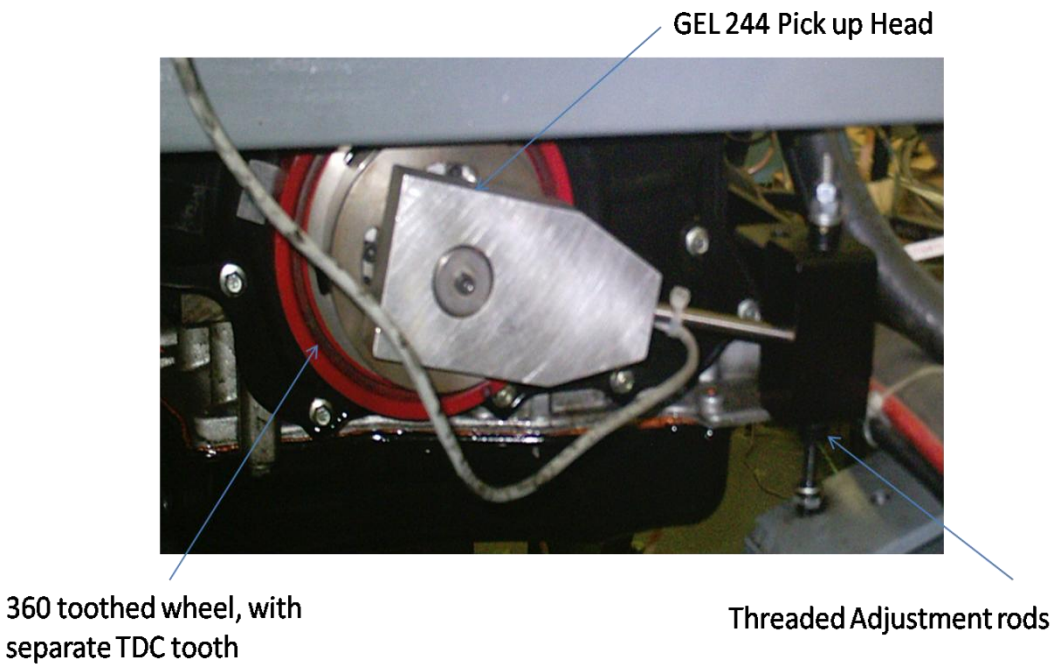

Figure 7 Shaft encoder set up

3.5.4 In-cylinder Pressure Measurement

The in-cylinder pressure from cylinder 1 on the engine was measured using a Kistler type 6125A piezoelectric pressure transducer. The pressure transducer was fitted into the modified hole for the glow plug, as shown in Figure 8. This transducer is a high-temperature, ground insulated pressure sensor specifically designed for in-cylinder pressure measurements. It does not require cooling, and it is resistant to thermal shocks. Over time the transducer can become affected by the build up of soot, but this is easily rectified by a manufacturer's service.

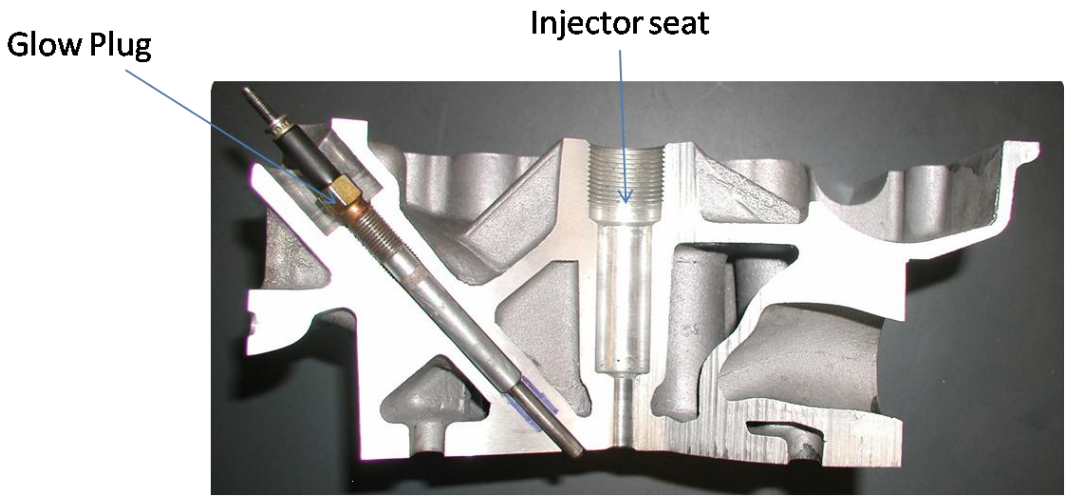

Figure 8 Cut away of cylinder head showing injector seat and glow plug hole

A piezoelectric pressure transducer contains a quartz crystal. The crystal is exposed to the cylinder pressure through a diaphragm at one end. As the crystal is compressed it produces an electrical charge proportional to the pressure exerted on the crystal. The charge produced by the Kistler 6125 A pressure transducer is known to be 16 pC/bar. The pressure transducer is shown in Figure 9.

Figure 9 Kistler 6125A pressure transducer

The transducer was held in the modified glow plug hole by a sleeve manufactured by Ford. The signal was passed through a charge amplifier to boost it, and together with the crank angle signal provided from the shaft encoder, was used to log the change in cylinder pressure versus crank angle using a PC. A LabVIEW version 6.0 program was developed at Brunel University to capture the pressure data, and export it for further analysis.

3.5.5 EGR Control

On the Duratorq engines a vacuum operated poppet valve mounted below the exhaust manifold controls the Exhaust Gas Recirculation (EGR) mass flow rate. The vacuum applied to the valve diaphragm is controlled by a current-to-vacuum transducer. The diaphragm then directly manipulates the valve.

The EGR level can be set using GrEDI. Although the GrEDI software estimates the EGR level, it was found to be much more accurate to directly measure the levels. This was done using the carbon dioxide (CO2) levels in the exhaust manifold and the inlet manifold according to the equation shown in Equation 1.

$$EGR\ \% = \frac{CO_{2in}}{CO_{2out}} \times 100$$

Equation 1 EGR percentage calculation [Zhao (2001)]

3.6 Exhaust Sampling

A modified down-pipe from the exhaust manifold allowed easy exhaust gas sampling from the engine. A number of outlets were drilled into the pipe, and fitted with the various fixtures needed for the specific analysers used. A picture of the exhaust down-pipe, showing all the sampling points, is shown in Figure 10.

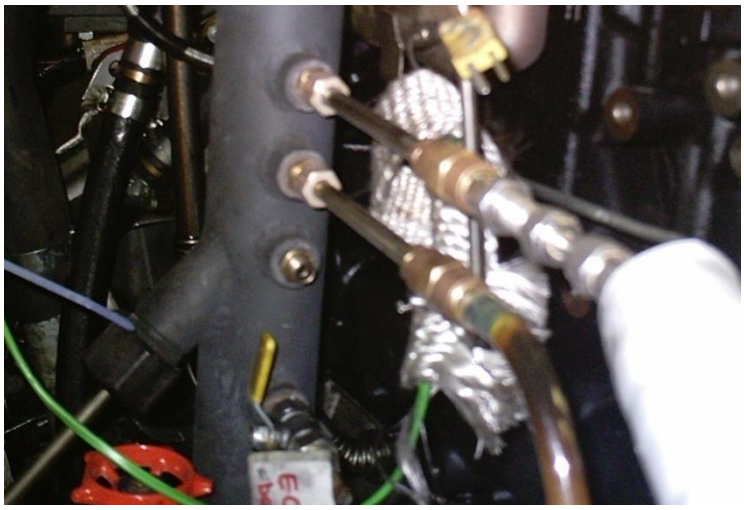

Figure 10 Exhaust downpipe showing sampling ports

Each of the sampling ports was fitted with a stainless steel sampling pipe, drilled with a number of openings. This meant that the gas samples were all collected from the central part of the exhaust pipe, and collected at 90° to the exhaust gas flow. This reduces any errors or discrepancies which could be caused by the wall effects of the flow through the down-pipe.

3.6.1 Exhaust Gas Measurements

The exhaust gas emissions were measured using a Horiba 7170DEGR gas analyser. The analyser is capable of measuring carbon monoxide (CO), carbon dioxide (CO_2), exhaust gas oxygen (O_2), total unburnt hydrocarbons (THC) and nitrogen oxides (NO_X). The analyser also has a facility which allows the CO_2 present in a secondary feed to be measured. This was used to measure the CO_2 present in the exhaust and the inlet manifold simultaneously, and calculate the EGR levels.

3.6.1.1 CO and CO_2 Measurements

The measurement of CO and CO_2 was conducted by the AIA-72X module of the Horiba gas analyser, by non-dispersive infrared analysis (NDIR). NDIR works on the principle that molecules absorb infrared radiation at specific wavelengths. The level of absorption is proportional to the concentration of the molecule. Different molecules have different absorption spectra. Examples of the absorption spectra for carbon monoxide, carbon dioxide and water are shown in Figure 11 [Horiba 7179DEGR Users Manual].

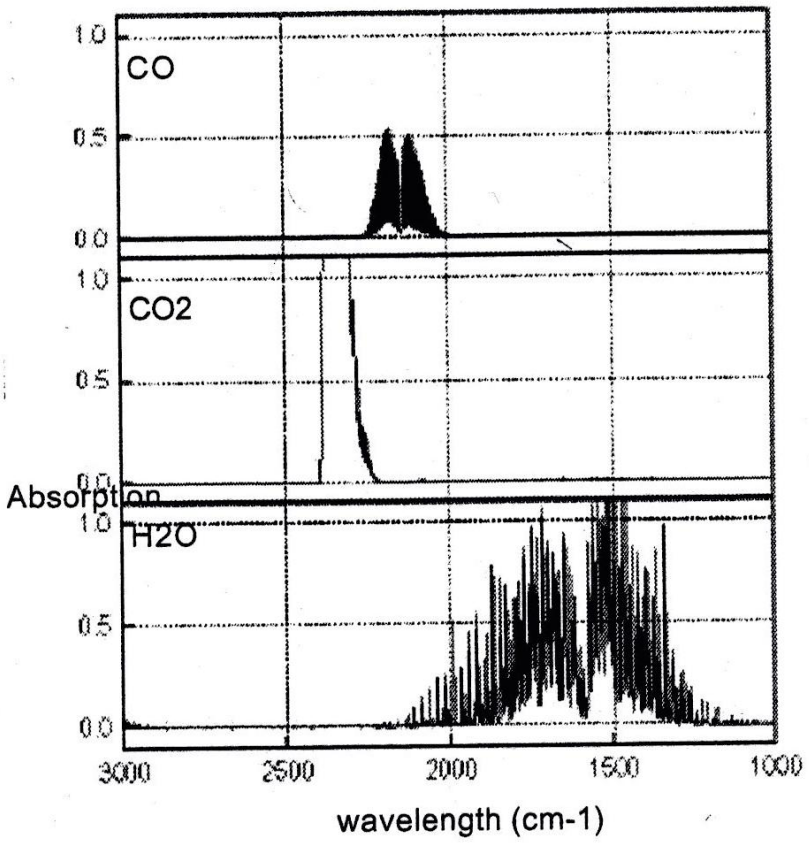

Figure 11 Absorption spectra for CO, CO_2 and H_2O [Horiba 7170DEGR Users Manual]

A typical NDIR set up consists of an infrared light source, a detector, a sample cell, a comparison cell and an electrical system, as shown in Figure 12. The comparison cell contains a gas, such as nitrogen, which does not absorb infrared radiation. The sample cell has a continuous supply of the sample gas. The infrared beam from the light source is passed through both cells, giving values for l and l_0, which can then be inserted into Equation 2 to calculate the concentration of the sample gases [Horiba 7170DEGR Users Manual].

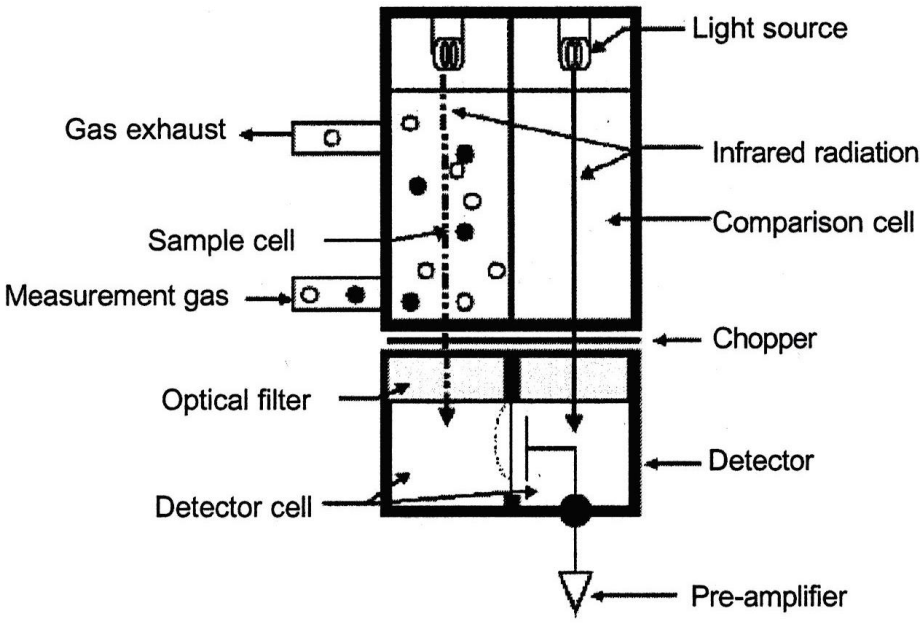

Figure 12 Typical non-dispersive infrared analyser set-up [Horiba 7170DEGR Users Manual]

$$\alpha(\lambda) = log\left[{l(\lambda)}/{l_0(\lambda)}\right] = \varepsilon(\lambda)CL$$

Equation 2 Relationship between the degree of absorption and the concentration of the sample gas

3.6.1.2 O_2 Measurements

The measurement of the oxygen contained in the exhaust gas was achieved by magneto-pneumatic detection within the MPA-720 unit in the Horiba analyser. The magneto-pneumatic detection works by applying an alternating current to the electromagnet arrangement as shown in Figure 13. The pressure around the magnetic poles changes in relation to the concentration of O_2, because the oxygen is attracted to the poles. A condenser microphone is used to detect the changes in pressure [Horiba 7170DEGR Users Manual].

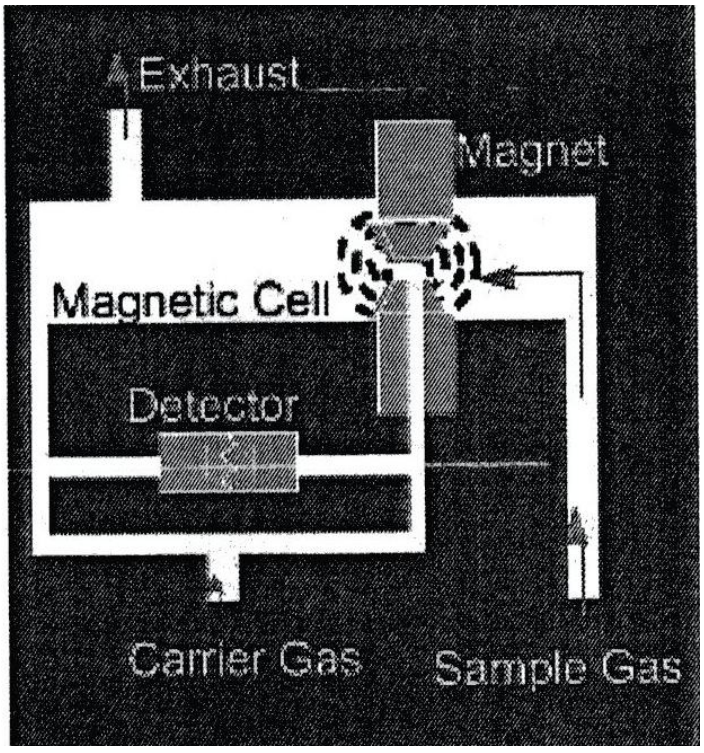

Figure 13 Configuration of magneto-pneumatic oxygen analyser [Horiba 7170DEGR Users Manual]

3.6.1.3 NO_X Measurements

The measurement of NO_X is achieved by chemiluminescence detection within the CLA-720A module of the Horiba analyser. Chemiluminescence works by reacting the nitrogen oxides with ozone. This converts the NO to NO_2. A proportion of the NO_2 created in this manner will produce an excited NO_2 molecule. The excited molecules emit light on return to the ground state. This light emitted is proportional to the number of nitrogen oxides preset in the original gas sample [Horiba 7170DEGR Users Manual].

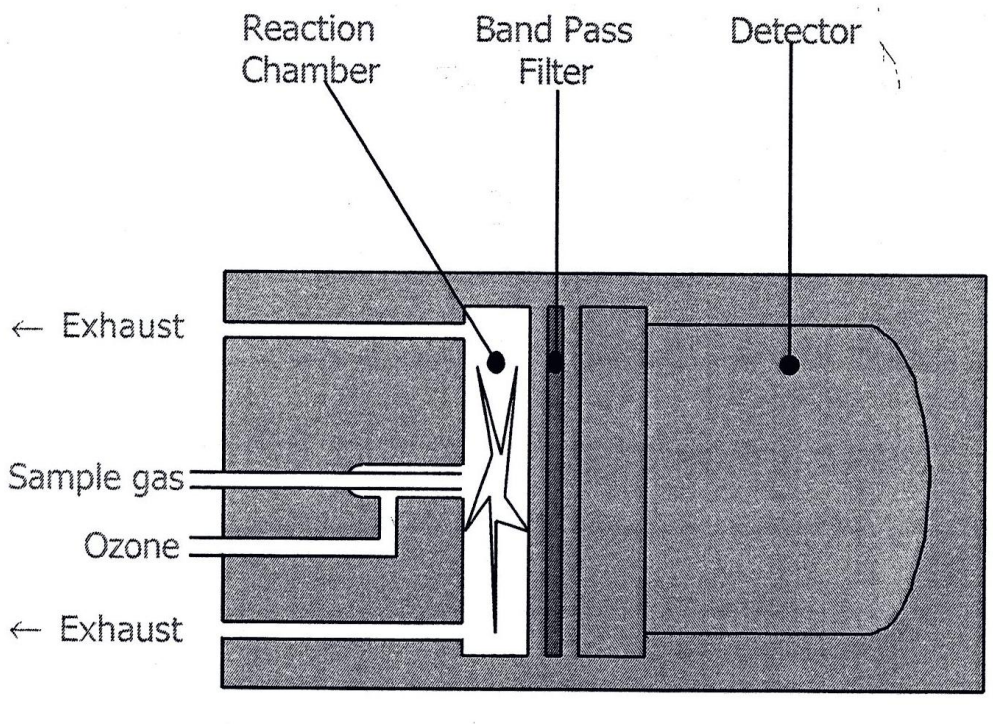

Figure 14 Chemiluminescence Detector Schematic [Horiba 7170DEGR Users Manual]

3.6.1.4 THC Measurements

The FIA-720 module of the Horiba analyser uses Flame Ionisation Detection (FID) to measure the concentration of Total Unburnt Hydrocarbons (THC). When hydrocarbons are introduced to a hydrogen flame, the number of ions produced is proportional to the number of carbon atoms. This in effect gives the THC as an equivalent number of methane ions. An example of a FID set up is given in Figure 15 [Horiba 7170DEGR Users Manual].

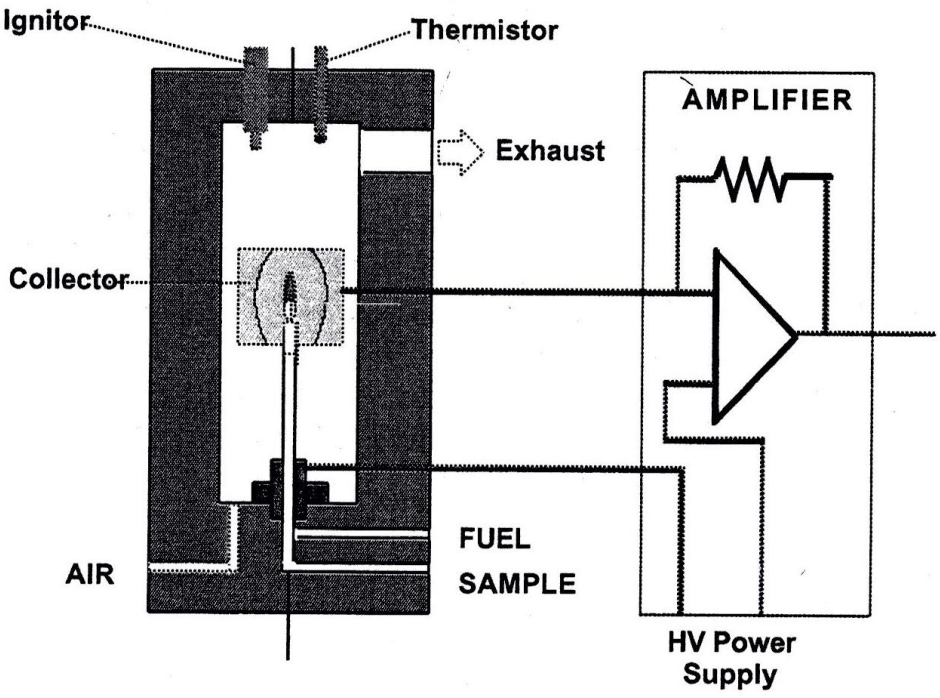

Figure 15 Flame Ionisation Detector Schematic [Horiba 7170DEGR Users Manual]

3.6.2 Smoke Measurements

An AVL 415S smoke meter was used to record the filter smoke number (FSN). This smoke meter uses a photoelectric measuring head to evaluate the blackening of the filter paper caused by a known volume of exhaust gas

sample passing through. The meter automatically varies the sampling volume, or effective length, to the most appropriate for the soot concentration, making it accurate to 0.002 FSN [AVL Data Sheet]. All the measurements taken in the experimental work were the average of three samples, automatically taken and averaged by the meter. A schematic of the filter method, reproduced from the AVL data sheet for the 415S, is shown in Figure 16.

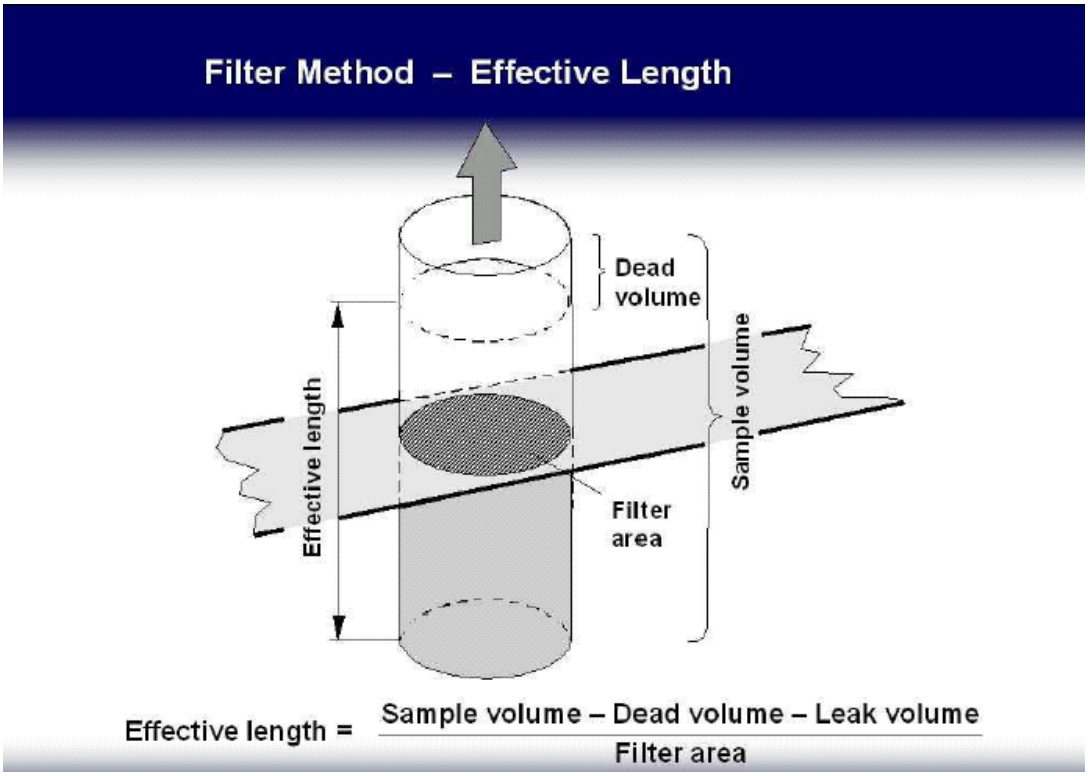

Figure 16 Filter method for the AVL 415S Smoke Meter [AVL Data Sheet]

3.7 Hydrogen Induction System

A custom hydrogen induction system was developed for the purpose of this project. A schematic of the gas feed to the engine is shown in Figure 17. A

flame arrester was fitted to ensure the safety of the laboratory and the operator. A flow meter was used to determine the volume of hydrogen gas supplied to the engine at any given time. A standard K-type thermocouple was fitted into the flow meter and was used to measure the temperature of the hydrogen. The hydrogen was supplied at room temperature and ambient pressure so as to avoid a temperature or pressure gradient between the hydrogen and the intake air as they mixed.

The hydrogen was introduced to the engine immediately below the air filter. This meant that the air and hydrogen were sufficiently mixed prior to entering the inlet manifold, and therefore eliminated any discrepancies between the supplies to each cylinder. This is important for the stable running of the engine.

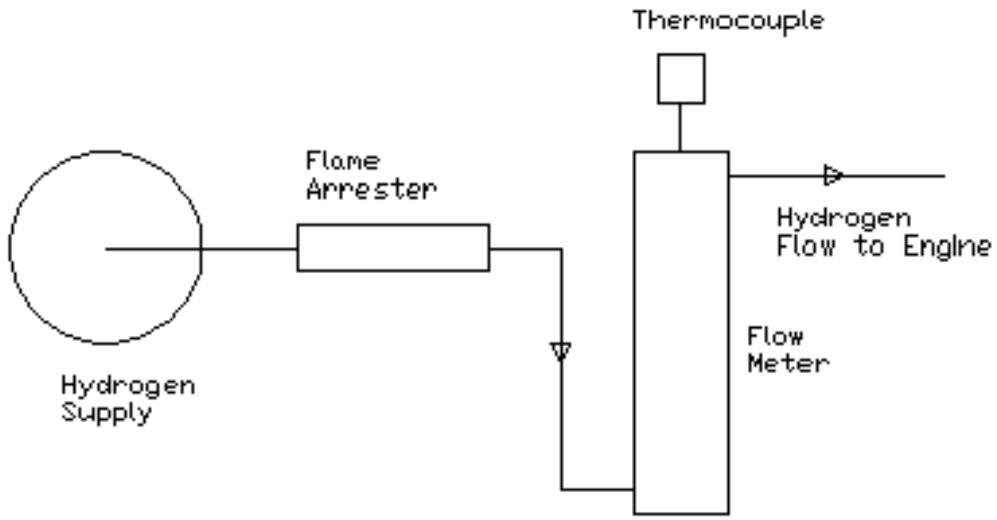

Figure 17 Hydrogen feed to the induction system

Hydrogen was introduced to the engine was measured as a percentage of the air intake volume.

3.8 MOUDI Set-up

In order to measure the particulate matter size distribution a MSP 110 rotating nano-Micro-Orifice Uniform Deposit Impactor (nano-MOUDI) was used. The nano-MOUDI separates the particulate matter (PM) into progressively smaller cut sizes based on the apparent aerodynamic diameter, as listed in Table 5. This is achieved by maintaining a constant flow of 30 L/min through the MOUDI tower, and accelerating the PM through the nozzle plates, shown in Figure 18. As the PM is accelerated through the nozzles, the larger particles will gain a higher momentum than the smaller ones. As the larger particles are not influenced as much as the smaller ones by the air current, they continue on a more linear path, and are impacted. The smaller particles are dragged away from the impaction plate by the air flow through the MOUDI, and down onto the next stage. The size of the nozzles in each plate is smaller than the one above, and therefore a smaller cut size achieves the required momentum through the acceleration to be impacted on the collecting substrate.

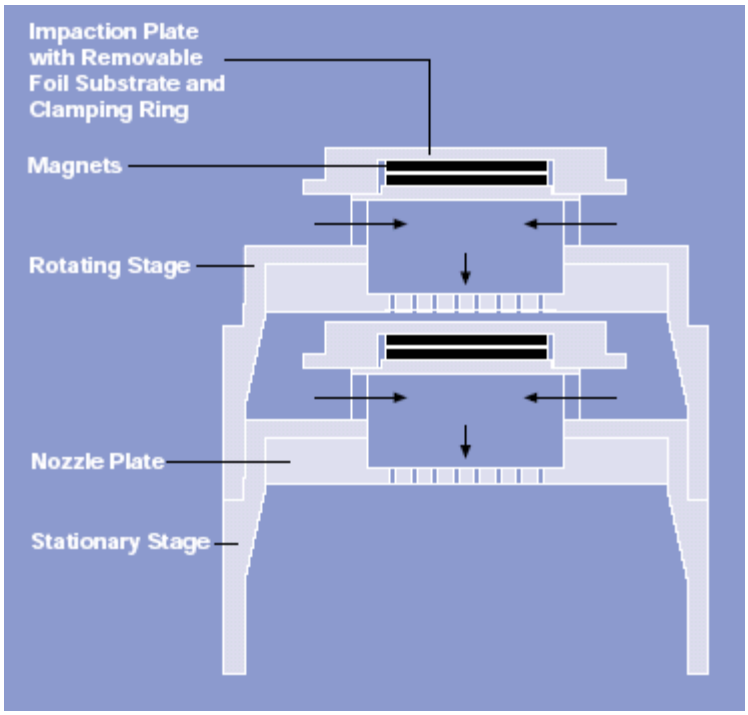

Figure 18 Components of the MOUDI stages [MOUDI (1999)]

The nano-MOUDI does not rotate, and a lower flow rate of 10L/min is used for these stages. In order to achieve the required flow rate through the instrument a vacuum pump is used. The pressure drop through stages 1 to 6 was measured, and maintained at a pressure drop equivalent to the 30 L/min. The nano-MOUDI has a choke to manage the flow through that part of the instrument.

MOUDI stage	Particulate Matter size / m
1	1.8×10^{-5} <
2	1.0×10^{-5} <
3	5.6×10^{-6} <
4	3.2×10^{-6} <
5	1.8×10^{-6} <
6	1.0×10^{-6} <
7	5.6×10^{-7} <
8	3.2×10^{-7} <
9	1.8×10^{-7} <
10	5.6×10^{-8} <
11	3.2×10^{-8} <
12	1.8×10^{-8} <
13	1.0×10^{-8} <

Table 5 Cut sizes for the nano-MOUDI

The PM collected by the MOUDI was analysed gravimetrically. The set of 13 collection substrates were weighed before and after impaction, making the difference in mass the collected PM. A micro balance was used to weigh each substrate in grams, correct to 5 decimal places. Each substrate was weighed at least twice, and more if the final decimal place was more than 1 digit out of agreement. This negates any discrepancies due to the air motion in the balance room.

3.9 GC-MS Set-up

The Gas Chromatography – Mass Spectrometry (GC-MS) set-up in the engines lab at Brunel University was used to analyse the chemical composition of the unburnt hydrocarbons present in the exhaust emissions. This is a highly specialist piece of equipment, more commonly used by chemists than engineers.

3.9.1 Mass Spectrometer

The mass spectrometer (MS) used was a TRIO-1, quadrupole mass analyser. The components of the mass spectrometer are the ion source, an arrangement of ion optics designed to accelerate and focus the ion beam, the quadrupole filter, control voltage supply, exit aperture, ion detector and a high-vacuum system, as shown in Figure 19. The TRIO-1 mass spectrometer is a constantly kept under a -4.0 bar vacuum. The detector is connected, via the interpretation electronics, to a PC running MassLAB. This allows the chromatogram to be interpreted in terms of the mass spectra and retention times.

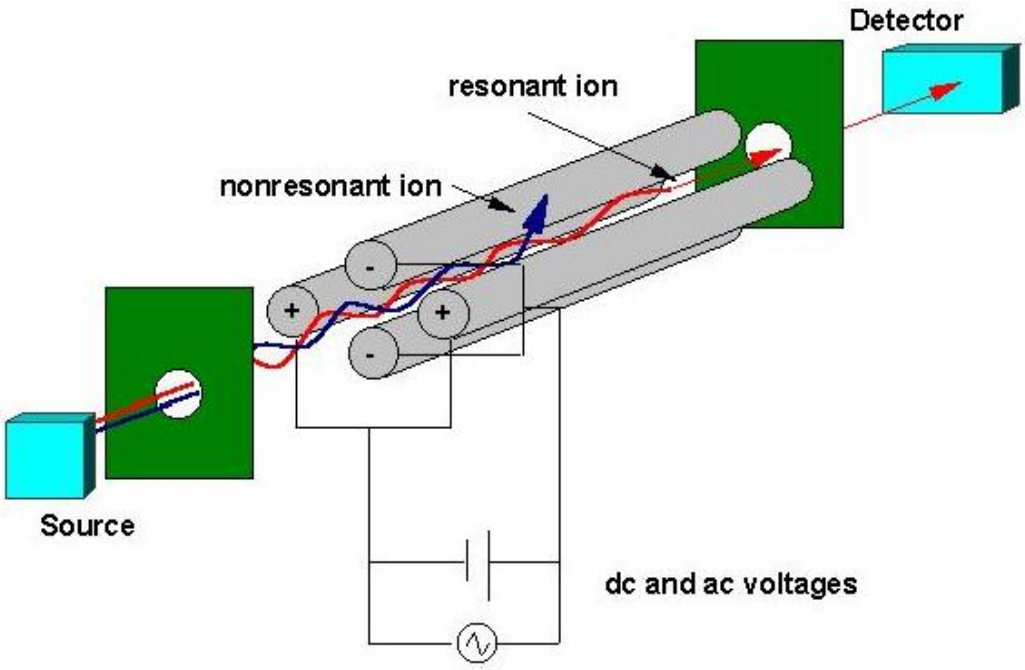

Figure 19 Schematic of a quadrupole mass spectrometer [Quadrupole Set up]

Prior to testing, the mass spectrometer must be tuned. The ion optics, which consists of a series of 4 electric fields, is electronically controlled within MassLAB, and must be focused. The detector must also be tuned to

the range of ions expected. If care is not taken with this process, the resulting chromatograms will not be reliable.

The quadrupole filter separates the ions according to the mass-to-charge ratio (m/z). The four parallel rods are connected electrically in opposing pairs. A shifting radio frequency current is applied to one pair of rods, and a direct current voltage is superimposed on all the rods. The selected ion m/z which will reach the detector is set by the ratio of the radio frequency voltage to the DC voltage. All other ion m/z ratios will have an unstable trajectory, and will collide with the rods. The quadrupole filter can be set up to look for a specific ion, or can scan through a range of m/z ratios by varying the radio frequency voltage.

3.9.2 Gas Chromatograph

The gas chromatograph (GC) used was an HP 5890. A GC consists of an injector port, a column within an oven, and a transfer pipe to the detector, in this case the mass spectrometer discussed in the previous section. This GC has both a split/splitless inlet, for liquid samples, and a 6 port inlet, for the gas samples. Both are heated to prevent the sample condensing in the inlet and not progressing to the column and the oven. Schematics of both injectors are shown in Figure 20 and Figure 21.

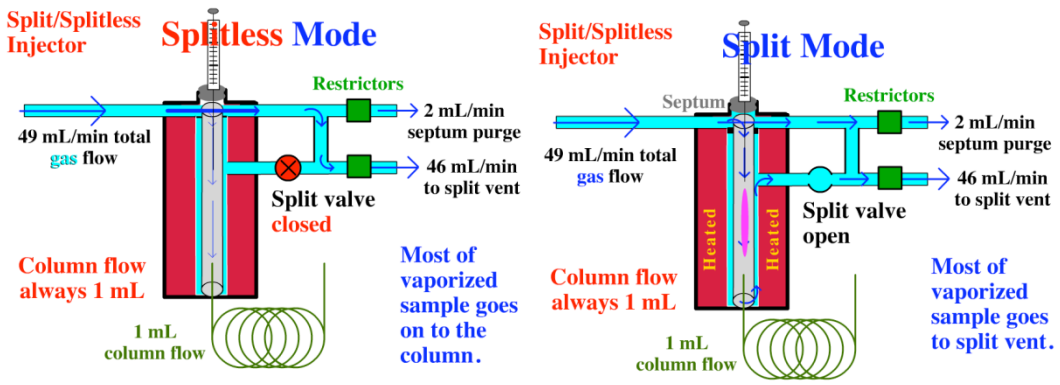

Figure 20 Schematic diagram of split and splitless injectors [Chasteen]

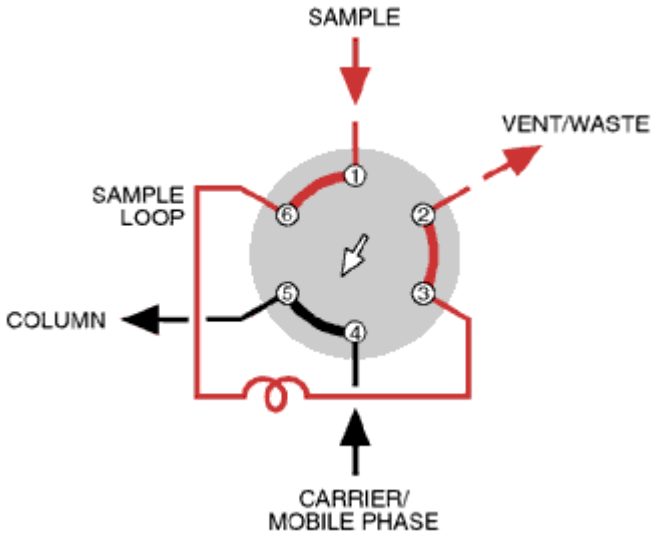

Figure 21 Schematic diagram of a 6 port injector [Sample injection with 6-port valve]

The column used was a (5%-Phenyl)-methylpolysiloxane (DB-5) stationary phase column, of 30 m length, 0.25 mm internal diameter and a 0.25 µm film thickness. The mobile phase, or carrier gas, used was helium. This is a multipurpose column, which can effectively separate a wide range of molecular masses. This is important for use with exhaust gas where some of the hydrocarbons present will be unburnt diesel fuel, as well as the products of incomplete combustion.

The oven temperature program is very important to the separation of the compounds. If the temperature is ramped up too quickly the peaks will merge, and the compounds cannot be identified. However, if the temperature ramp is too slow the elution times increase significantly, increasing the cost of the procedure. This means careful set up of the temperature program is required.

3.10 Summary

In this chapter a description is given of the various pieces of equipment used through this project. Further details, where required, will be given in later chapters.

CHAPTER 4

COMBUSTION PROPERTIES OF DIESEL AND DIESEL/HYDROGEN COMBUSTION

4 CHAPTER 4 COMBUSTION PROPERTIES OF DIESEL AND DIESEL/HYDROGEN COMBUSTION

4.1 Introduction

Individual cylinder pressure based feedback control is an ideal method to optimise engine operation. In-cylinder pressure is a fundamental combustion variable, which can be used to characterise the combustion process for each combustion event. Optimal engine control can be maintained by monitoring the pressure in each cylinder and using this information for feedback control in order to minimise the exhaust gas emissions. The availability of low cost and robust pressure sensors, such as the glow plug installed pressure sensor (GPPS) developed by Siemens, is expected to lead to the wide adoption of cylinder-pressure-based engine control for both gasoline and diesel engines.

In order to identify the most effective parameters to use when controlling combustion based on cylinder pressure information, a series of experiments were carried out with varying injection timings and EGR levels. This chapter presents the results obtained and discusses the potential key parameters that may be used for closed loop control using an in-cylinder pressure transducer.

This chapter will also look at the combustion properties for combined hydrogen/diesel combustion. It was necessary prior to the start of the experimental work to find an appropriate running point for the engine in purely diesel mode to act as a base point. Once this point was found, an experimental test matrix for the combined EGR and hydrogen investigation was set up.

4.2 Injection Timing and EGR Experimental Test Matrix

The injection strategy for this part of the investigation was a single injection at 1200 bar, maintained via the high-pressure common rail, at injection timings varying from 14 CAD BTDC and 0 CAD BTDC. The EGR level was varied, in 5% steps, from 0% and 40%.

A set operating point of 1500 rpm and 2.7 bar BMEP was used. The exhaust gas emissions were all measured as described in the previous chapter. This information was then used to plot correlations between the in-cylinder pressure and the related combustion properties and the resultant exhaust gas emissions.

4.3 Results and Discussion for the Injection Timing Investigation

The results are obtained for a range of EGR and fuel injection timings.

4.3.1 Combustion Parameters

The followings are a summary of results obtained.

Figure 22 shows that with increasing levels of EGR the 50 % MFB point is delayed. It can also be seen that higher levels of EGR have more of an effect than lower levels as the lines diverge with increasing EGR. This effect becomes more pronounced as the injection timing is retarded.

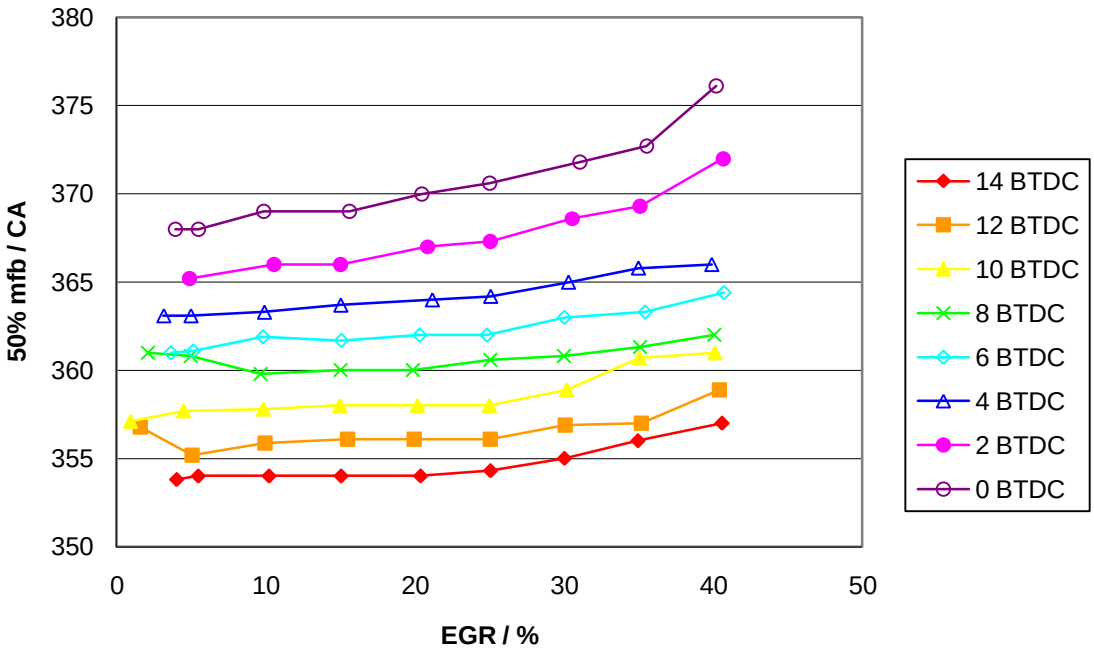

Figure 22 Correlation between 50 % mass fraction burnt, EGR and injection timing

From Figure 23 it can be seen that as the EGR level is increased, the maximum in-cylinder pressure decreases. This is a known effect of EGR addition. The maximum pressure decreases as the injection timing is retarded. As the injection timing is retarded the effect of EGR addition becomes more pronounced.

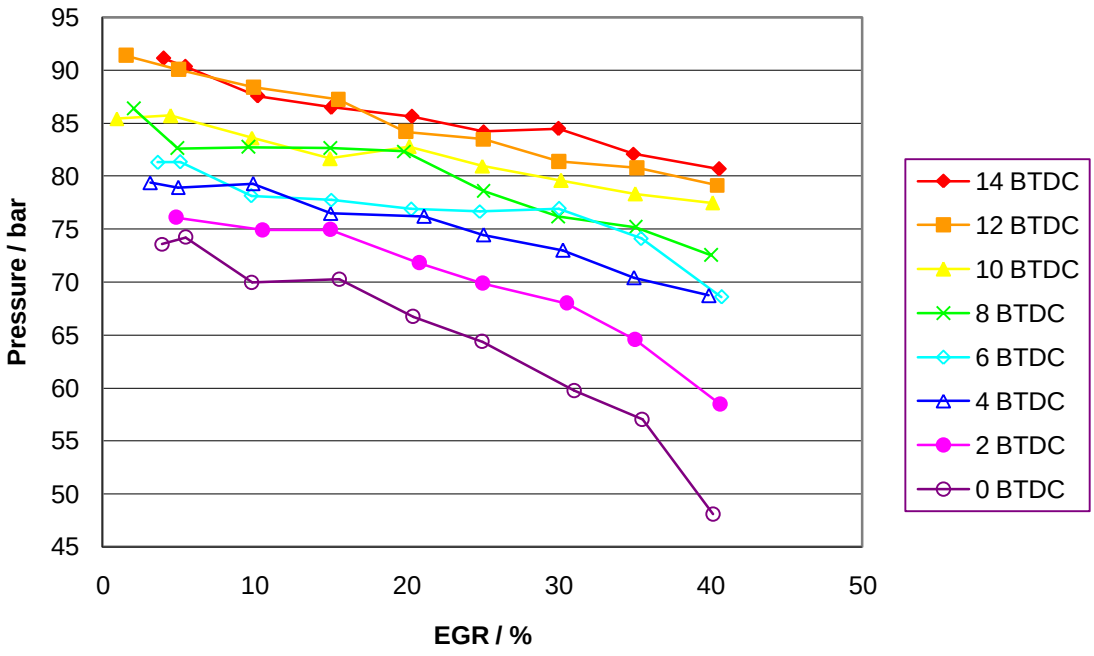

Figure 23 Correlation between maximum pressure, EGR and injection timing

From Figure 24 it can be seen that increasing the EGR level delays the position of the maximum in-cylinder pressure. The position of the maximum pressure is also delayed as the injection timing is retarded. As the injection timing is retarded, the effect of the EGR is increased.

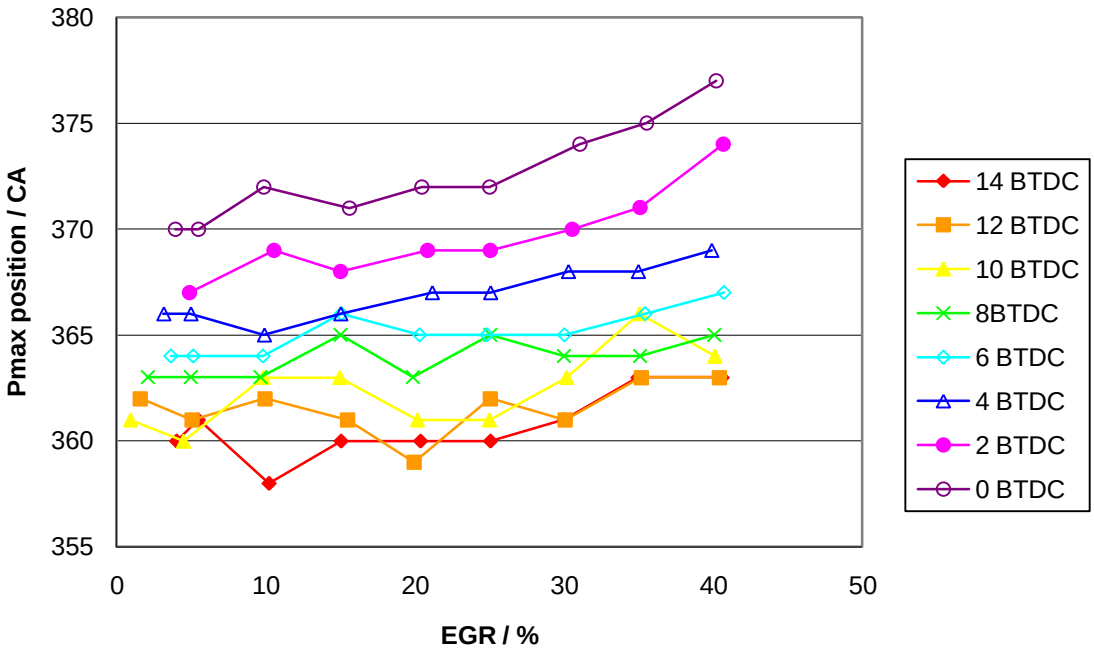

Figure 24 Correlation between the position of the maximum pressure, EGR and injection timing

From Figure 25 it can be seen that with increasing levels of EGR, the maximum pressure rise rate decreases. As the injection timing is retarded, the pressure rise rate decreases. The effects of EGR appear to be greater with retarded injection. The results of different injection timings are not well separated. Hence, this is not a particularly reliable parameter.

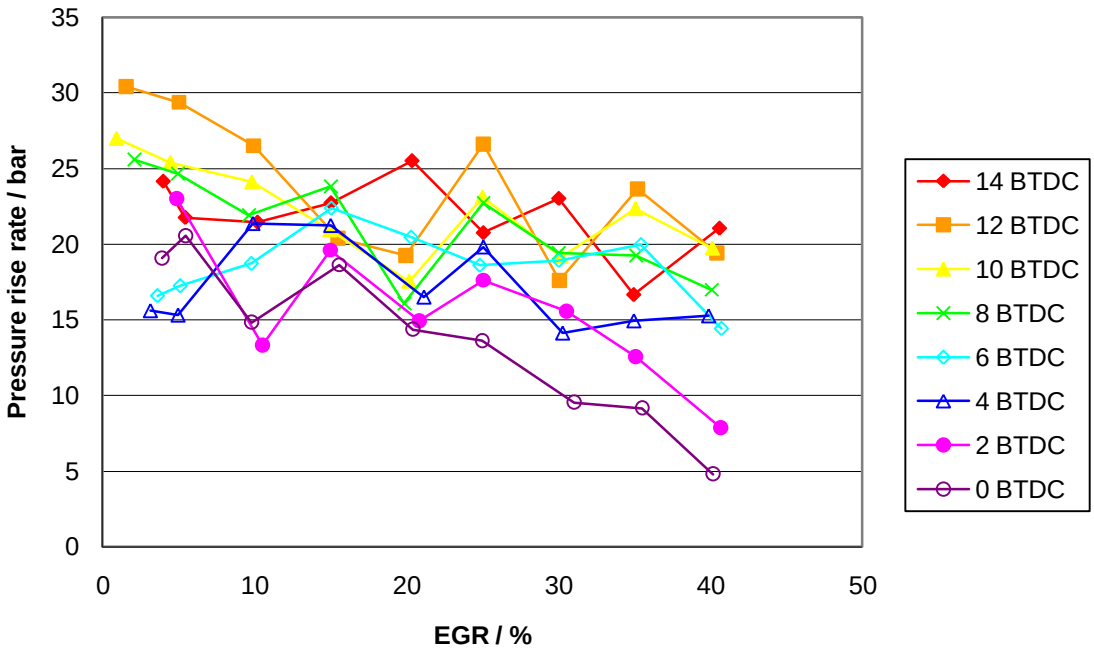

Figure 25 Correlation between the maximum pressure rise rate, EGR and injection timing

Figure 26 shows that the position of the maximum pressure rise rate is delayed with increased levels of EGR. It can also be seen that as the levels of EGR increases, the delay is also increased. As the injection timing is retarded, the position of the maximum pressure rise rate is delayed. This is all due to the increased ignition delay.

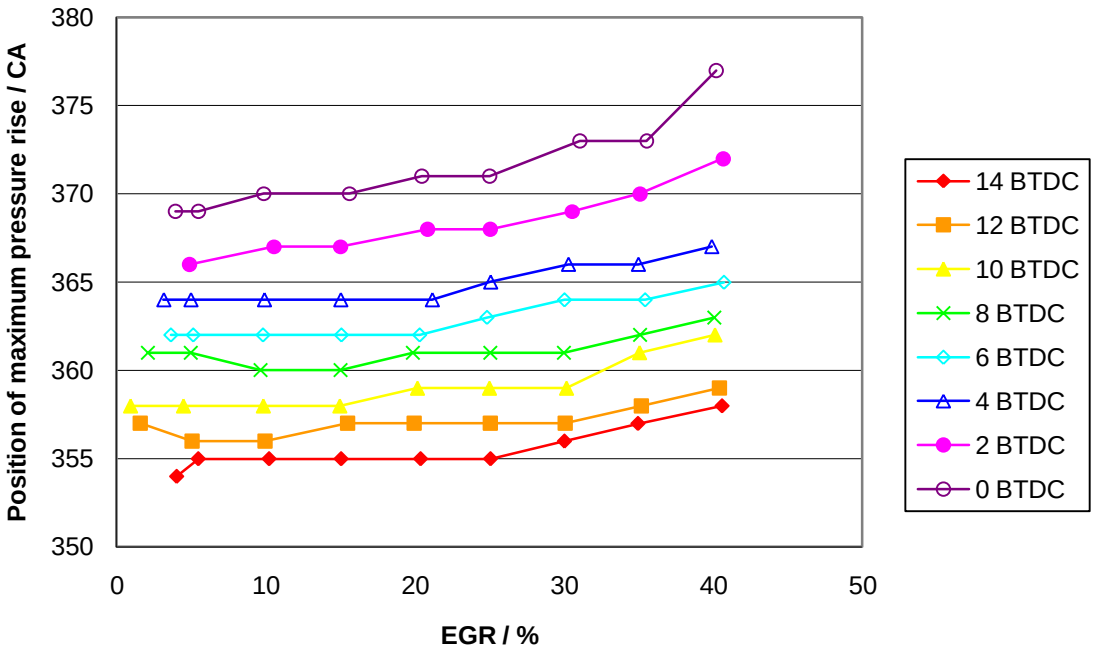

Figure 26 Correlation between the position of the maximum pressure rise rate, EGR and injection timing

Figure 27 shows that the motoring pressure at 20 crank angle degrees before TDC decreases as the level of EGR increases, as was the case for the maximum in-cylinder pressure. The motoring pressure decreases as the injection timing is retarded. This is a parameter which needs further investigation before it could be recommended for a closed loop control system.

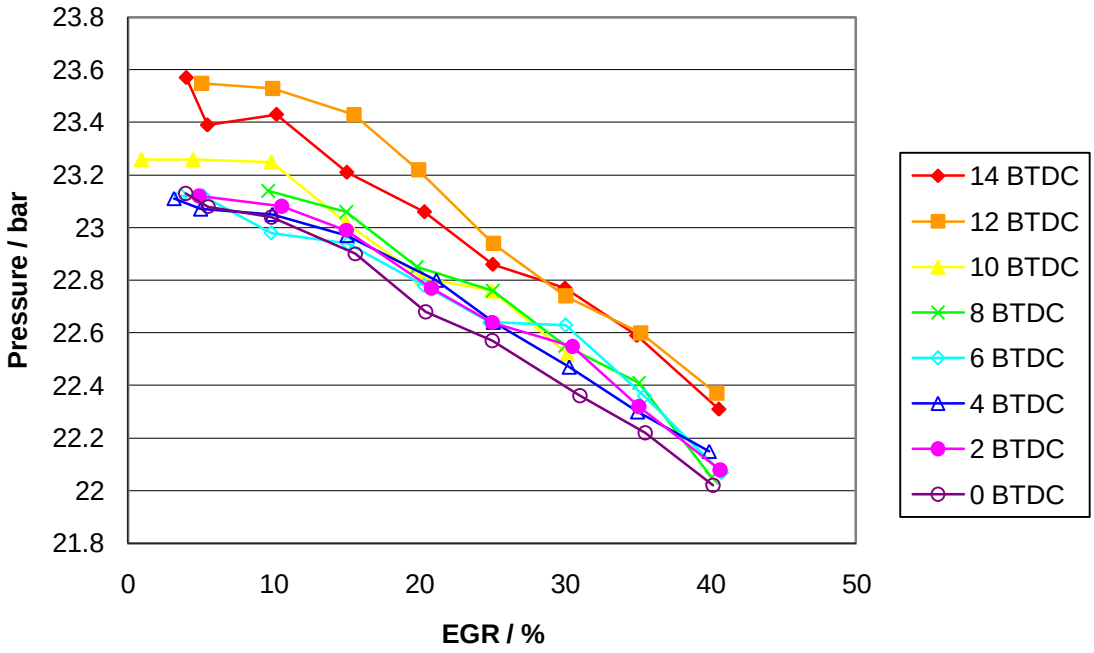

Figure 27 Correlation between the pressure at 20 degrees before TDC, EGR and injection timing

4.3.2 Emissions

From Figure 28 it can be seen that increasing EGR decreases the emission of nitrogen oxides (NO_X). Retarding the injection timing also decreases the emission of NO_X. At earlier injection timings, the effect of EGR is more pronounced, as can be seen from the converging lines in Figure 28.

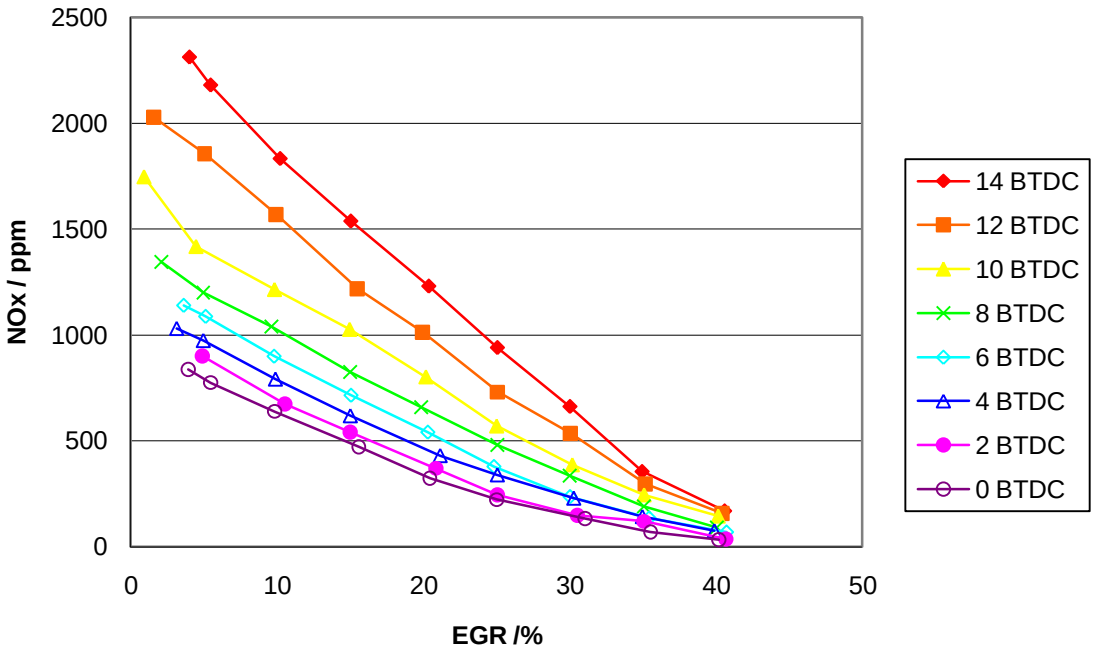

Figure 28 Correlation between Nitrogen Oxides emissions, EGR and injection timing

Figure 29 clearly shows that retarding the injection timing increases the total unburnt hydrocarbons (THC). As is known, increasing EGR level also increases the total unburnt hydrocarbons. The combined effect of retarded injection and high levels of EGR means a significant increase in the total unburnt hydrocarbons. This makes it necessary to optimise the injection strategy to minimise the THC emissions.

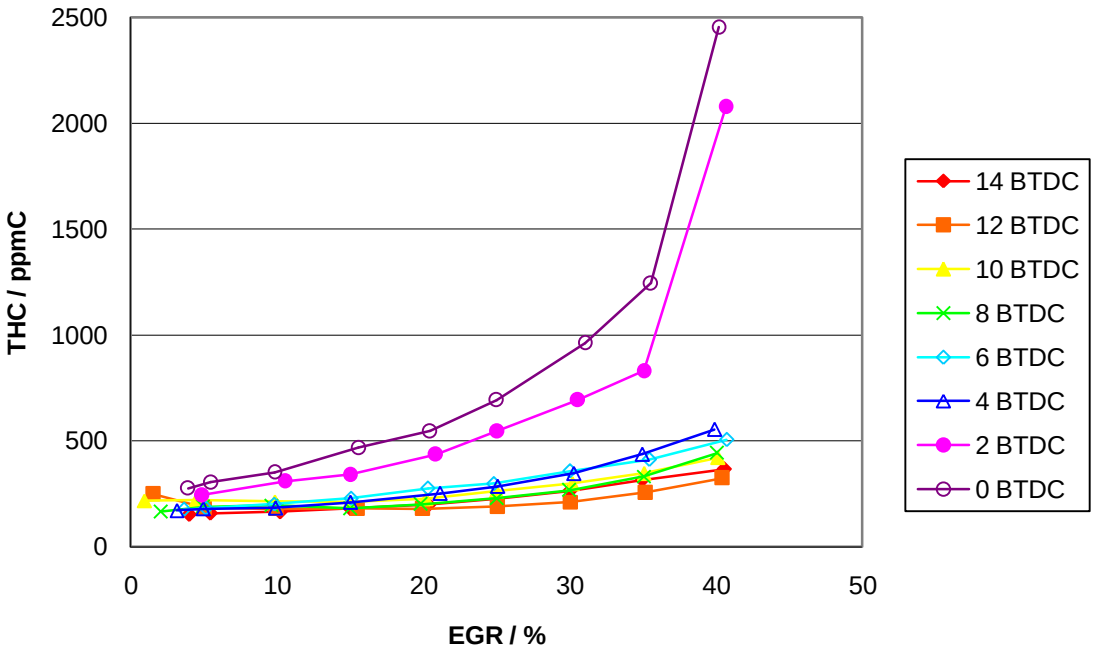

Figure 29 Correlation between total unburnt hydrocarbons, EGR and injection timing

Although not quite so clear, Figure 30 shows that increasing the EGR by a small percentage does not have much of an effect on the smoke number. With more than approximately 20% EGR, increasing the EGR significantly increases the smoke number. Broadly, retarded injection timing increases smoke number after the 20% EGR level.

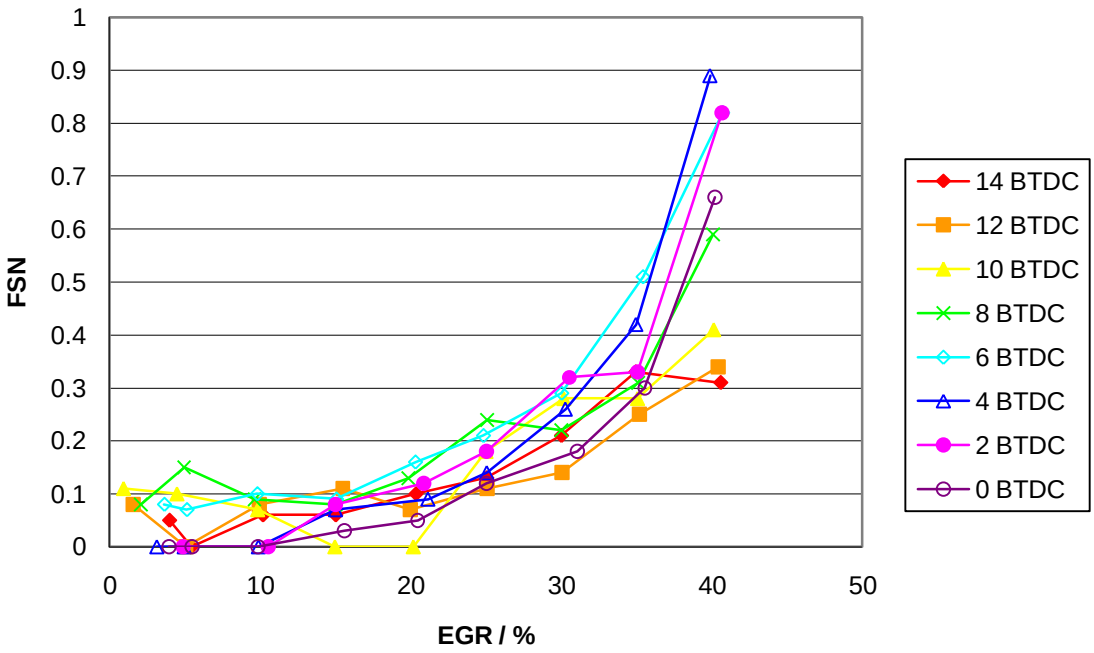

Figure 30 Correlation between the smoke number, EGR and injection timing

In can be seen from Figure 31 that increasing EGR levels increases the emissions of carbon monoxide (CO). It can also be seen that retarding the injection timing increases the emission of carbon monoxide. The effect of EGR increases both with retarded injection timing and increasing EGR levels.

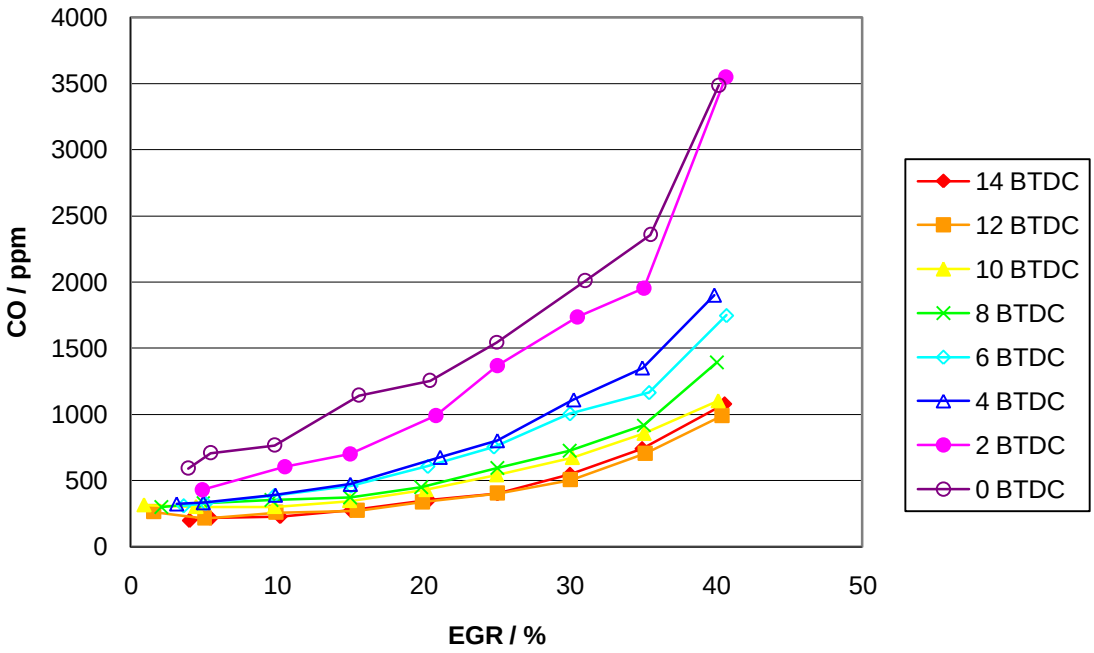

Figure 31 Correlation between carbon monoxide, EGR and injection timing

Figure 32 shows that the specific fuel consumption decreases with EGR. The specific fuel consumption also decreases with retarded injection timing. Figure 32 also shows that this parameter is variable, and not appropriate for use as a closed loop control.

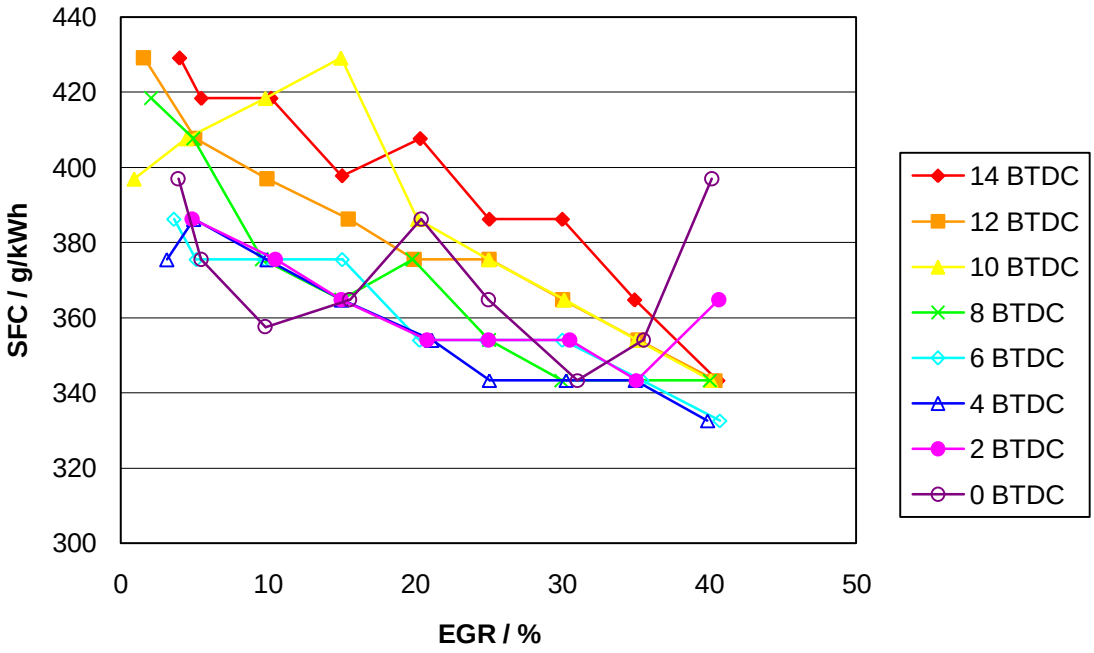

Figure 32 Correlation between the brake specific fuel consumption, EGR and injection timing

4.3.3 Correlation between Parameters

In Figure 33

- EGR increases towards the bottom of the graph
- Injection timing is retarded from left to right

Figure 33 shows that the position of the 50% MFB is retarded as nitrogen oxides are decreased.

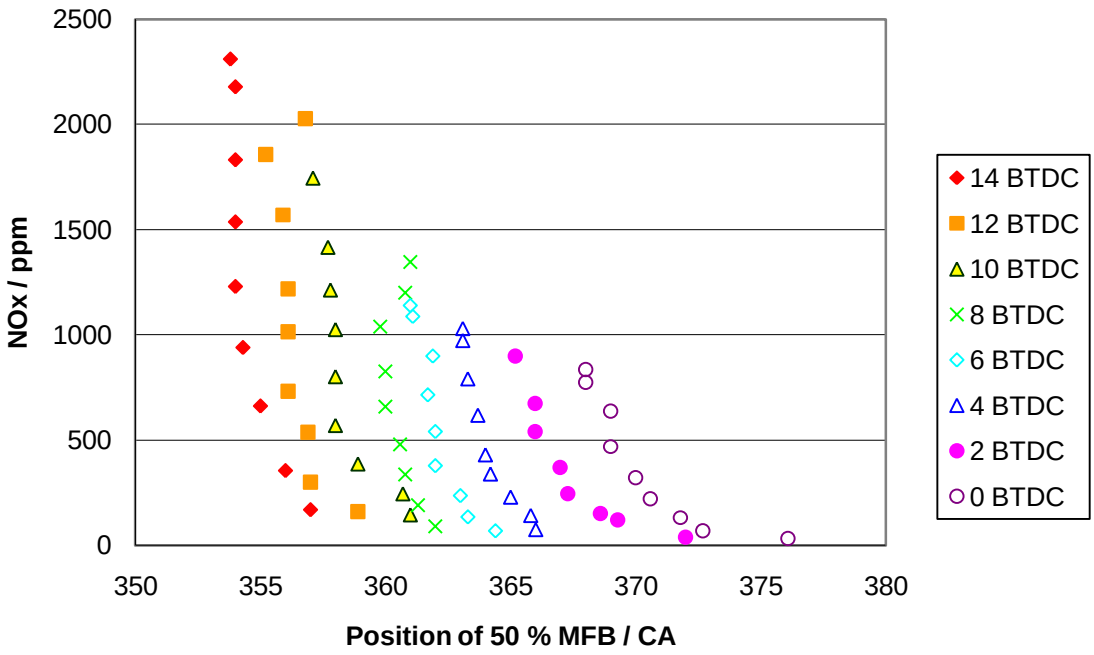

Figure 33 Correlation between the position of 50% MFB, nitrogen oxides, EGR and injection timing

Unlike in the previous figure, in Figure 34 EGR increases towards the top of the graph. The injection timing is still retarded from left to right.

From Figure 34 it can be seen that as the 50% MFB position is delayed the total unburnt hydrocarbons increases. This is the usual diesel trade of off: as NO_X is decreased, THC increases.

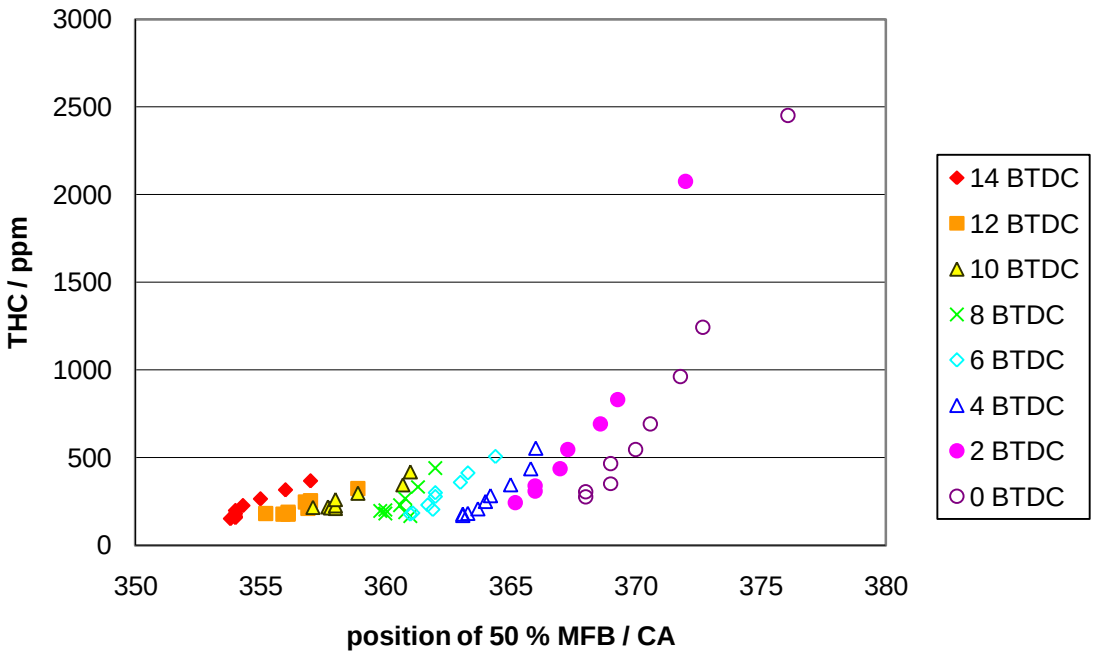

Figure 34 Correlation between total unburnt hydrocarbons, the position of 50% MFB, EGR and injection timing

Similar to Figure 34, Figure 35 follows

- EGR increases towards the top of the graph.
- Injection timing is retarded from left to right.

As was the case for the total unburnt hydrocarbons, as the 50% MFB position is delayed, the filter smoke number is increased, as shown in Figure 35. This directly follows the THC emissions, which contributes to the smoke number, and is a direct result of the higher incomplete combustion.

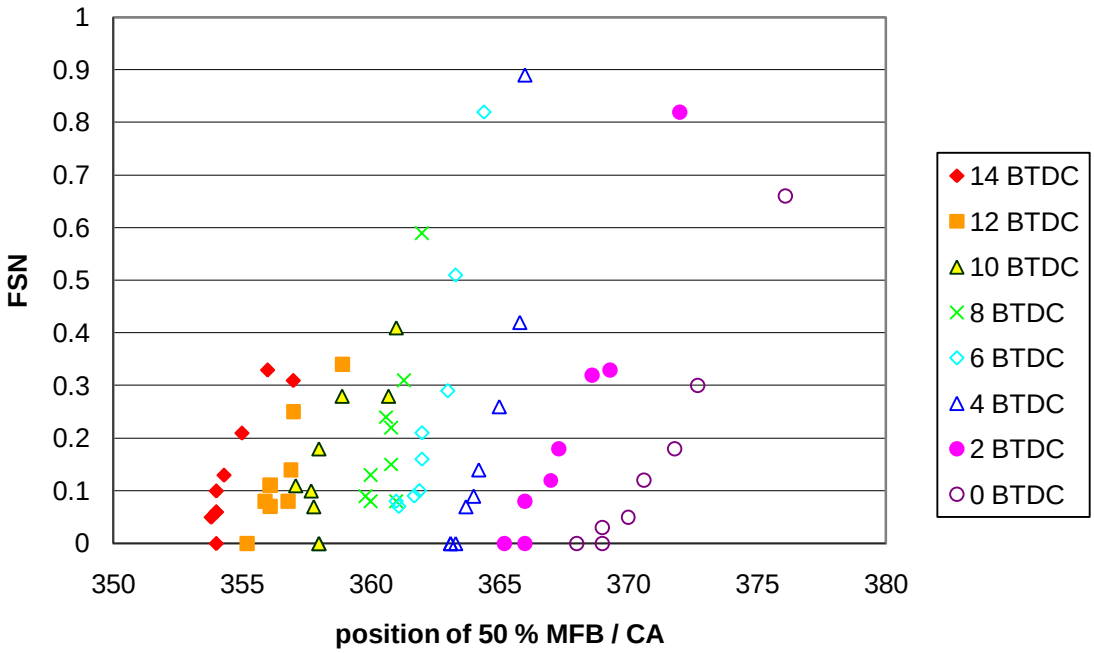

Figure 35 Correlation between the position of 50% MFB, smoke number, EGR and injection timing

As with the previous two figures, with Figure 36

- EGR increases towards the top of the graph
- Injection timing is retarded from left to right.

It follows that as the 50% MFB position is delayed, and therefore the ignition delay, there is less time for the combustion event to occur. This means that incomplete combustion was increased, resulting in higher carbon monoxide emissions, as can be seen in Figure 36.

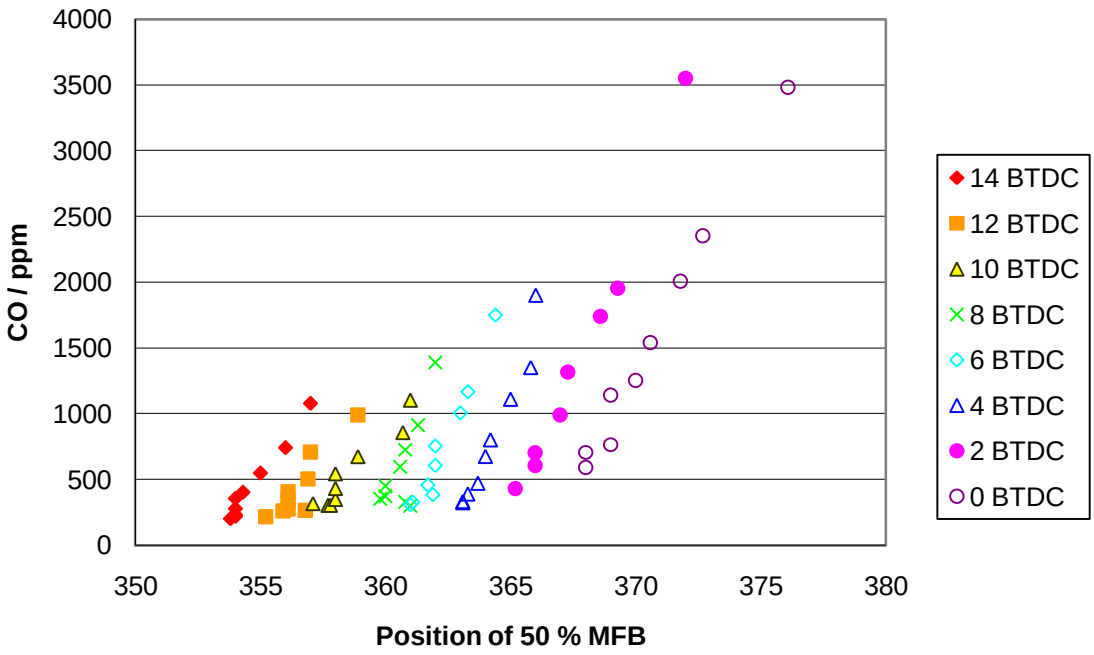

Figure 36 Correlation between the position of 50% MFB, carbon monoxide, EGR and injection timing

For Figure 37

- EGR increases towards the bottom of the graph
- Injection timing is retarded from left to right.

As the position of the 50% MFB is delayed, the specific fuel consumption increases, as is shown in Figure 37. The increase in incomplete combustion means lower fuel efficiency, and therefore higher fuel consumption.

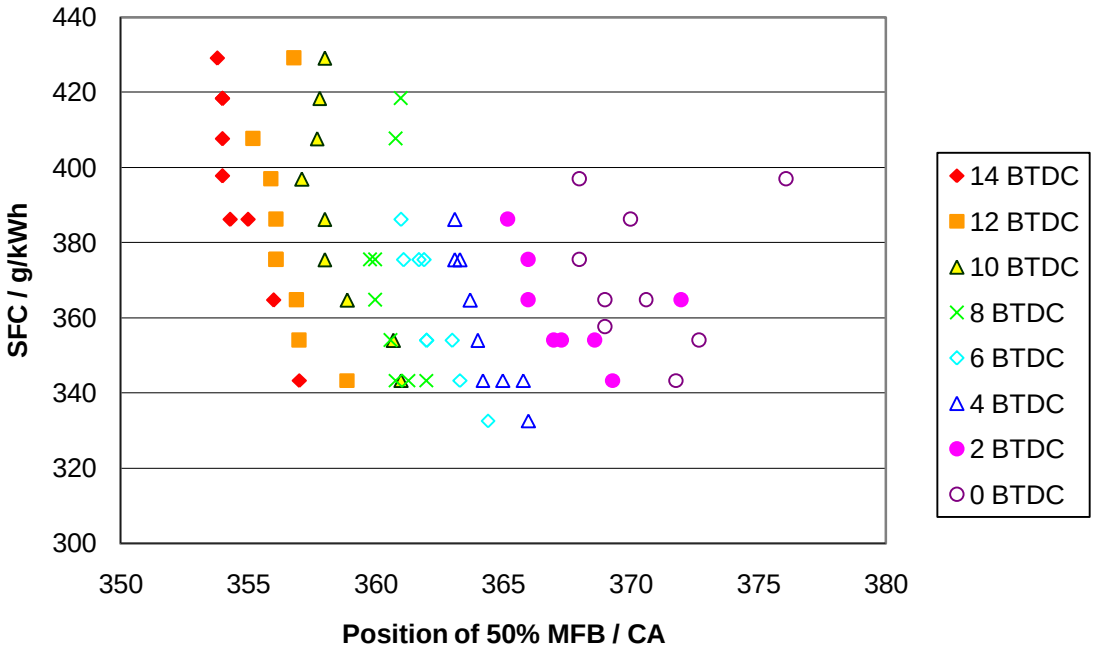

Figure 37 Correlation between the position of 50% MFB, the specific fuel consumption, EGR and injection timing

For Figure 38

- EGR increases from the top to the bottom of the graph.
- Injection timing is retarded from left to right.

As the position of the maximum rate of pressure rise rate is retarded, the NO_X emissions decrease, as shown in Figure 38. This decrease in NO_X emissions corresponds to the in-cylinder pressure decrease brought about by the increasing EGR levels, as well as the decreased time for the combustion event, and therefore NO_X formation time.

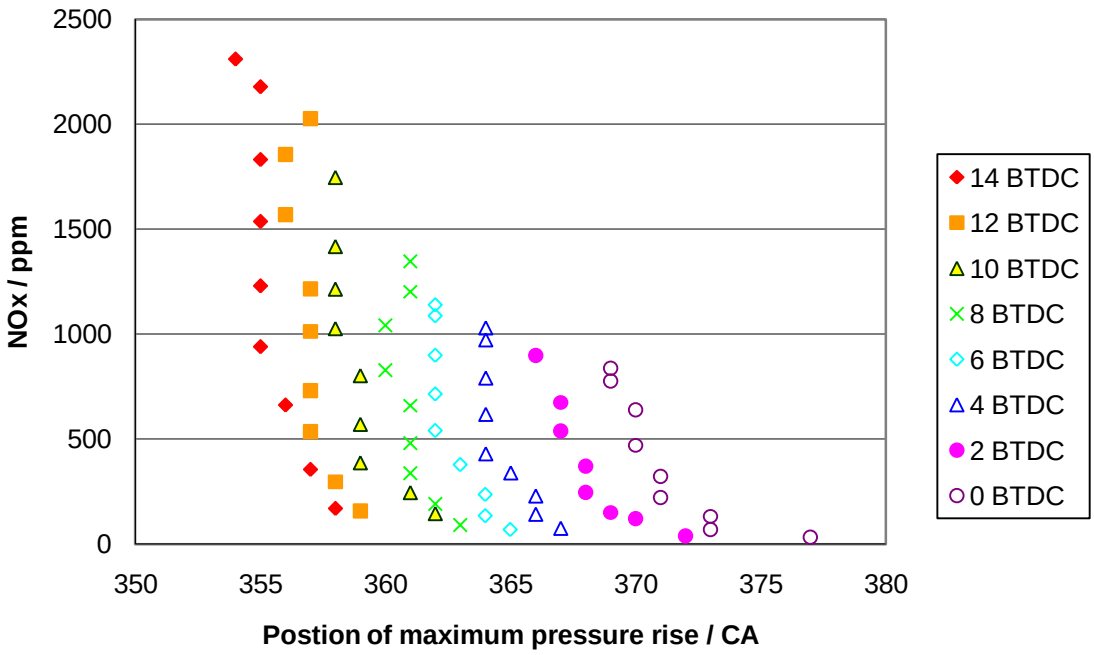

Figure 38 Correlation between the position of maximum pressure rise rate, nitrogen oxides, EGR and injection timing

For Figure 39

- EGR increases from the bottom of the graph to the top.
- Injection timing is retarded from left to right.

As could be seen in Figure 34, Figure 39 shows an increase in THC as the position of maximum in-cylinder pressure rise rate is retarded. The same mechanisms that reduce the production of NO_X – the shorter combustion duration and the decrease in in-cylinder pressure – mean an increase in incomplete combustion.

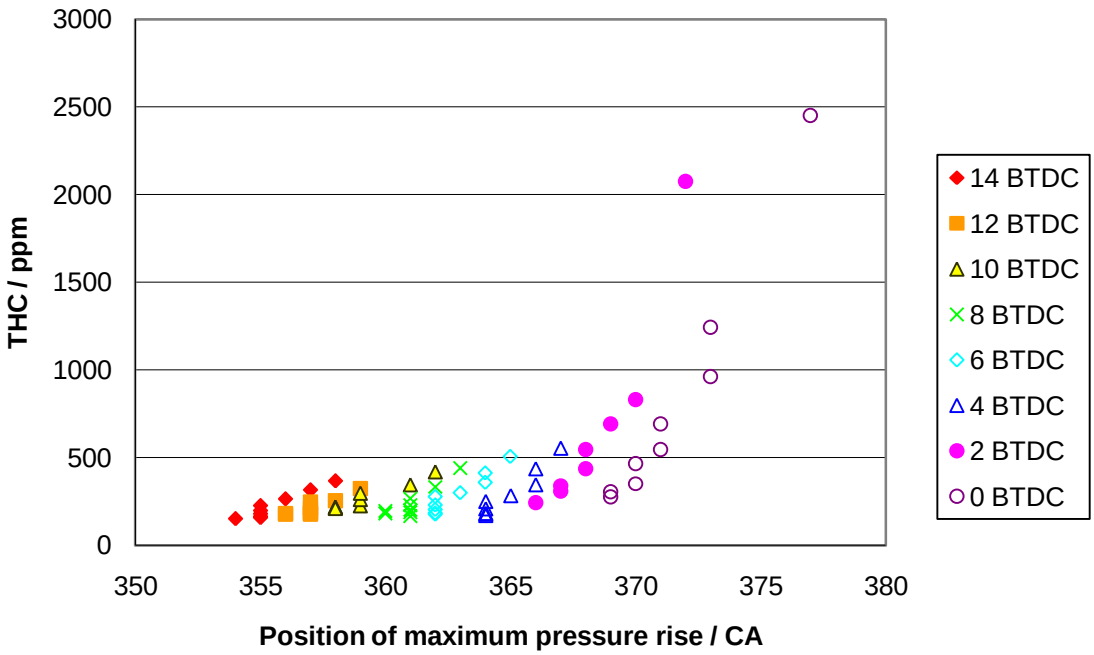

Figure 39 Correlation between the position of the maximum pressure rise rate, total unburnt hydrocarbons, EGR and injection timing

For Figure 40

- EGR increases from the bottom of the graph towards the top
- Injection timing is retarded from left to right.

As is the case for the THC, Figure 40 shows the corresponding increase in filter smoke number as the position of the maximum in-cylinder pressure rise rate is retarded. This increase is due to the increase in incomplete combustion, producing more soot particulates.

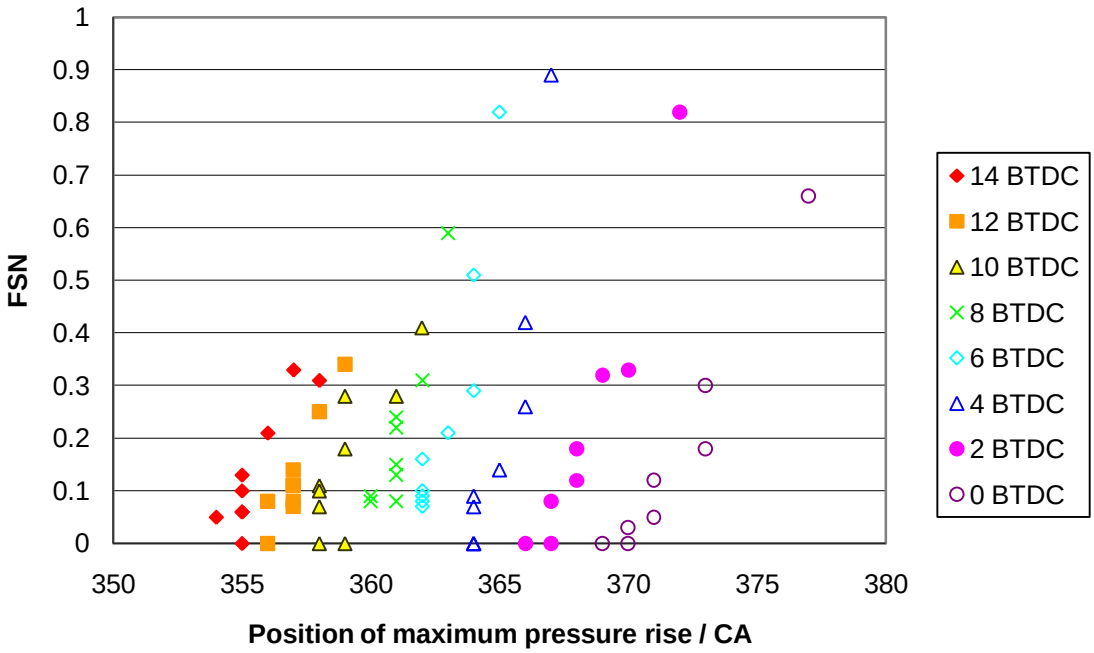

Figure 40 Correlation between the position of the maximum pressure rise rate, the smoke number, EGR and injection timing

For Figure 41

- EGR increases from the bottom of the graph towards the top.
- Injection timing is retarded from left to right.

Following on from both the THC and FSN, the emissions of carbon monoxide, which are also a by-product of incomplete combustion, increase with the retardation of the position of the maximum in-cylinder pressure rise rate. This is shown in Figure 41.

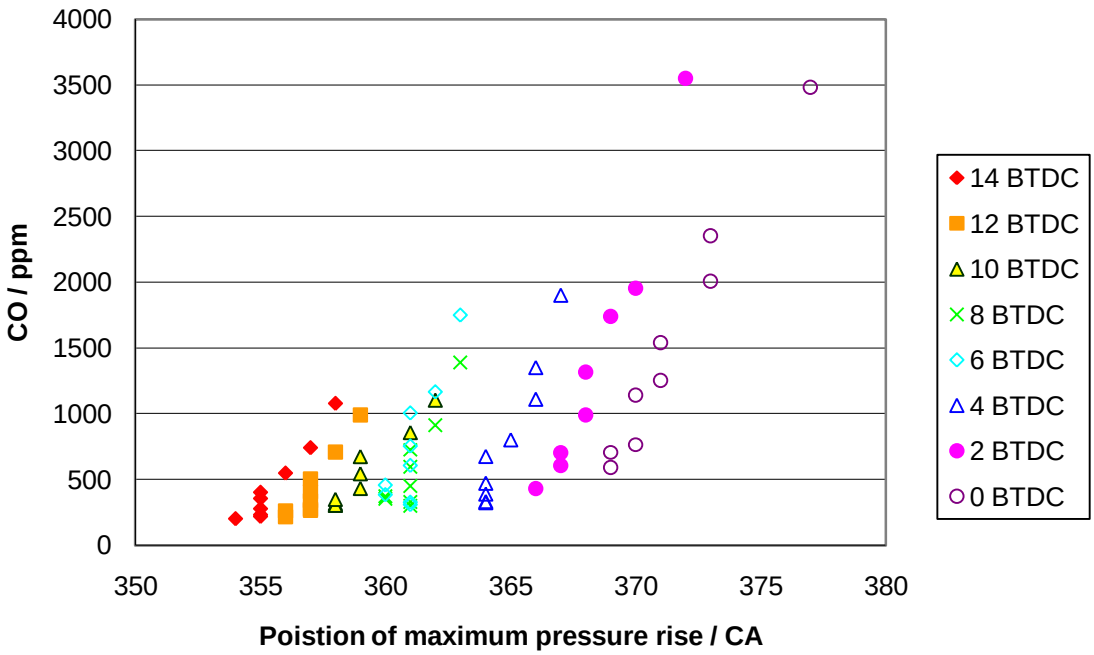

Figure 41 Correlation between the position of maximum pressure rise rate, carbon monoxide, EGR and injection timing

For Figure 42

- EGR increases from the top of the graph down to the bottom.
- Injection timing is retarded from left to right.

Incomplete combustion means that more fuel is wasted, reducing the thermal efficiency, and increasing the specific fuel consumption. Figure 42 shows the increase in SFC as the position of maximum in-cylinder pressure rise rate is retarded, due to the increase in incomplete combustion. This graph does show some scattering of the points, much more than is seen in the 50% MFB correlation graph, particularly at high EGR levels.

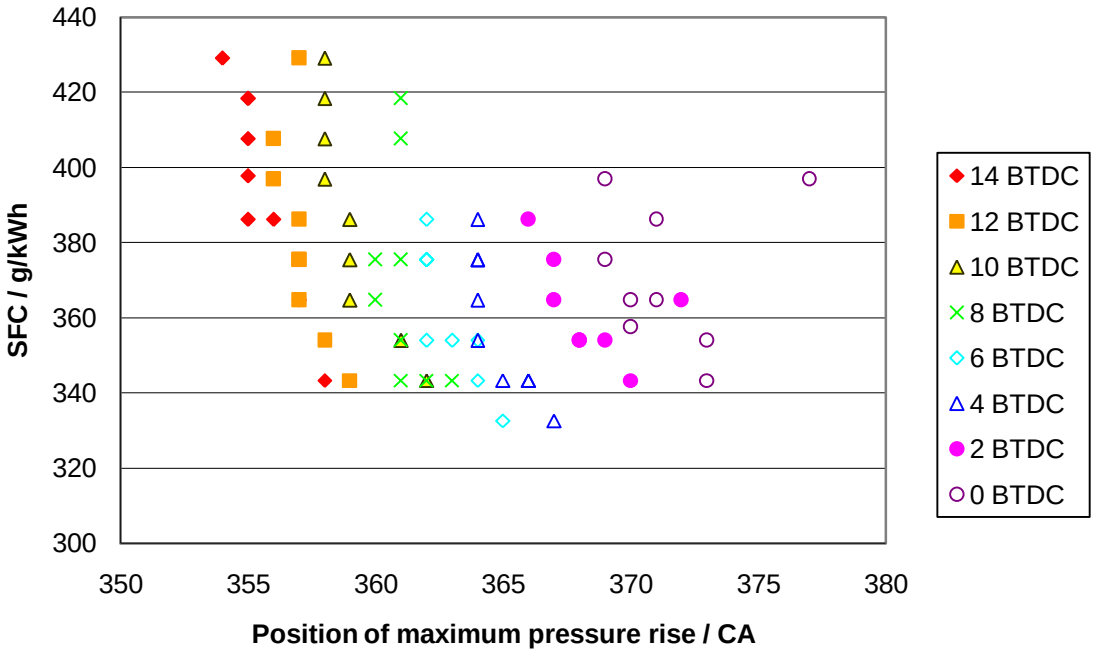

Figure 42 Correlation between the position of the maximum pressure rise rate, the specific fuel consumption, EGR and injection timing

4.4 Injection Timing and Pressure Investigation

In order to find an appropriate base point for the hydrogen experiments, an investigation of injection pressures and timings for a single diesel injection strategy was conducted. Injection pressures were varied from 400 to 1400 bar. The injection timing was varied between 0 and 14 Crank Angle Degrees Before Top Dead Centre (CAD BTDC).

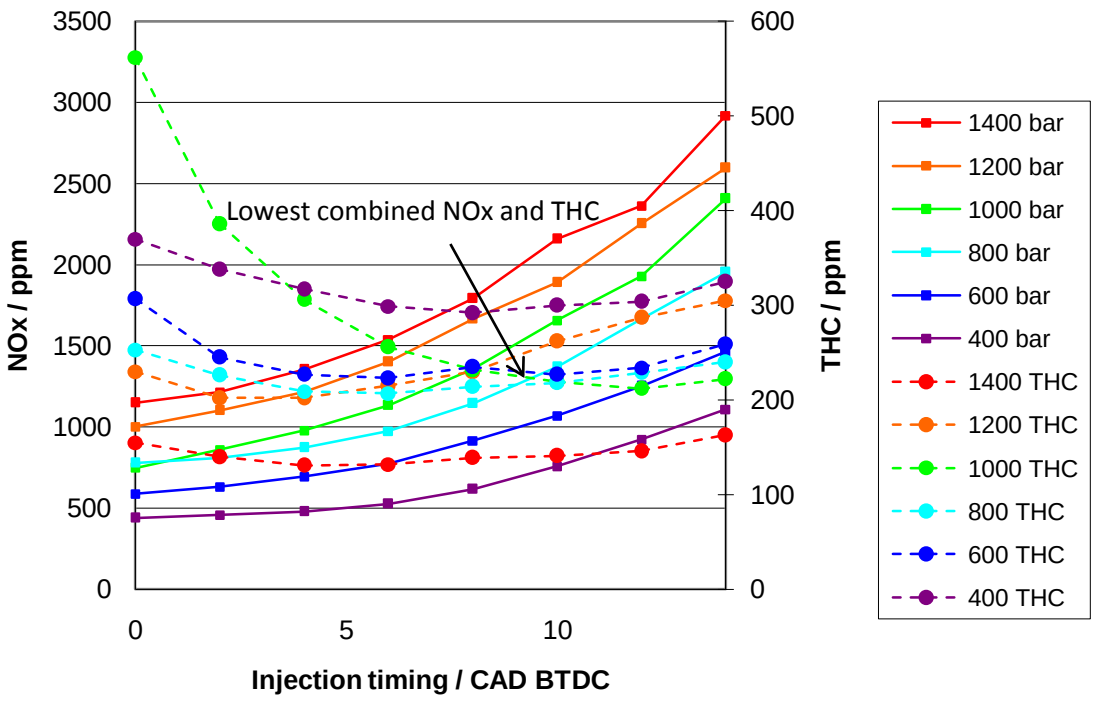

Figure 43 Lowest combined NO_X and THC over various injection pressures and timings

As can be seen from Figure 43, NO_X emissions increase as the injection timing is advanced, and as the injection pressure is increased. This is to be expected, as NO_X emissions increase with temperature and with lower flame speeds. Earlier injection timings allows for a higher portion of the diesel fuel to be burnt during the premixed phase of combustion. This leads to higher rates of in-cylinder pressure rise, higher maximum in-cylinder pressures, and therefore higher temperatures.

Conversely, the total unburnt hydrocarbons decrease as the injection timing is retarded and there is more time to allow for complete combustion. As the injection pressure is increased, the fuel atomises better, allowing for better fuel air mixing and therefore more complete combustion. This trade off is typical of diesel combustion.

This being the case, it was necessary to find the compromise point where the NO_X and THC were each as low as possible. This has been highlighted in Figure 43, making the base point for the hydrogen and EGR investigation 800 bar injection pressure and 9 CAD BTDC.

4.5 Hydrogen and EGR Experimental test matrix

In order to investigate the effects of combined hydrogen/diesel combustion with EGR addition, various levels of EGR and hydrogen addition were used. The EGR levels were varied between 0% and 40%, where the engine was capable of running this level, in 5% steps.

Hydrogen was supplied as shown in the previous chapter, and the levels were varied between 0 and 10% of the volume of the inlet charge, in 2% vol. steps. In the case of running both hydrogen and EGR, the hydrogen always replaced air.

Two engine speeds were run, 1500rpm and 2500rpm, and 3 engine loads. The 3 engine loads were 0 bar BMEP, 2.7 bar BMEP and 5.4 bar BMEP, referred to as no load, medium load and high load throughout this thesis.

Since not all combinations of the speeds and loads were capable of supporting the maximum levels of hydrogen and EGR, Table 6 shows the achieved levels for each operating point.

Operating Point	Hydrogen Level	0% vol.	2% vol.	4% vol.	6% vol.	8% vol.	10% vol.
1500 rpm 0 bar		40 % EGR	30% EGR	30% EGR	Not run	Not run	Not run
1500 rpm 2.7 bar		40% EGR	35% EGR	40% EGR	10% EGR	Not run	Not run
1500 rpm 5.4 bar		30% EGR	30% EGR	30% EGR	15% EGR	15% EGR	10% EGR
2500 rpm 0 bar		40% EGR	40% EGR	35% EGR	Not run	Not run	Not run
2500 rpm 2.7 bar		40% EGR	40% EGR	40% EGR	35% EGR	Not run	Not run
2500 rpm 5.4 bar		15% EGR	15% EGR	15% EGR	15% EGR	Not run	Not run

Table 6 Experimental Test Matrix

4.6 Results and Discussion for the Hydrogen Investigation

4.6.1 Pressure and Heat Release Rate

As described in the previous chapter, the in-cylinder pressure data was captured using a Kistler pressure transducer connected to a PC running LabVIEW via a charge amplifier. This in-cylinder pressure data, combined with the crank angle data captured simultaneously from the shaft encoder, was used to analyse the combustion process. The data capture was averaged over 20 cycles. The heat release rate was calculated using Equation 3.

$$HRR = \frac{\gamma}{\gamma - 1} p \frac{dV}{d\theta} + \frac{1}{\gamma - 1} V \frac{dp}{d\theta}$$

Equation 3 Heat Release Rate, where γ=1.3

The heat release rate trace was used to determine the nature of the combustion. As can been seen by comparing Figure 44 and Figure 45, the addition of hydrogen has increased the maximum heat release rate. This is due to the increased ignition delay, and the great proportion diesel fuel

being burned in the premixed phase of combustion. This increased rate of heat release is only true while stable combustion can be maintained, as will be discussed later in this section. Looking at Figure 45 and Figure 46 it can be seen that the maximum rate of heat release actually decreases slightly, although the hydrogen level supplied has increased. This shows that the limit of stable combustion has been reached, and the benefits of the hydrogen addition will begin to decrease.

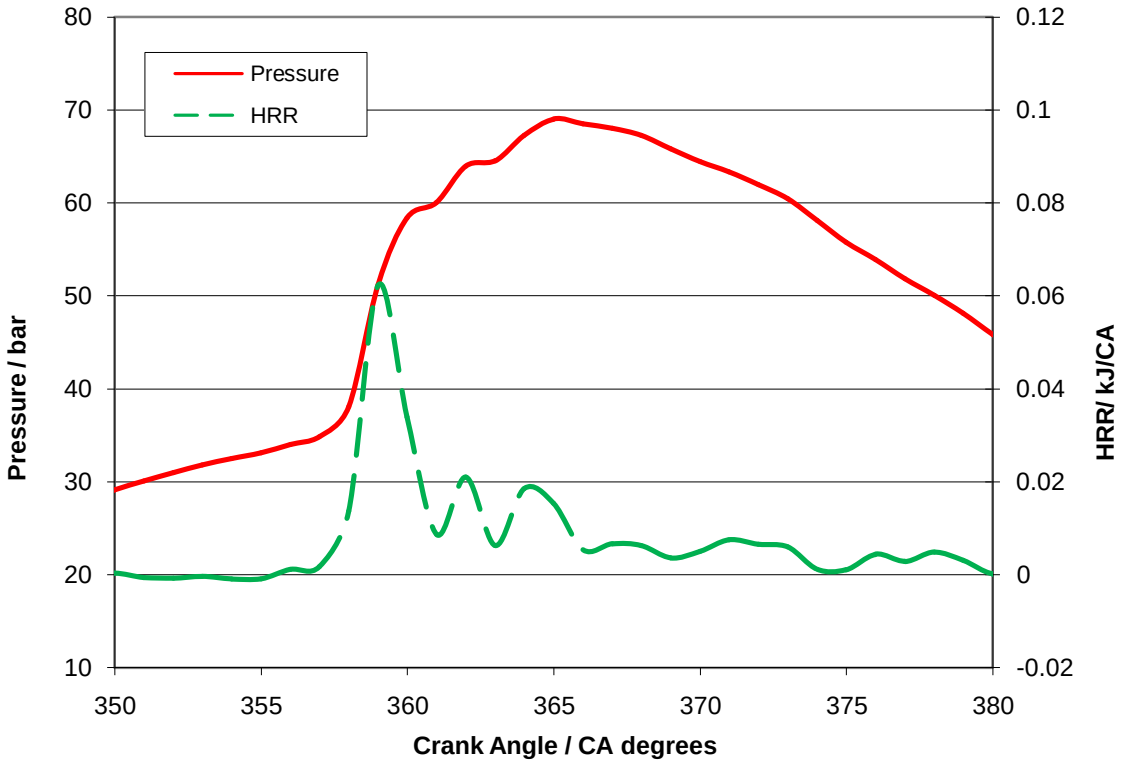

Figure 44 In-cylinder pressure and Heat Release Rate at 2500 rpm and 5.4 bar BMEP, 0% vol. hydrogen, 20% EGR

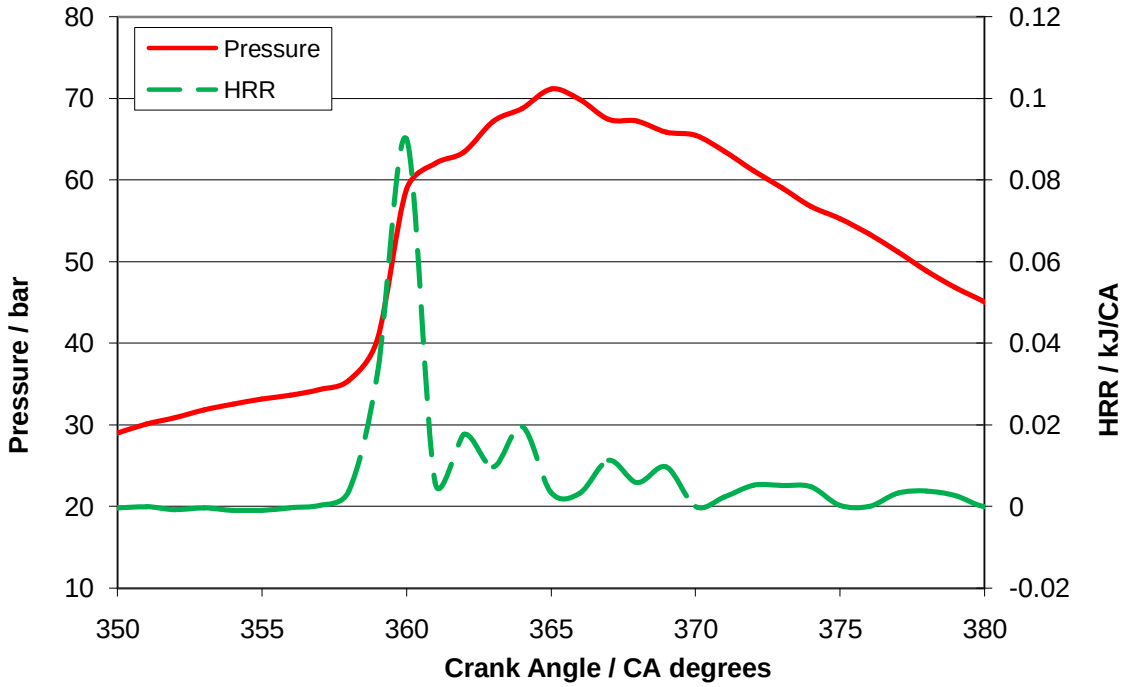

Figure 45 In-cylinder pressure and Heat Release Rate at 2500rpm and 5.4 bar BMEP, 2% vol. hydrogen and 20% EGR

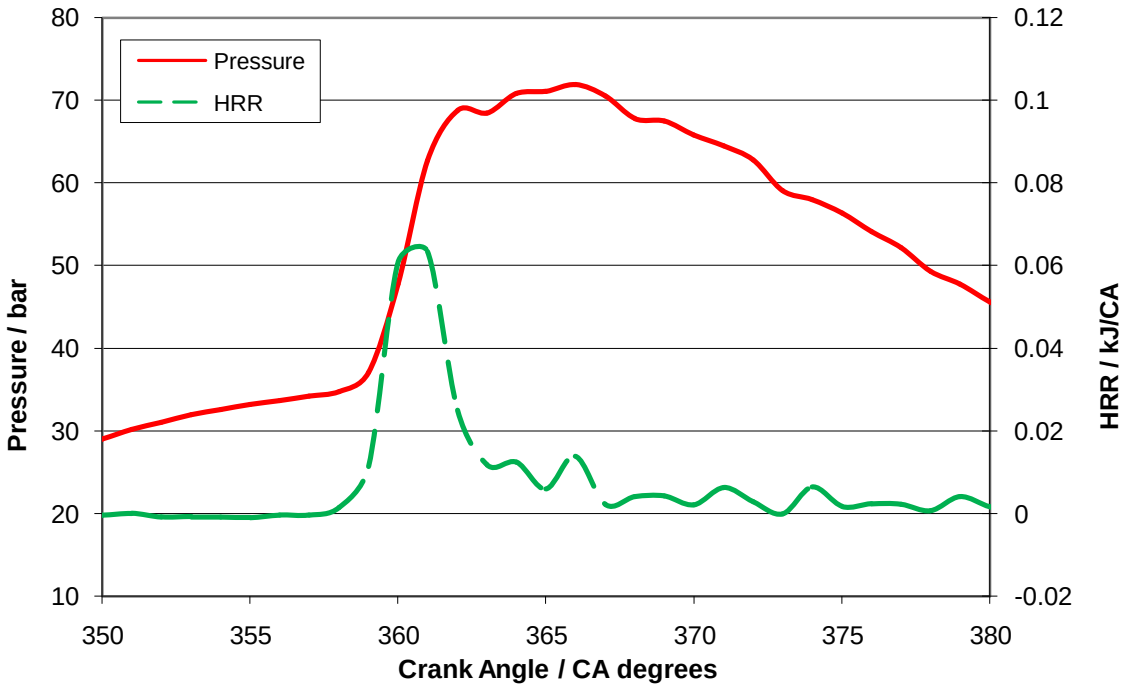

Figure 46 In-cylinder pressure and Heat Release Rate at 2500rpm and 5.4 bar BMEP, 4% vol. hydrogen and 20% EGR

As can be seen from Figure 47 the maximum pressure for medium and high loads increases with hydrogen at 2500rpm. For the case of no load, increasing hydrogen decreases the maximum pressure. This is due to the unstable nature of hydrogen combustion at low loads. Unstable combustion was taken to be a greater than 5% Coefficient of Variation (CoV) of maximum in-cylinder pressure. (This has also been observed in previous studies where at low loads, the in-cylinder conditions were not always favourable for the efficient oxidation of hydrogen and the engine combustion stability could deteriorate [Tsolakis (2004)].) There is higher maximum cylinder pressure with no EGR, due to the effect of EGR of lowering the maximum pressure.

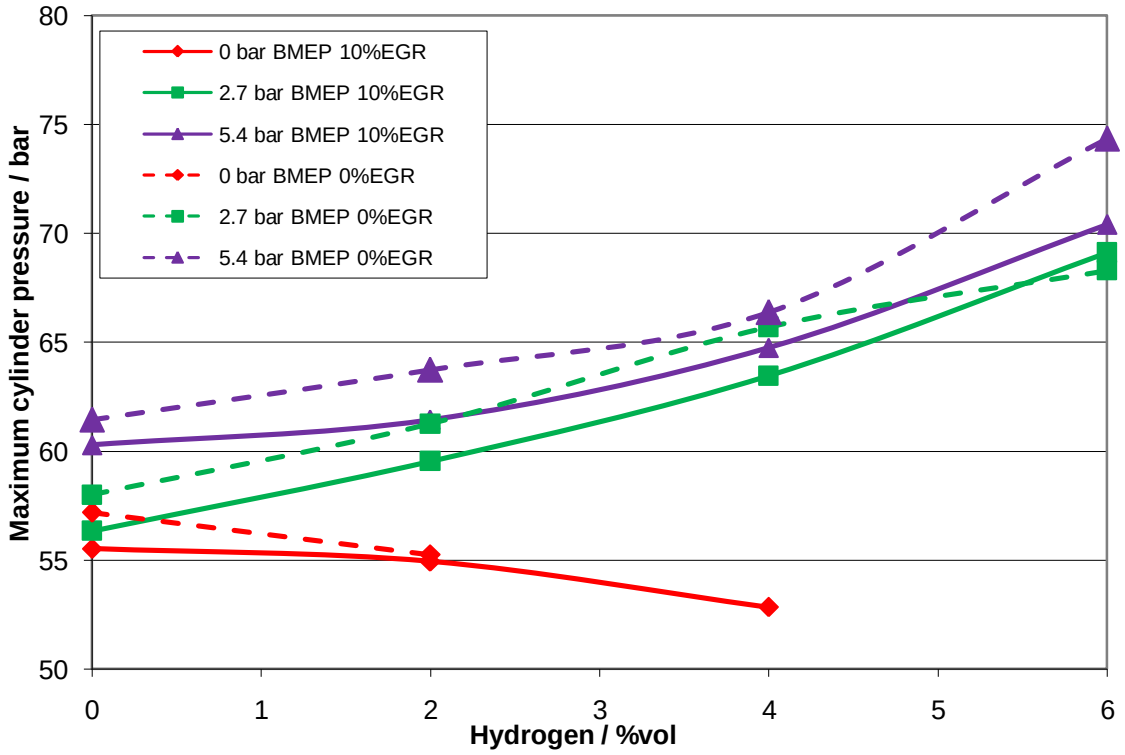

Figure 47 Maximum in-cylinder pressure at 2500 rpm

The 1500 rpm case is slightly different from the 2500 rpm case, as can be seen from Figure 48. The onset of unstable combustion at 1500 rpm occurs

at a lower load than at 2500 rpm. The advantages of hydrogen induction are clearer at high loads at low speeds.

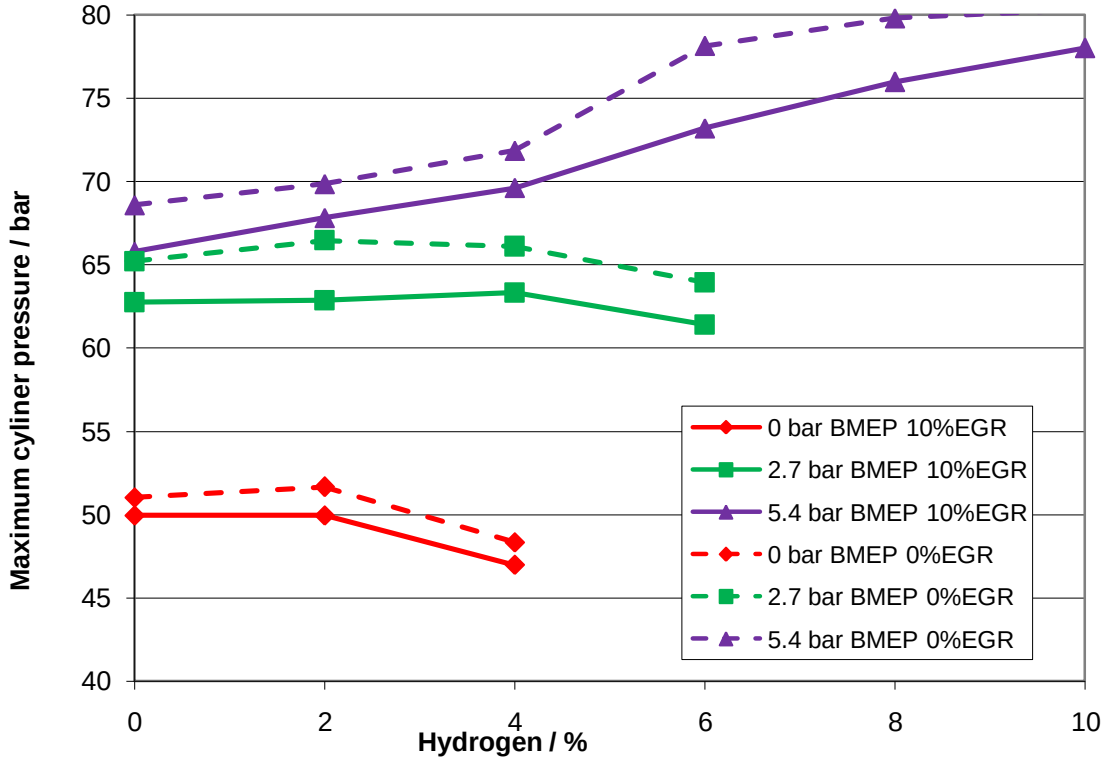

Figure 48 Maximum in-cylinder pressure at 1500 rpm

4.6.2 Ignition Delay

As can be seen from Figure 49 as the hydrogen addition level increases the ignition delay increases, except in the no load case. Ignition delay was taken as the time between the start of fuel injection signal and the start of combustion. The start of combustion in this instance was taken as the point on the heat release rate curve after injection where the value changed from negative to positive [Heywood (1988)]. The decreased ignition delay in the no load case is interesting as it is not what would normally be expected with hydrogen addition, but is also reflected in the unusual trends in the emissions. The no load case needs further investigation to establish the

exact chemical kinetics at this point. It may also be useful to measure the hydrogen emissions to establish whether or not the hydrogen is burning as the combustion at this point is unstable.

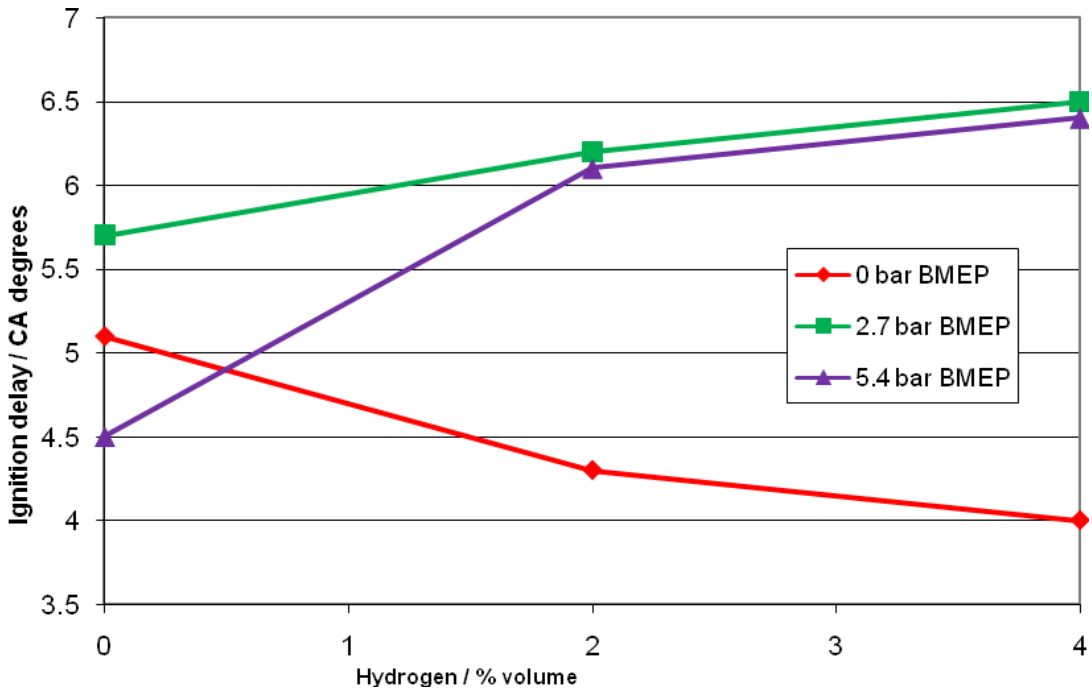

Figure 49 Ignition delay at 2500 rpm

Hydrogen addition also resulted in increase of the peak heat release rate until the onset of unstable combustion. This is a result of the longer ignition delay, and therefore a greater volume of diesel fuel being burnt during the premixed phase of combustion. This in turn makes the combustion noisier.

4.6.3 Maximum Rate of In-cylinder Pressure Rise

Similarly, as shown in Figure 50, the maximum rate of cylinder pressure rise increases with hydrogen (until the combustion becomes unstable) for medium and high loads, but decreases in the case of no load. With EGR the maximum rate of pressure rise was decreased. The increased maximum

rate of cylinder pressure rise means that the combustion using hydrogen is noisier than using exclusively diesel.

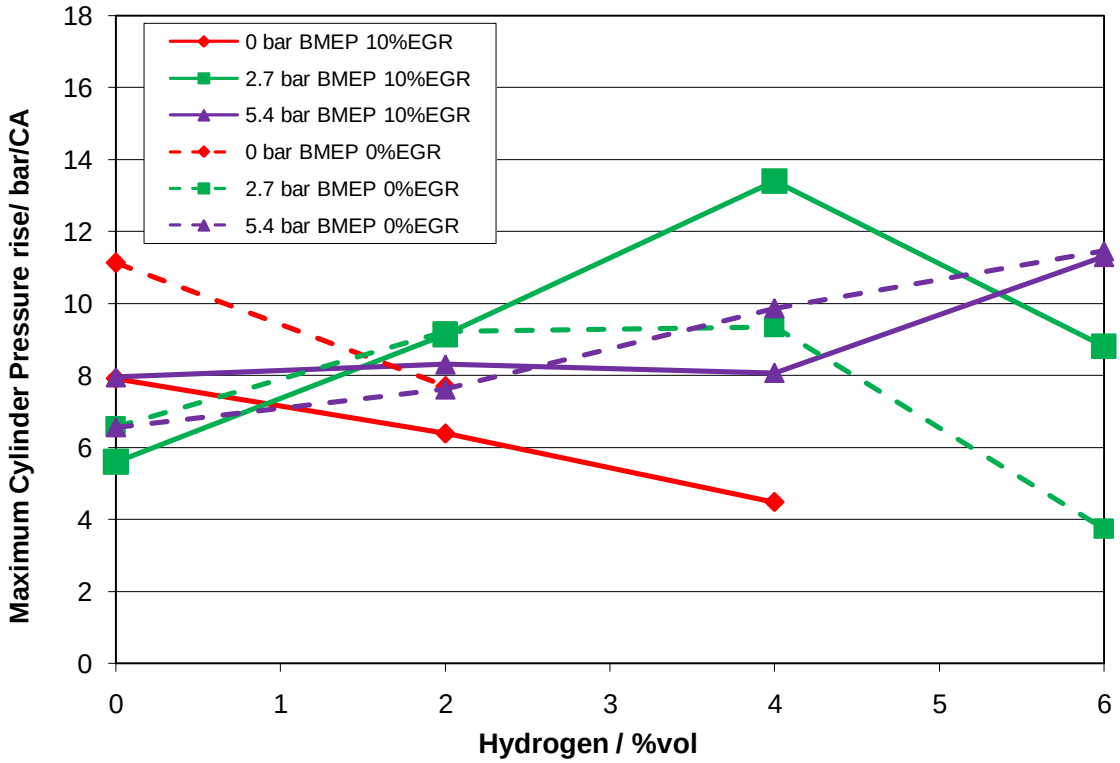

Figure 50 Maximum rate of in-cylinder pressure rise rate at 2500rpm

In the case of the 1500 rpm speed, there is an unexpected dip in the rate of maximum in-cylinder rise at 4% vol. hydrogen addition for medium and high loads. This is shown in Figure 48.

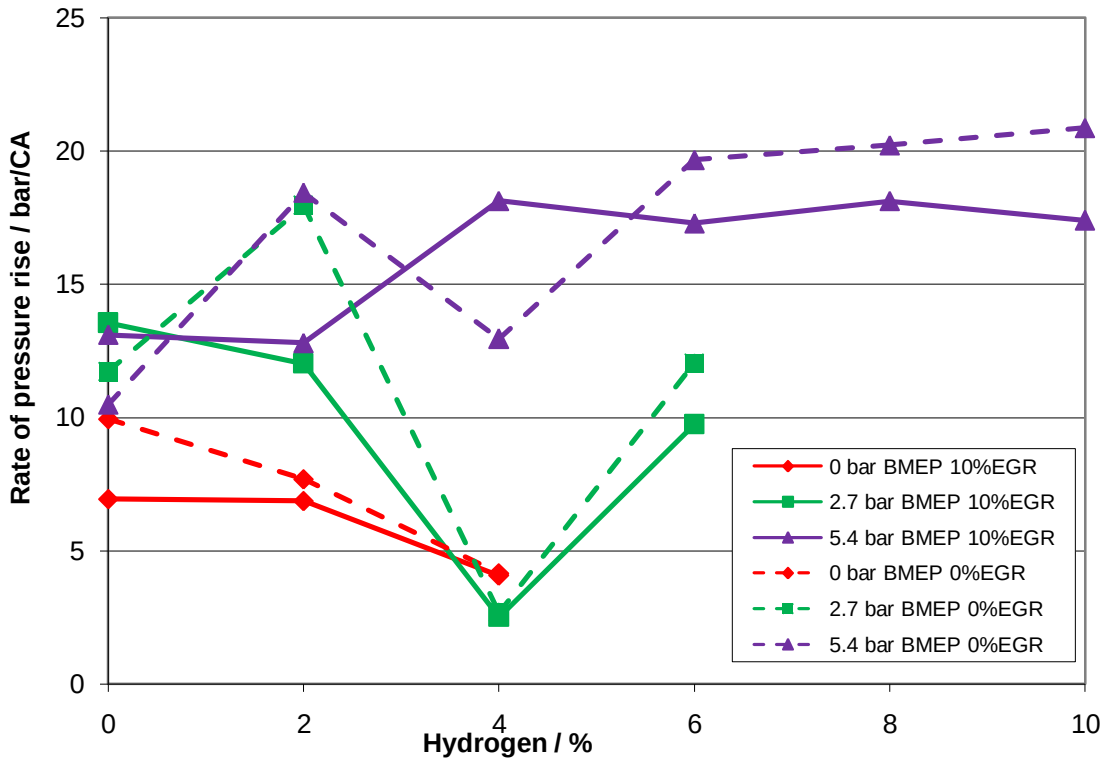

Figure 51 Maximum rate of In-cylinder pressure rise at 1500 rpm

4.7 Summary

This chapter has looked at various combustion parameters and their correlations with the exhaust gas emissions in order to make suggestions for a closed loop control system using an in-cylinder pressure transducer. The effects of hydrogen addition on the combustion parameters are also examined.

CHAPTER 5

EFFECTS OF HYDROGEN ADDITION ON EXHAUST GAS EMISSIONS AND PARTICULATE MATTER SIZE DISTRIBUTION

5 CHAPTER 5 EFFECTS OF HYDROGEN ADDITION ON EXHAUST GAS EMISSIONS AND PARTICULATE MATTER SIZE DISTRIBUTION

5.1 Introduction

This chapter will look at the exhaust gas emissions and the particulate matter size distribution, based on a gravimetric analysis, from combined hydrogen/diesel combustion. Ultimately the aim of this investigation was to determine if a combination of hydrogen induction and exhaust gas recirculation (EGR) could be used to simultaneously reduce the carbon monoxide, total unburnt hydrocarbons and nitrogen oxides emissions. This being the case, an operating strategy for each of the investigated speeds and loads has been proposed.

The size distribution was determined using a nano-Micro Orifice Uniform Deposit Impactor (nano-MOUDI) described in Section 3.7 MOUDI Set-up. Since the nano-MOUDI was not specifically designed to be coupled directly to an engine exhaust system, it was necessary prior to beginning the investigation to find an appropriate set-up. Once this set-up was determined, an experimental test matrix for the combined hydrogen and EGR investigation was set up. The ultimate aim of this part of the investigation was to find out if the use of hydrogen addition to diesel combustion could reduce the total mass of particulate matter, and what is the effect on the particulate matter size distribution. A shift towards smaller particulates, which could potentially be more harmful to health, would be best to be avoided.

5.2 Substrate Investigation

Due to the high concentration of particulate matter in pure diesel exhaust, it was necessary to find a more suitable substrate than the normally used aluminium foils coated in silicon gel. The purpose of the silicon gel is to minimise particle bounce off the substrates. If the larger cut size particulate matter is not impacted onto the appropriate level of the nano-MOUDI then this could result in a nozzle blockage further down the impactor tower. Unfortunately, the silicon gel was not capable of preventing enough particulate bounce when subjected to the high concentrations in the diesel exhaust. The gel compounded the problem of large apparent aerodynamic diameter particulate matter causing blockages further down the nano-MOUDI because the silicon was also dragged down the tower with the particulate matter, acting almost like glue. This problem of blocking meant that tests could not be conducted of sufficient length to collect a measurable weight of particulate matter on the substrates.

A set of 5 different substrates were investigated to solve the problem of the aluminium foils and silicon gel. The substrates needed to have low reactions to atmospheric conditions, because the gravimetric analysis was measuring the weights to five decimal places of a gram, produce low particulate bounce, be able to withstand the flow rate of 30L/min and be able to withstand the bombardment of the high concentration of particulate matter. The substrates investigated were uncoated aluminium foils, cellulose filters, bonded glass fibre filters, Durapore® filters and Nuclepore® filters. The Durapore® and Nuclepore® substrates are both polycarbonate filters. The difference between them is that Nuclepore® is hydrophobic, whereas Durapore® is not.

Given the work previously done by Kittelson (1998), the expected particulate matter size distribution for a diesel engine running without EGR was known, as is shown in Figure 52. Using this information, each of the substrates was evaluated based on their performance in the nano-MOUDI, the repeatability of the tests and the maximum length of time for which the tests could be run. The substrates were all tested at 1200 bar injection pressure, 0.5 CA BTDC injection timing, 2.7 bar BMEP and 1500rpm. The results for each of the substrates are discussed in the following sections.

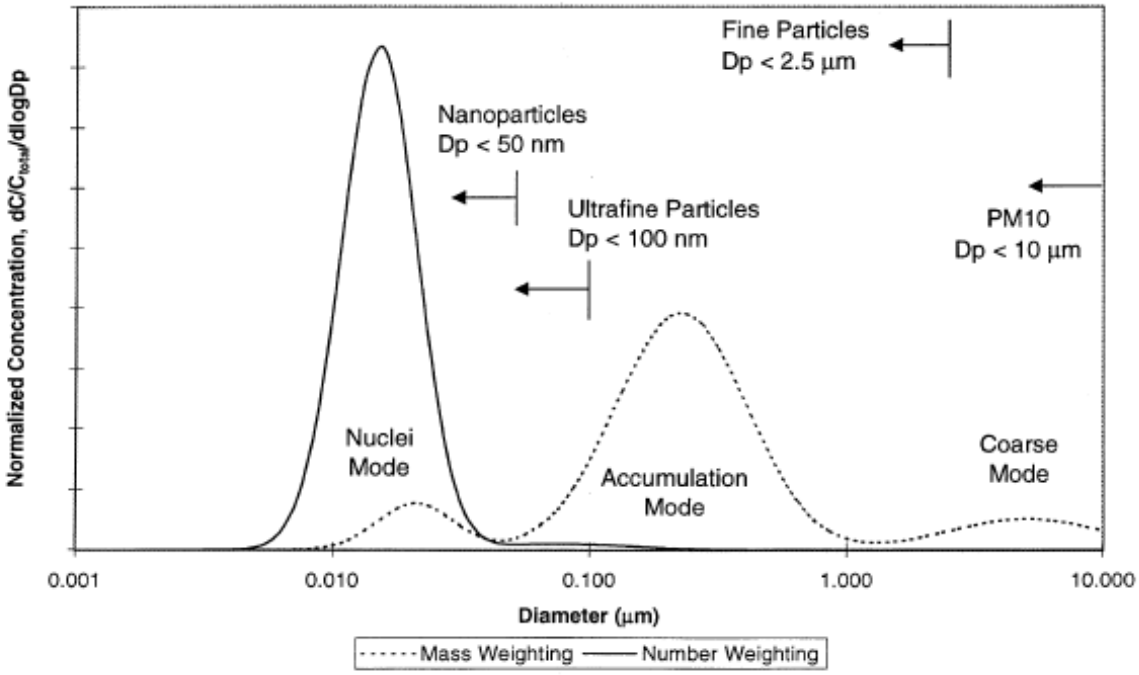

Figure 52 Particulate matter size distribution reproduced from Kittelson (1998)

5.2.1 Aluminium substrates

Aluminium foils were tested without silicon gel to assess the particulate matter bounce. Unfortunately, without the silicon gel the particulate matter bounced and quickly clogged the nozzle plates of the nano-MOUDI, meaning

that the length of the test could not be sufficient to allow for accurate measurement of the mass of the particulate matter collected.

5.2.2 Cellulose substrates

With cellulose substrates, the variation with atmospheric conditions was problematic. Because there was no way to hermetically seal the test area, the effects of the weather, and specifically the humidity, meant that the mass of the cellulose substrates changed throughout the day. One solution to this problem was to bake the cellulose substrates for an hour at 52°C before measurement, and again after collection of the substrates. However, increasing the temperature of the substrates only increases the ability to absorb moisture from the atmosphere.

The cellulose substrates also collected the water from the exhaust gas stream. The water was mainly absorbed in the first few stages, decreasing the further down the tower the exhaust gas progresses. This trend was overlaid on the expected particulate mass size distribution, as shown in Figure 53.

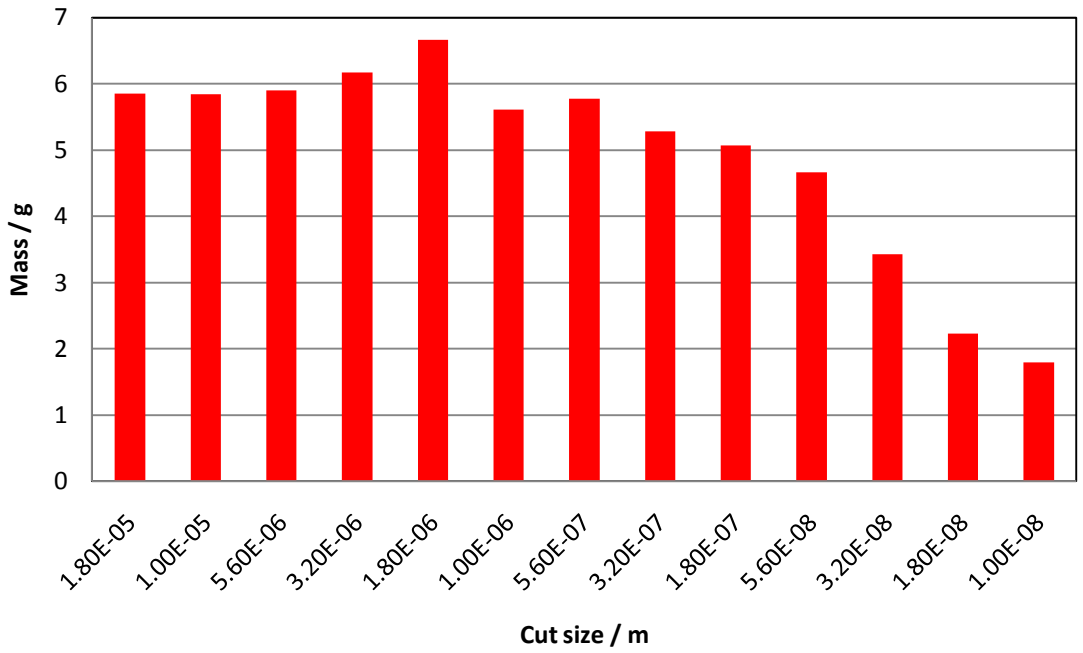

Figure 53 Particulate mass size distribution after 1 hour with cellulose substrates

5.2.3 Bonded Glass Fibre substrates

Bonded glass fibre substrates are hydrophobic, so will not be effected by the changes in atmospheric humidity. The glass fibre is softer than aluminium substrates, so should avoid the problems of particulate bounce. However, with the high concentration of particulate matter in the diesel exhaust stream and the 30 L/min flow rate the glass fibre substrates deteriorated. Although bonded glass fibre was used, the individual fibres were easily stripped and removed from the substrates. This very quickly clogged the nano-MOUDI meaning no meaningful test could be conducted. In fact, it was impossible to even collect a single complete set of results with the glass fibre substrates.

5.2.4 Durapore® substrates

Durapore® filters are a polycarbonate substrate manufactured for use in high precision filtration systems. The Durapore® substrates did not suffer problems with particulate matter bounce, and held up under the flow rate through the nano-MOUDI.

Although not completely hydrophobic, the Durapore® substrates are resistant to changes in atmospheric conditions. However, the high water content in the exhaust stream meant that even the Durapore® absorbed water to such an extent as to make the mass of the water captured higher than the mass of the particulate matter collected. The main problem with the Durapore® substrates was the very high levels of particulate matter bounce, as shown in Figure 54. The expected trend is completely lost in the errors created by the particulate bounce.

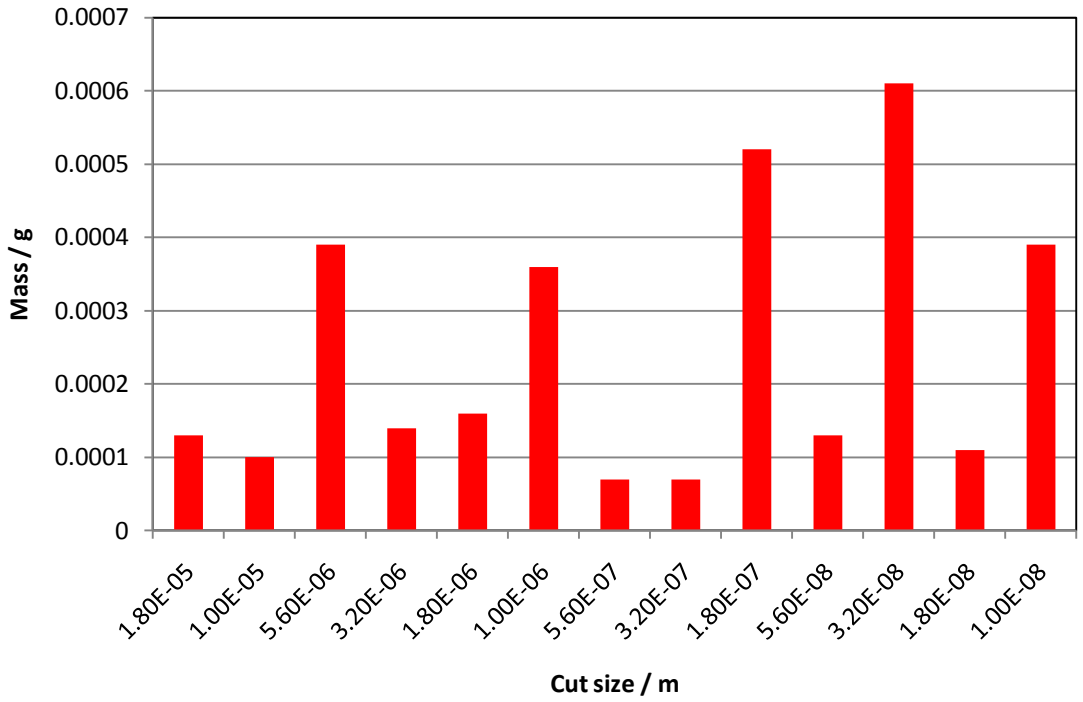

Figure 54 Particulate matter size distribution after 1 hour with Durapore® substrates

5.2.5 Nuclepore® substrates

Given the results of the Durapore® substrates, it is clear that polycarbonate substrates do not have the problems of degradation under the 30 L/min flow rate. The other problem with the absorption of water can be solved by using hydrophobic substrates. Nuclepore® is designed to be hydrophobic, and so was tested in the nano-MOUDI. The subsequent results were as expected, so Nuclepore® was used for the main testing.

5.3 Dilution System

A simple dilution system was used to decrease the concentration of the particulate matter in the feed stream to the nano-MOUDI. The exhaust gas

was mixed with compressed air from the laboratory supply via a t-junctions as shown in Figure 55. This was necessary to increase the maximum length of time the test could be run. Since the valve on the nano-MOUDI were used to control the total flow through the tower, it was possible to set the dilution ratio by measuring the flow of the compressed air. A float flow meter was connected on the compressed air feed to the t-junction. A dilution ratio of 2:1 was used by maintaining the compressed air flow rate to 15 L/min.

The secondary purpose of the dilution system is to ensure the exhaust gas has cooled to below 52 ^{o}C. This satisfies the definition of diesel particulate matter as laid out by the USEPA [Kittelson (1998)].

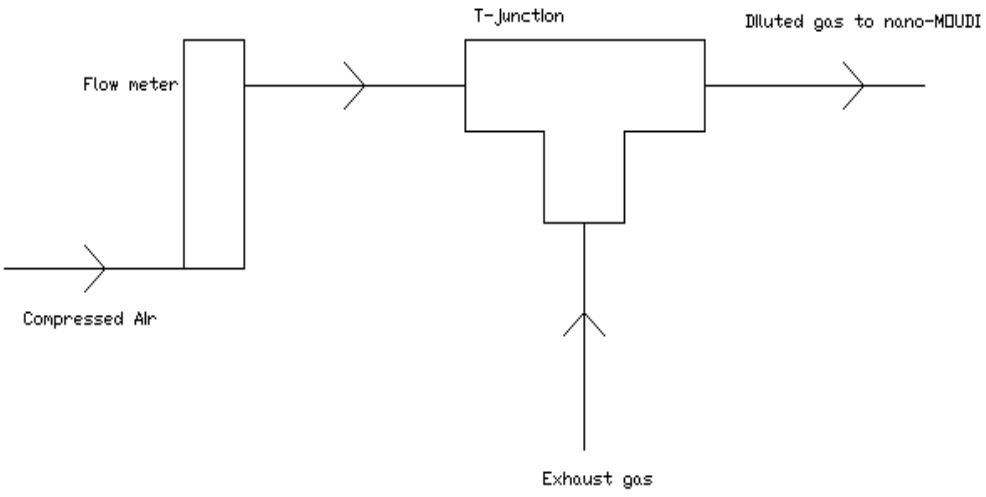

Figure 55 Dilution set-up for the nano-MOUDI feed

5.4 Experimental Test Matrix

5.4.1 Emissions Tests

As was stated in the previous chapter, in order to investigate the effects of combined hydrogen/diesel combustion with EGR addition, various levels of EGR and hydrogen addition were used. The EGR levels were varied between 0% and 40%, where the engine was capable of running this level, in 5% steps.

Hydrogen was supplied as shown in chapter 3, and the levels were varied between 0 and 10% volume of the inlet charge, in 2% vol. steps. In the case of running both hydrogen and EGR, the hydrogen always replaced air.

Two engine speeds were run, 1500rpm and 2500rpm, and 3 engine loads. The 3 engine loads were 0 bar BMEP, 2.7 bar BMEP and 5.4 bar BMEP.

Since not all combinations of the speeds and loads were capable of supporting the maximum levels of hydrogen and EGR, Table 6 shows the achieved levels for each operating point.

Operating Point	Hydrogen Level	0% vol.	2% vol.	4% vol.	6% vol.	8% vol.	10% vol.
1500 rpm 0 bar		40 % EGR	30% EGR	30% EGR	Not run	Not run	Not run
1500 rpm 2.7 bar		40% EGR	35% EGR	40% EGR	10% EGR	Not run	Not run
1500 rpm 5.4 bar		30% EGR	30% EGR	30% EGR	15% EGR	15% EGR	10% EGR
2500 rpm 0 bar		40% EGR	40% EGR	35% EGR	Not run	Not run	Not run
2500 rpm 2.7 bar		40% EGR	40% EGR	40% EGR	35% EGR	Not run	Not run
2500 rpm 5.4 bar		15% EGR	15% EGR	15% EGR	15% EGR	Not run	Not run

Table 7 Experimental Test Matrix

5.4.2 MOUDI Tests

For the purpose of this part of the investigation the engine was operated at one speed, 1500rpm, three loads, 0 bar BMEP, 2.7 bar BMEP and 5.4 bar BMEP. The EGR level was varied from 0 to 15%, in 5% intervals. The hydrogen levels used were 0, 2 and 4% vol. of the intake charge. When both EGR and hydrogen were used, the hydrogen replaced air in the intake charge. In order to negate any changes in boost pressure at the varying loads and EGR levels, the engine was run in naturally aspirated mode.

Each of the filter substrates were weighed using a microbalance with a resolution of 10 μg. In order to reduce errors, each substrate was weighed at least twice, until the final decimal place was within 10μg agreement. This procedure was repeated after collection of the particulate matter, again weighing each substrate at least twice.

The nano-MOUDI was run for 30 minutes at each engine operating point. It is important that each test was the same length of time, because as the substrates collect particulate matter the properties of the particulate bounce change.

5.5 Results and Discussion

5.5.1 Emissions

5.5.1.1 Carbon Monoxide Emissions

As can be seen from Figure 56, carbon monoxide emissions decrease with an increase in hydrogen percentage. This is true for all loads. The increase in hydrogen means there is a lower percentage of hydrocarbons available for combustion, resulting in lower carbon monoxide emissions for the same load output. This alone cannot fully explain the reduction in CO emissions. It is more likely that the nature of the more complete mixing of the fuel and air brought about by the ignition delay results in more complete combustion. As can be seen from the case of the high load lines in Figure 56, the use of EGR increases CO emissions, but the use of hydrogen goes some of the way towards offsetting this.

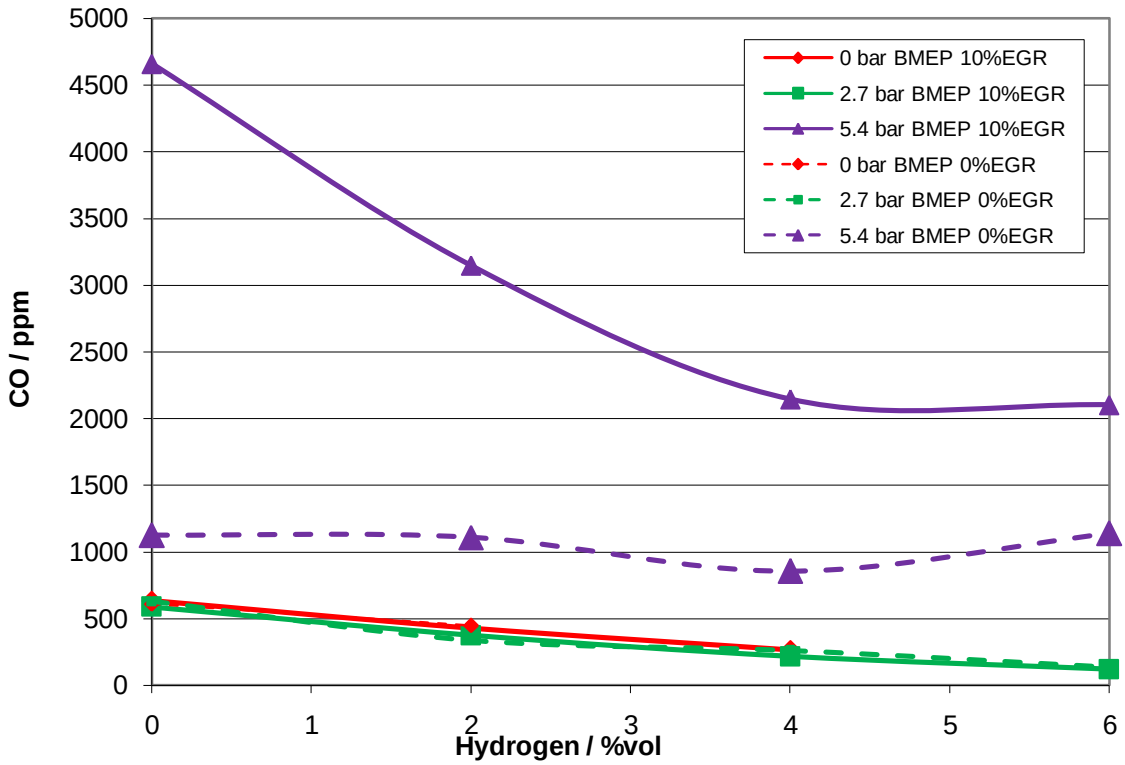

Figure 56 Carbon Monoxide emissions at 2500rpm

As was seen with the 2500 rpm case, carbon monoxide decreases with hydrogen addition in the case of 1500 rpm, as shown in Figure 57. There is however a spike in CO production at 8% vol. Hydrogen induction at 5.4 bar BMEP. This is due to the onset of unstable combustion, and therefore the increase in products of incomplete combustion. There is a corresponding increasing in THC at this point as expected, which is discussed in a later section.

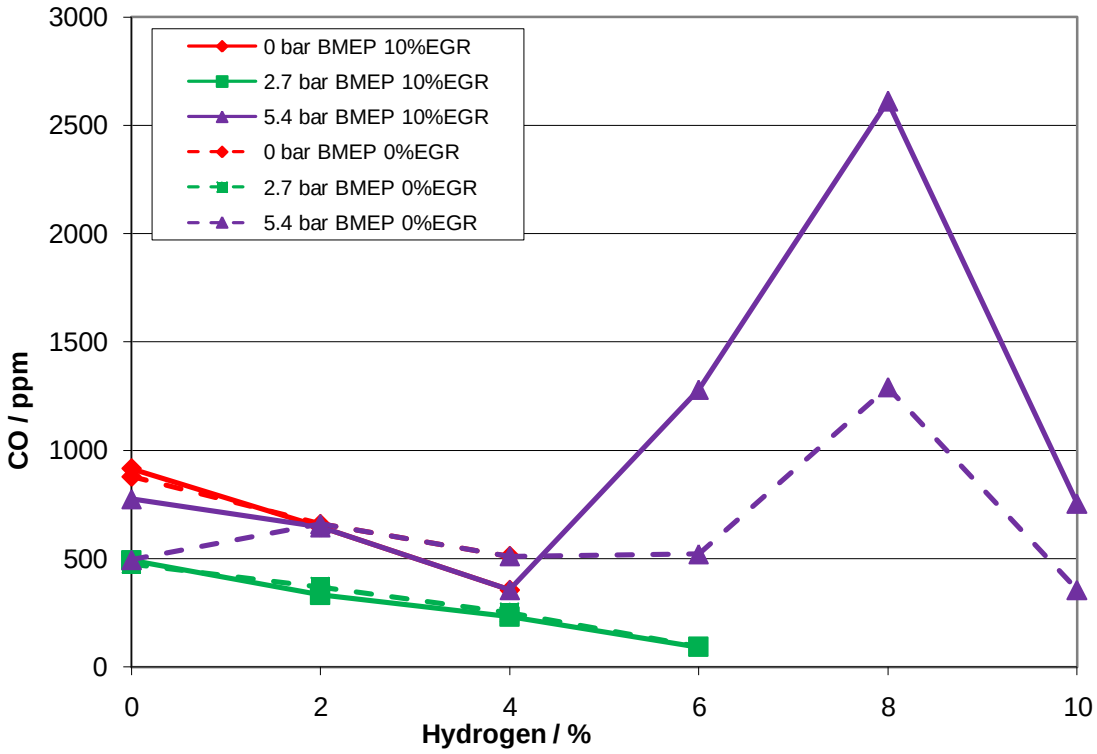

Figure 57 Carbon Monoxide emissions at 1500rpm

5.5.1.2 Nitrogen Oxide Emissions

As can be seen from Figure 58 nitrogen oxides are mainly increased by the increasing hydrogen. This is to be expected with the increased premixed combustion experienced with hydrogen combustion. However, in the case of no load with 10% EGR it can be seen that NO_X actually decreased. Unfortunately, this is also the higher limit of using hydrogen with no load, so a way would have to be found to allow stable combustion.

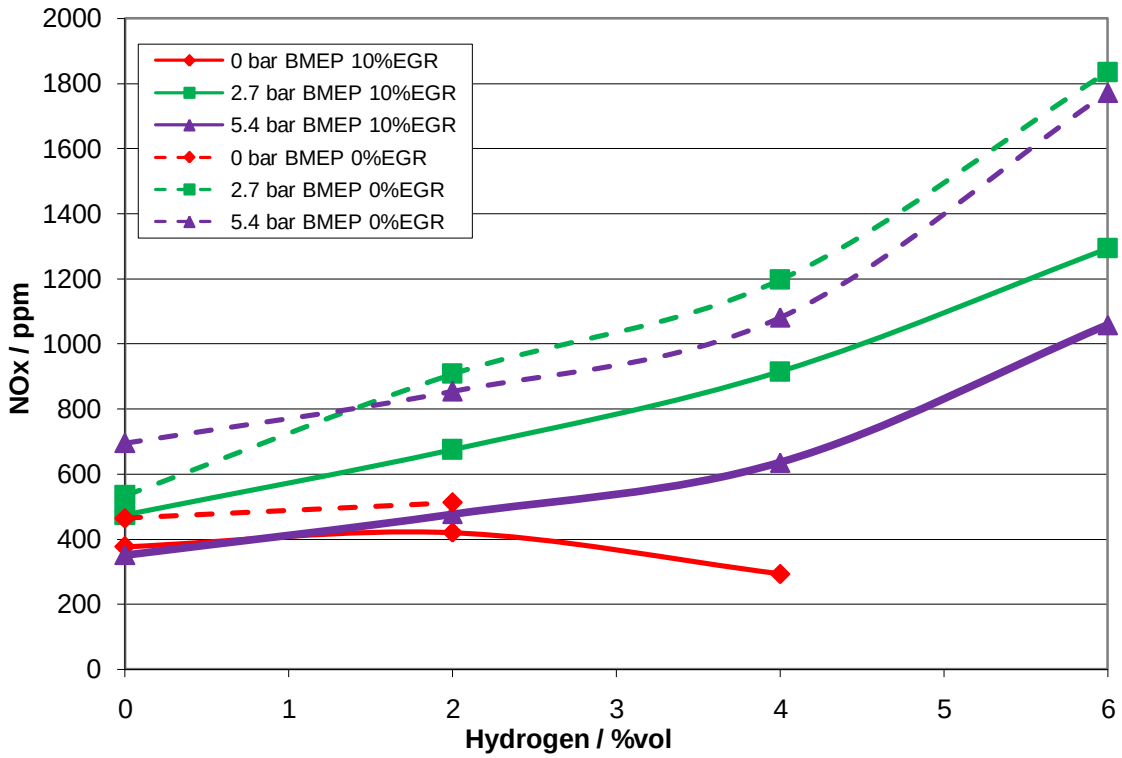

Figure 58 Nitrogen oxides emissions at 2500rpm

Since the production of NO_X is controlled by both the in-cylinder temperature and the flame speed, the introduction of hydrogen influences NO_X production in more than one way. Hydrogen increases the ignition delay, resulting in faster combustion due to the better mixing of the fuels. This high temperature combustion would be expected to increase the NO_X production. It would also be expected that as the mixture became leaner, and the flame speed slower, the time allowed for NO_X formation would be increased. The introduction of hydrogen does indeed increase the air/fuel ratio, for example in the case of high load at 2500 rpm and 10% EGR it increases from 16.6 at 0% vol. hydrogen all the way up to 30.0 at 4% vol. hydrogen, but the chemical kinetics are far too complex for the air/fuel ratio alone to account for the increased production of NO_X.

For the 1500 rpm case, the trend appears to be more complicated, as shown in Figure 59. The NO_X emissions for the no load and high load case actually decrease up to 4% vol. hydrogen addition. This is clearly due to the slower rates of in-cylinder pressure rise rates at these levels. Lower portions of diesel fuel burned during the premixed phase of combustion leads to lower NO_X production as the in-cylinder temperatures are lower.

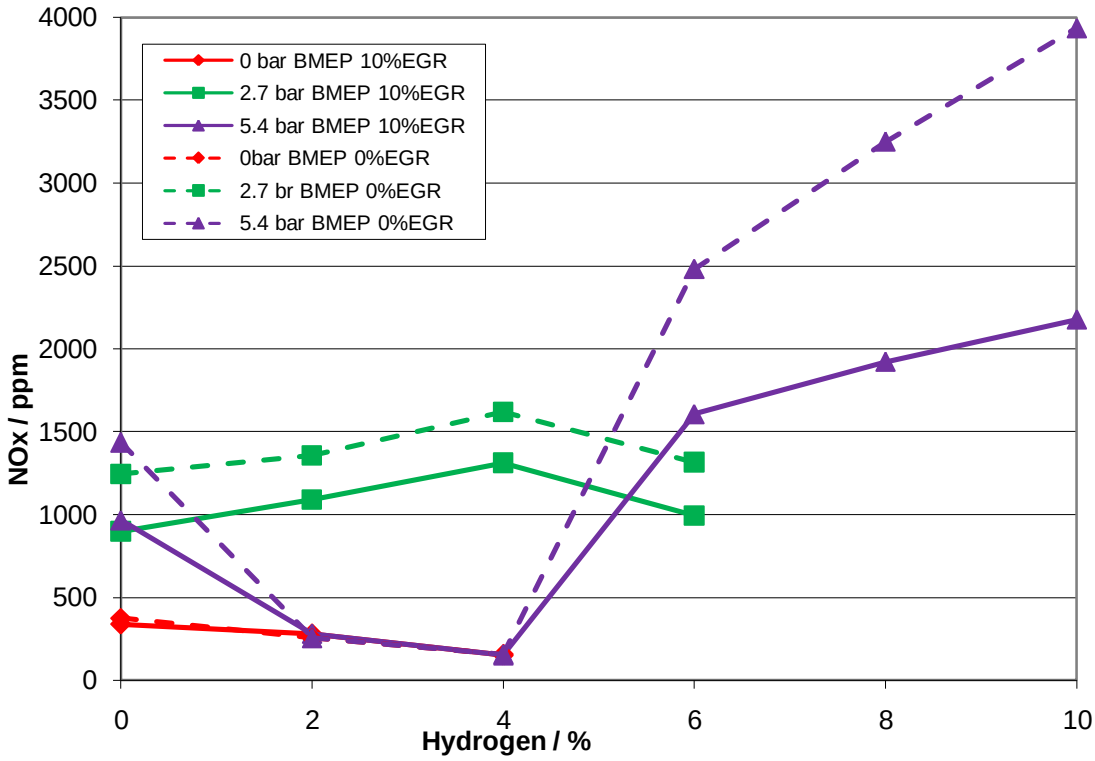

Figure 59 Nitrogen oxides emissions at 1500rpm

5.5.1.3 Total Unburnt Hydrocarbon Emissions

The total unburnt hydrocarbons (THC) decrease with hydrogen until the combustion becomes unstable. This can be explained by the lower carbon content in the supplied fuel, but also the more complete combustion. When the point of unstable combustion is reached, a sharp rise in the unburnt hydrocarbons can be observed, as is shown in Figure 60, around the 4% vol.

hydrogen for both medium and high loads. The point at which unstable combustion is reached changes with both load and speed. The effect of EGR on the THC is a general increase with increasing EGR. The high load 2% vol. hydrogen result is unexpected and needs further investigation.

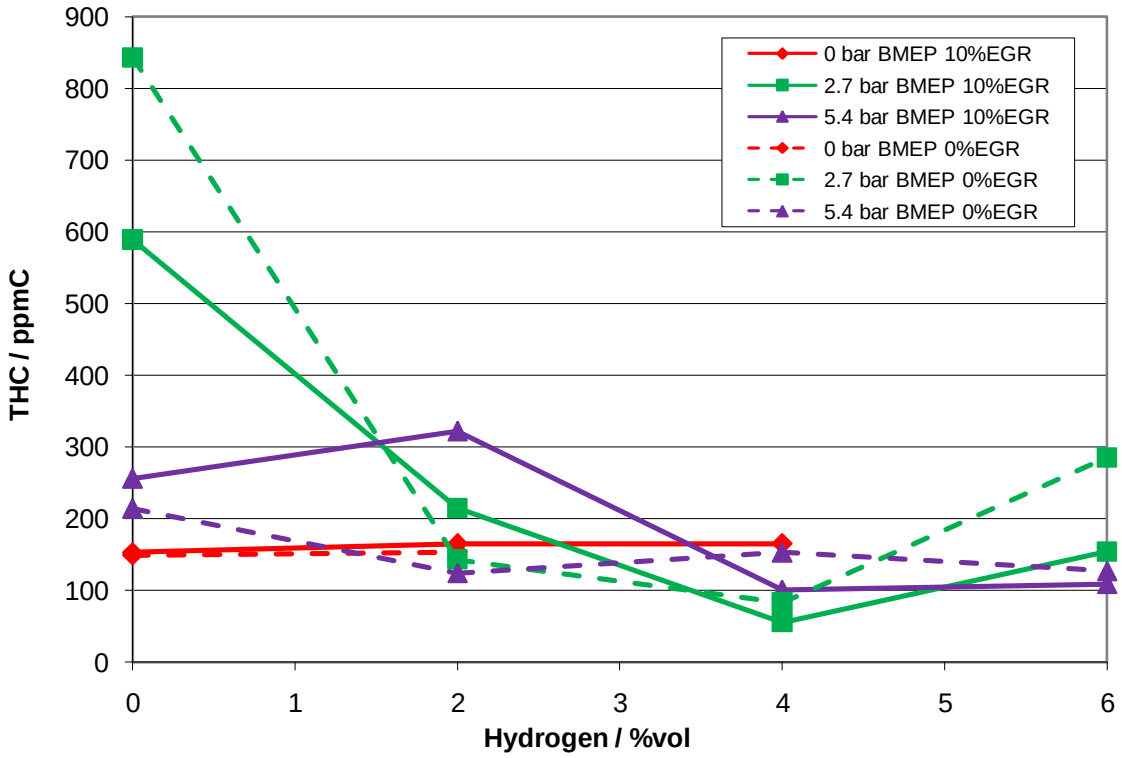

Figure 60 Total unburnt hydrocarbons at 2500rpm

Generally, the THC emissions decrease with hydrogen addition. The point where unstable combustion is reached does vary between the 1500 rpm and 2500 rpm cases, as is shown by Figure 60 and Figure 61. The onset of unstable combustion for the 1500 rpm case at 5.4 bar BMEP can be seen to be between 6 and 8 % vol. Hydrogen induction. The increase in THC emissions at 4% vol. Hydrogen addition for the 2.7 bar BMEP case reflects the dramatic decrease in maximum in-cylinder pressure rise rate. At this point the advantage provided by the premixed nature of combustion is lost.

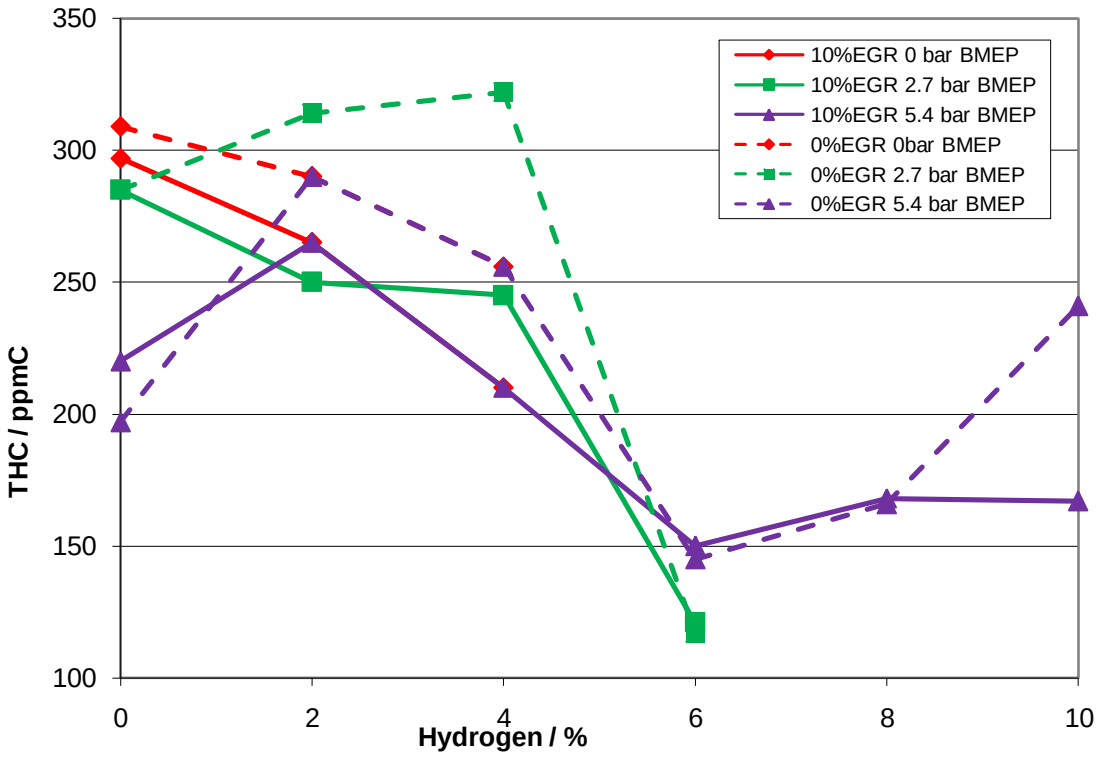

Figure 61 Total unburnt hydrocarbons at 1500rpm

5.5.1.4 Filter Smoke Number

The measurement of the filter smoke number (FSN) was hampered by the increased water contained in the hydrogen/diesel exhaust. This led to problems within the instrument where the paper used to collect the exhaust became soggy and broke during some measurements. It can still be seen from Figure 62 that the FSN decreases with hydrogen. The FSN always increases with EGR, but this effect is almost negated when EGR is combined with high levels of hydrogen addition. The fact that the 10% EGR shows lower smoke numbers with increasing hydrogen levels when compared to the 0% EGR might seem to be a surprising result. This can be explained by the change in nature of the particulate matter produced. Without hydrogen the PM is mainly sooty in nature, and is black. With hydrogen the PM grows more gummy and colourless as the hydrogen level increases. This shows a

shift from long chain carbon molecules towards shorter chain volatile organics.

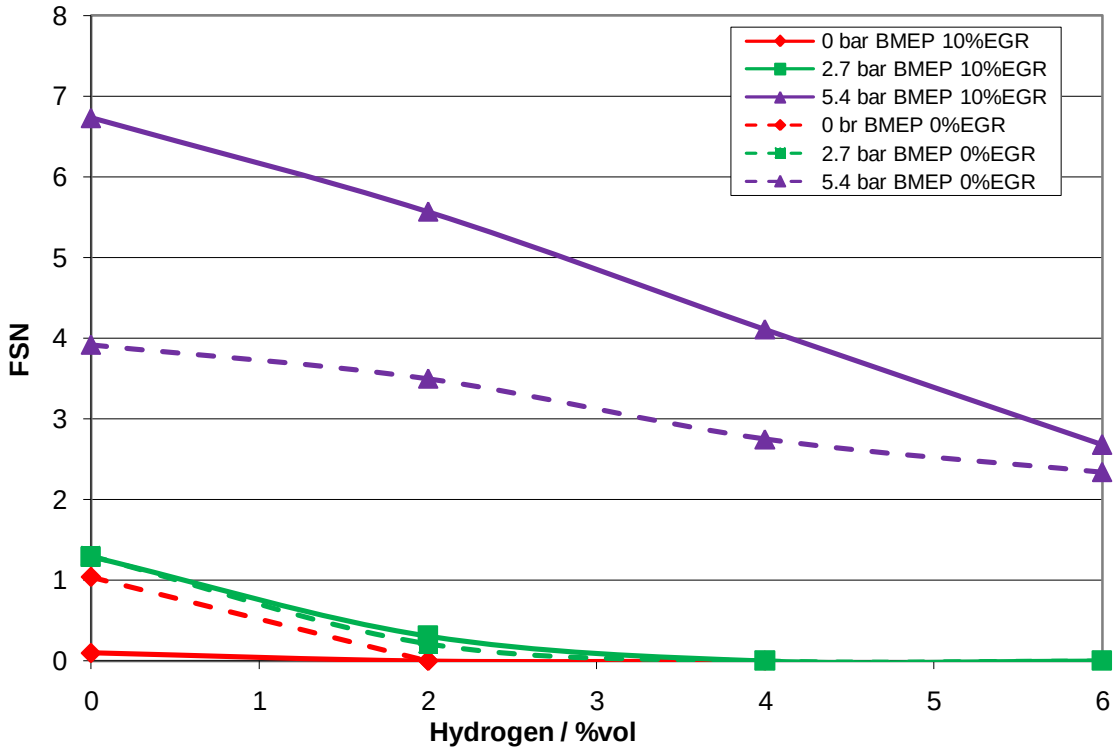

Figure 62 Filter smoke number at 2500rpm

Similarly for the case of 1500 rpm, the filter smoke number is heading towards zero with increasing hydrogen addition, as is shown in Figure 63. However, it can clearly be seen that the anomaly around 8% vol. Hydrogen induction. This is caused by the onset of unstable combustion.

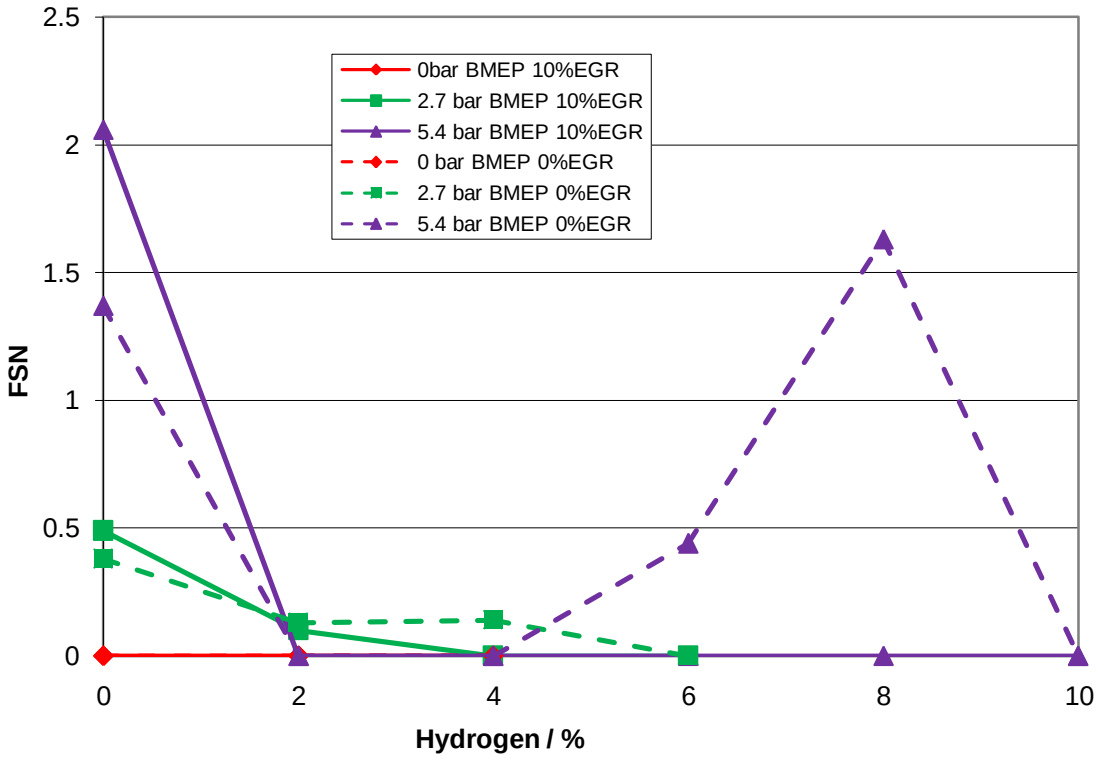

Figure 63 Filter smoke number at 1500 rpm

5.5.1.5 Specific Emissions

The emissions have been presented above in terms of the absolute values measured in this particular case. This has been necessary in order to examine the relationship between the hydrogen induction and the effects of load, as it is not possible to calculate the specific emissions at the no load case.

The specific emissions were calculated using the following method. Firstly, the chemical equation for the reaction was written out, as shown in Equation 4.

$$xC_{12}H_{23} + y\left(O_2 + \frac{79}{21}N_2\right) \rightarrow aCO + bCO_2 + cO_2 + dCH_4 + eNO + fH_2O + gN_2$$

Equation 4 Chemical balance for the combustion reaction

If each of the values represented by the letters on the left hand side of Equation 4 were taken to be the % volumes of the emissions, then each part of Equation 5 must be satisfied in order to balance the equation.

$$a + b + c + d + e + f + g = 100kmol$$

$$x = \frac{a + b + d}{12}$$

$$y = {}^{1}/_{2}\,a + b + c + {}^{1}/_{2}\,e + {}^{1}/_{2}\,f$$

$$f = 11.5x - 2d$$

Equation 5 Solution to the chemical balance equations

Each of the specific emissions was calculated in the same way, as shown in Equation 6.

$$SCO = SFC \times \frac{m_{CO} \times N_{CO}}{m_{diesel} \times N_{diesel}}$$

Equation 6 Specific emission calculation for carbon monoxide

The number of moles of each chemical is determined by the balancing of the chemical equation, and the molecular mass was calculated by adding the atomic masses for each molecule.

Figure 64 shows the expected decrease in CO emissions with hydrogen addition. This is particularly apparent in the high load case in combination

with EGR. The mechanism for decreasing CO has two components. Firstly the addition of hydrogen as fuel reduces the carbon available in the cylinder. Secondly the premixed nature of the hydrogen/diesel combustion means there is more complete combustion, resulting in higher water and carbon dioxide emissions, rather than the incomplete combustion counterparts.

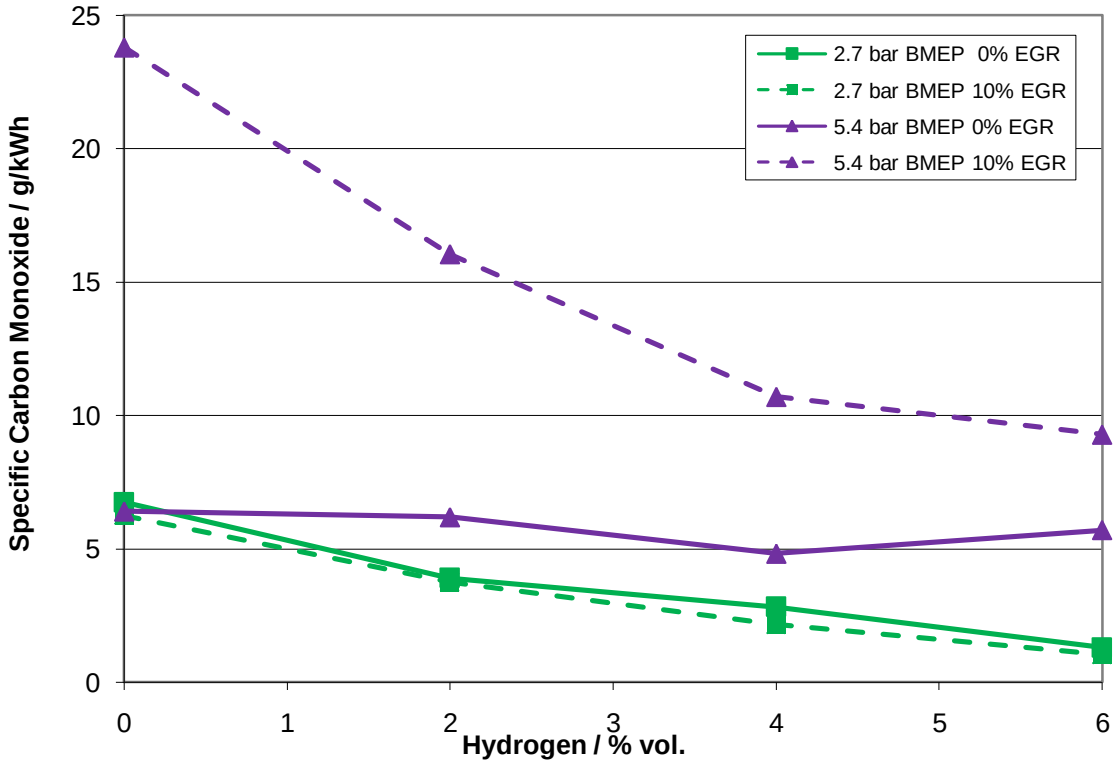

Figure 64 Specific Carbon Monoxide emissions at 2500rpm

Figure 65 shows the increase in NO_X emissions with hydrogen addition. It is important to note however, that the high load specific emissions of NO_X are lower than that of the medium load. The mechanisms for NO_X production during hydrogen combustion need further investigation.

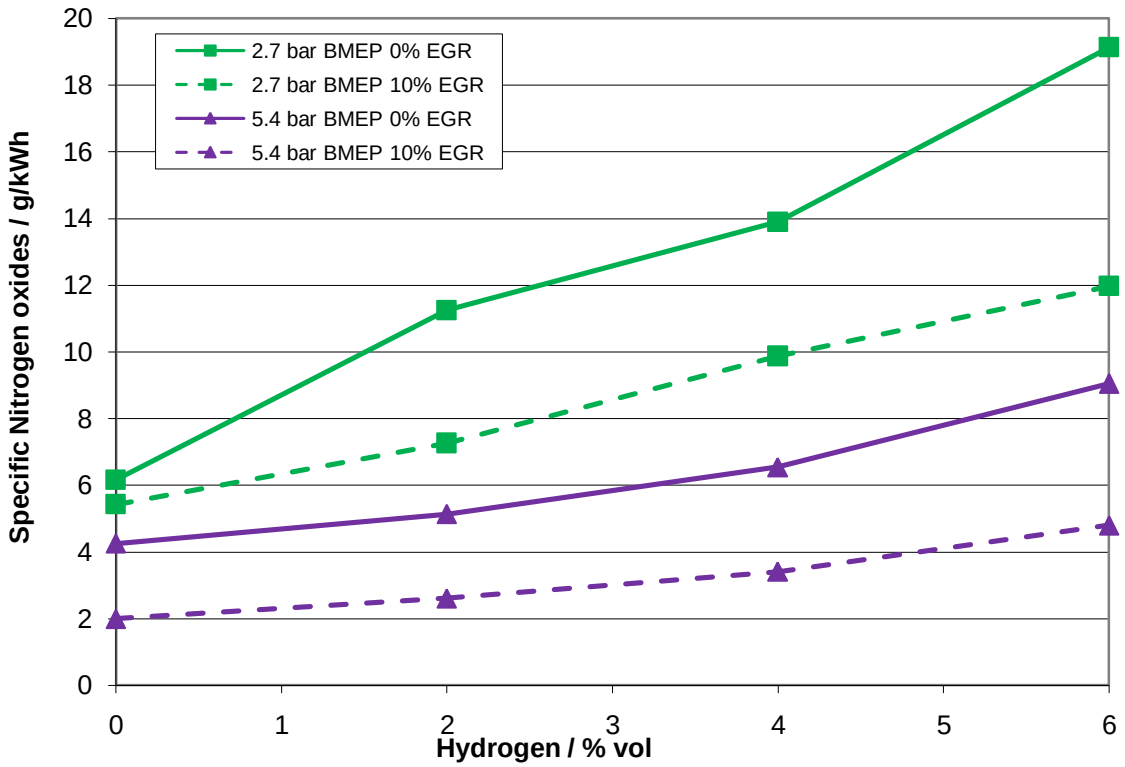

Figure 65 Specific Nitrogen oxides emissions at 2500rpm

Figure 66 shows the specific methane emissions. Methane is show here due to the analyzer measuring the unburnt hydrocarbons in terms of parts per million carbon (ppmC). The specific emissions of methane show a much clearer picture than the absolute values. There is a general decrease in methane emissions at both high and medium load with low levels of hydrogen. In the medium load case, with greater than 4% vol. hydrogen addition the methane emissions increase. This is due to the onset of unstable combustion, and therefore incomplete combustion. With low levels of hydrogen, the premixed nature of the combustion helps to promote complete combustion. It is clear that as the load increases so does the maximum level of hydrogen addition which can be beneficial.

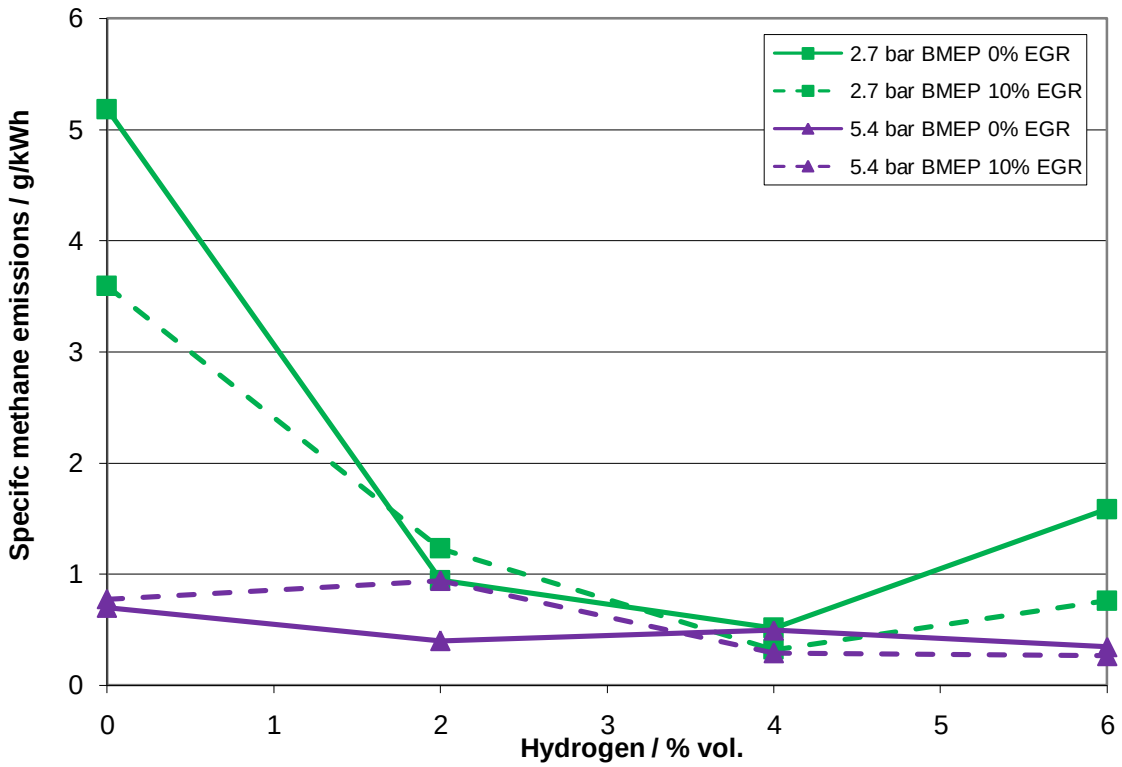

Figure 66 Specific methane emissions at 2500rpm

5.5.2 Efficiency

5.5.2.1 Thermal Efficiency

The fuel conversion efficiency (thermal efficiency) was calculated using equation 1 [Stone (1992)].

$$\eta = \frac{BP}{(\dot{m}_{fdiesel} \times CV_{diesel}) + (\dot{m}_{fH_2} \times CV_{H_2})}$$

Equation 7 Thermal efficiency

Where BP is the brake power and CV is the fuel calorific value (the calorific value of hydrogen is more than double that of diesel, ie. 120kJ/g for

hydrogen compared to 45kJ/g for diesel [Zumdahl (1995)]). As shown Figure 67, the efficiency is increased with hydrogen addition for both 2.7 and 5.4 bar BMEP, with maximum gains using EGR of around 8% at 2500 rpm.

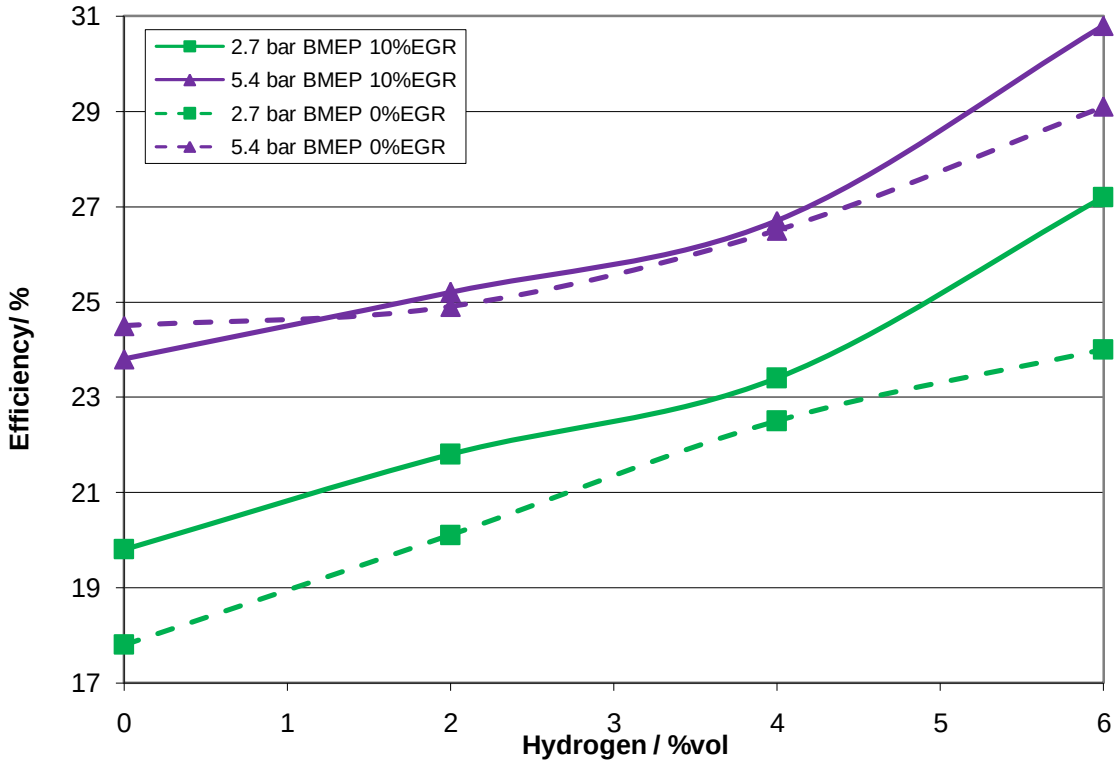

Figure 67 Thermal efficiency at 2500rpm

For the 1500rpm case however, the trend was not so good. As can be seen in Figure 68, the efficiency is increased with the addition of hydrogen apart from the anomaly around 6- 8% vol. Hydrogen addition at 5.4 bar BMEP. As has been discussed in the previous sections, there is something interesting happening at this point which needs further investigation to fully explain.

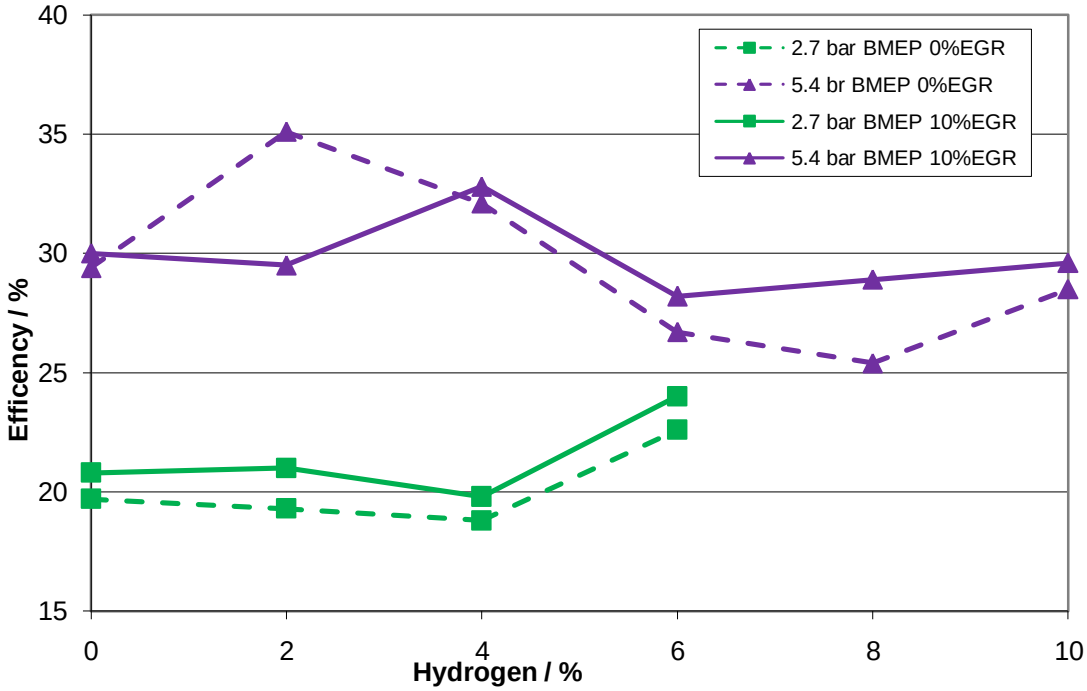

Figure 68 Thermal Efficiency at 1500rpm

It has to be mentioned here that in the case of an engine with on-board generation of hydrogen the overall fuel conversion efficiency of the engine/reformer system will also depend on the fuel reforming process efficiency and not only on the engine combustion process. Nevertheless, the obtained increased efficiencies show a clear benefit of hydrogen addition in terms of engine fuel conversion efficiency.

5.5.2.2 Energy Consumption

As the hydrogen level increases, the diesel fuel consumption decreases. This is partly due to the fact that the hydrogen is providing energy to the reaction, but also more of the diesel is being fully utilised, resulting is less wasted energy. As a way of visualising this effect, the total energy supplied the cylinder was calculated. The total energy was calculated using the

measured mass fuel flow rate of the diesel fuel and the volumetric fuel flow rate and the density of the hydrogen. As can clearly be seen in Figure 69, the total energy required to maintain the load decreases with hydrogen addition. This effect is more pronounced as the load increases. It is also important to note that the total energy needed to maintain the load is lower with EGR than without. The combined use of EGR and hydrogen delayed the onset of unstable combustion. This phenomenon needs further investigation to understand the chemical kinetics dictating the combustion.

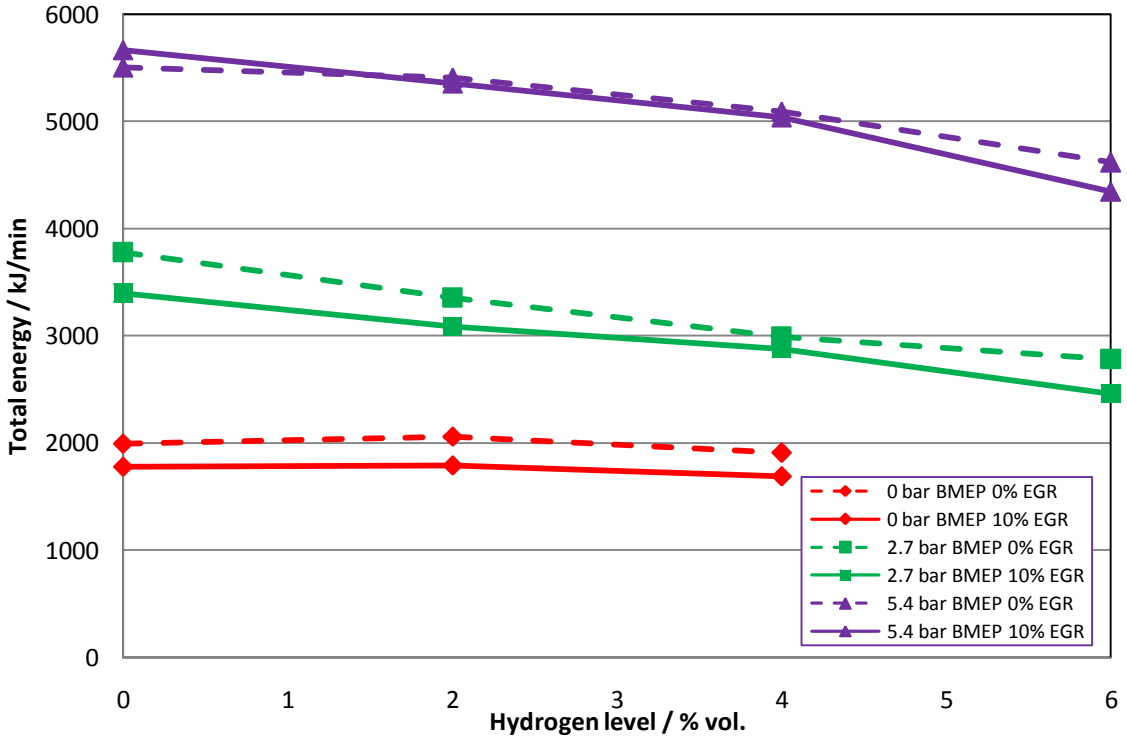

Figure 69 Total energy supplied to the engine at 2500rpm

As is shown in Figure 70 a similar effect is observed at 1500rpm. It is clear that at the no load case at 1500 rpm, the combustion is unstable, and therefore more energy must be supplied to maintain the engine operation during misfire. Again the energy consumption is lower with EGR than without, and the decrease with hydrogen addition is clear.

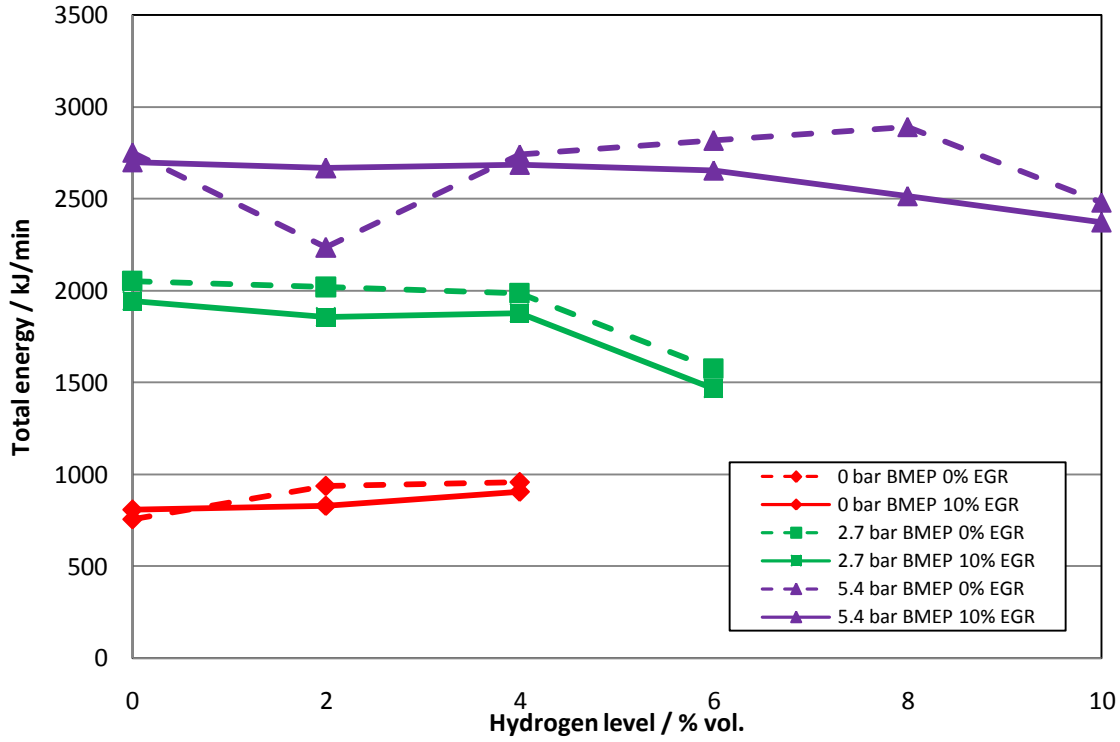

Figure 70 Total energy supplied to the cylinder at 1500rpm

The percentage of energy supplied by the hydrogen as the hydrogen levels increased was also calculated. Figure 71 clearly shows the higher percentage of energy supplied by the hydrogen with EGR. At 2500rpm the onset of unstable combustion occurs when the percentage of energy supplied by the hydrogen passes 50% for the lower load cases. In order to maintain a higher load, the maximum levels of hydrogen addition are lower, around 30% maximum.

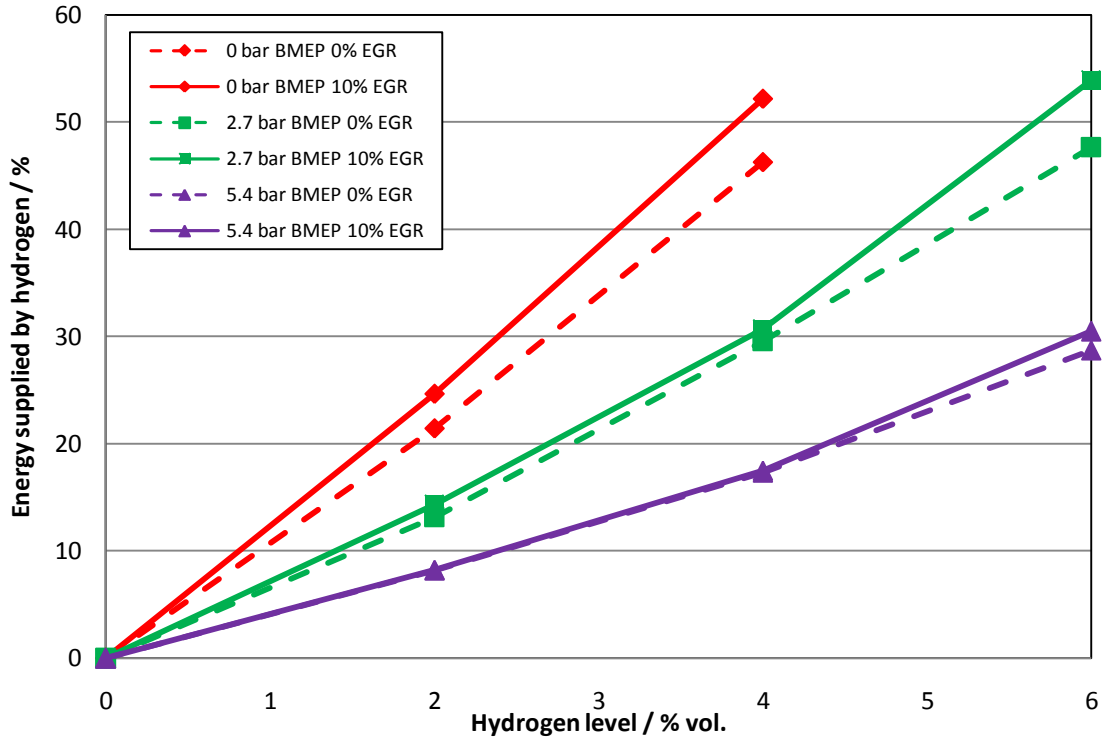

Figure 71 Percentage of total energy supplied by the hydrogen at 2500rpm

In the case of 1500rpm higher percentages of energy supplied by the hydrogen was possible, as shown in Figure 72. The onset of unstable combustion was with about 60% of the supplied energy coming from the hydrogen induction. For the medium and no load cases, the percentage of total energy supplied by the hydrogen is slightly higher with EGR than without, as the mass fuel flow rate of diesel fuel is lower with EGR than without.

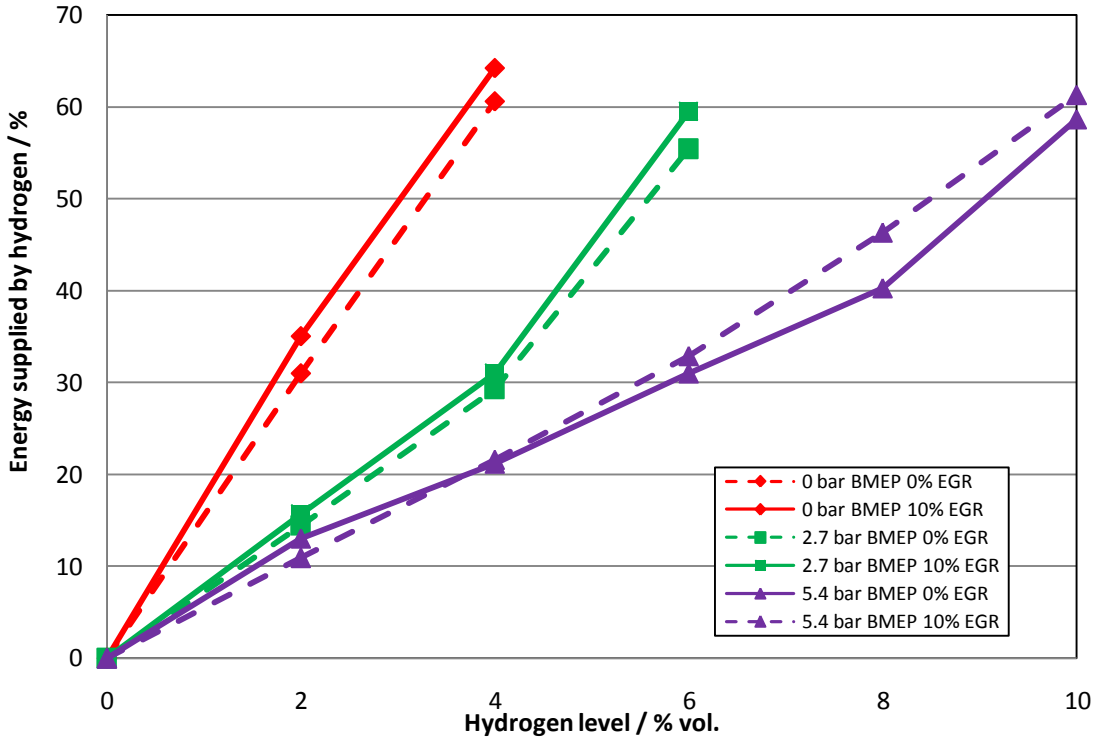

Figure 72 Percentage of total energy supplied by hydrogen at 1500rpm

5.5.3 Particulate Matter Size Distribution

5.5.3.1 Effects of hydrogen and load

In the case of 100% diesel fuelling, the PM size distribution was as to be expected [Kittelson (1998) and Burtscher (2001)] and is demonstrated by Figure 73 and Figure 74 (cases of 0% vol. H2). There is a large peak at the 3.2 µm cut point, which is the accumulation mode peak, as well as a secondary peak at 32 nm cut point. This second peak is in the nuclei mode. As can be seen from Figure 73 and Figure 74, the addition of hydrogen reduces the total particulate matter mass captured.

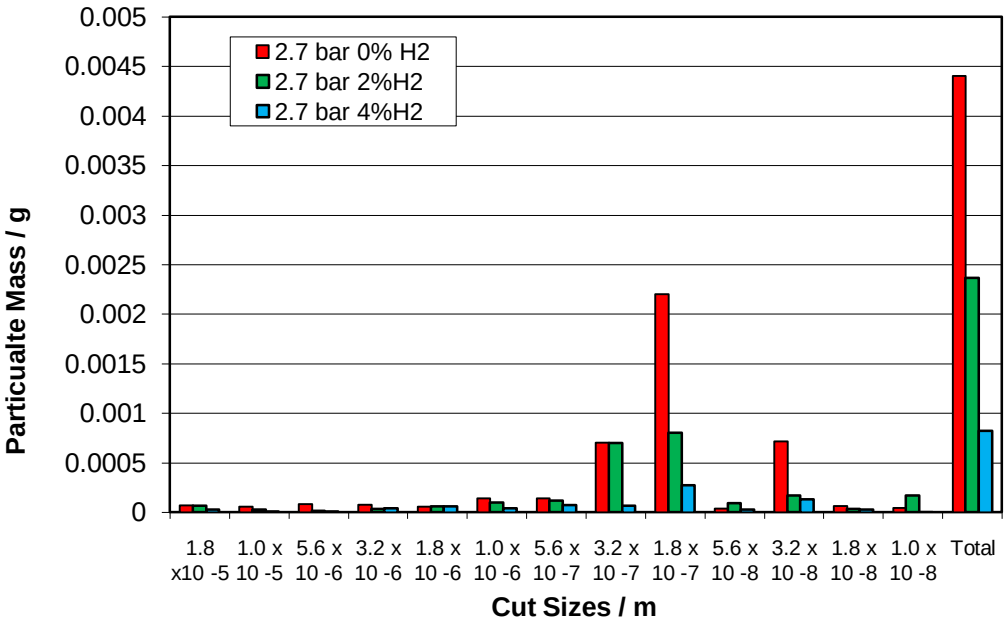

Figure 73 Particulate Matter size distribution at 5% EGR and 2.7 bar BMEP

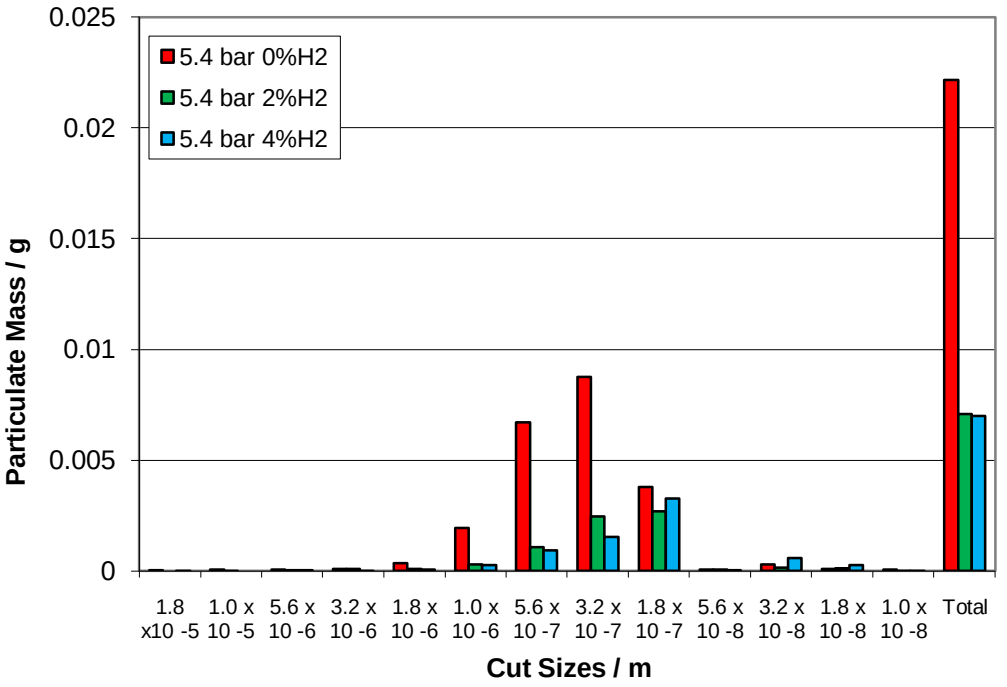

Figure 74 Particulate Matter size distribution at 5% EGR and 5.4 bar BMEP

In the case of the no load tests, it was not possible to run a MOUDI test with hydrogen and EGR conditions due to the nature of the particulate matter in the exhaust. The MOUDI clogged very quickly, and the PM was observed to be sticky on the impaction plates. This is due to the lower carbon and higher Soluble Organic Fraction (SOF) content in the exhaust.

In the case of medium load, shown in Figure 73 the total mass is significantly decreased with the addition of hydrogen. This phenomenon is not specific to the case of medium load operating conditions. A similar trend is shown in Figure 74 for high load, and was also observed with the no load condition at 0% EGR, as shown in Figure 75.

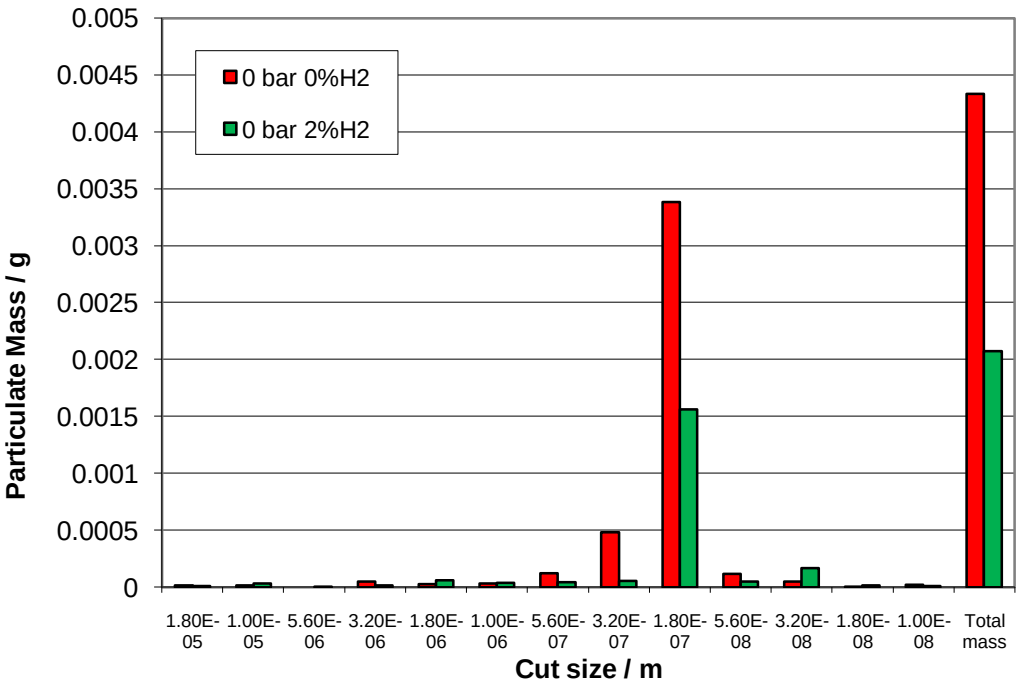

Figure 75 Particulate matter size distribution at 0 bar BMEP and 0% EGR

An observation of the PM collected shows that as the hydrogen levels increase the colouration on the impaction plates decreases. The PM becomes tackier, and the water collected in the condenser increases. The combustion

of the hydrogen alone cannot explain this increase in the water content in the exhaust, but must in fact be a by-product of the extra complete combustion of the diesel fuel achieved by premixing. This is supported by the decrease in energy supplied to the cylinder discussed in 5.5.2.2 Energy Consumption.

It can also be seen from Figure 73 and Figure 74 that as the hydrogen level increases the accumulation mode peak is moved nearer the nuclei mode. The pure nuclei mode peak is increased by comparison, but is still the secondary peak.

The shift in the main peak can be attributed to the lower availability of carbon. As the percent volume of hydrogen is increased, the diesel necessary to maintain the engine load is reduced, and so does the concentration of carbon atoms in the cylinder. Accumulation mode particulates are mainly carbonaceous agglomerates with SOF and sulphate molecules condensed on the carbon centres. It follows that as the availability of carbon decreases so does the abundance of these particulate agglomerates. The presence of hydrogen, and the products of incomplete and complete hydrogen combustion, could also be increasing the late oxidation of carbon compounds.

5.5.3.2Effects of hydrogen and EGR

Figure 76, Figure 77, Figure 78 and Figure 79 show the relationship between EGR level and hydrogen level. As can be seen, the general trend is as the EGR level increases the total PM increases (except for 5% EGR). This is to be expected. The size distribution with combined EGR and hydrogen does show a slight increase in larger sized coarse mode PM when compared to the 0% EGR case. Again, this is to be expected with the addition of EGR

[Aufdenblatten *et al* (2002)], but the effect is minimised with the combination of hydrogen, which pushes the size distribution towards the nuclei mode.

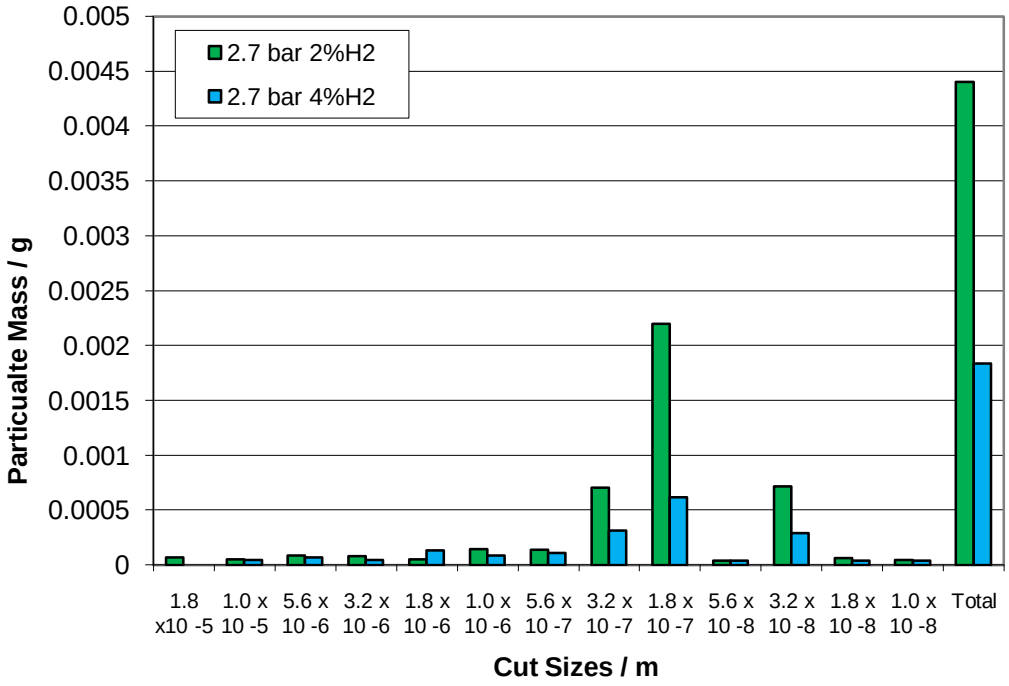

Figure 76 Particulate matter size distribution at 2.7 bar BMEP and 0% EGR

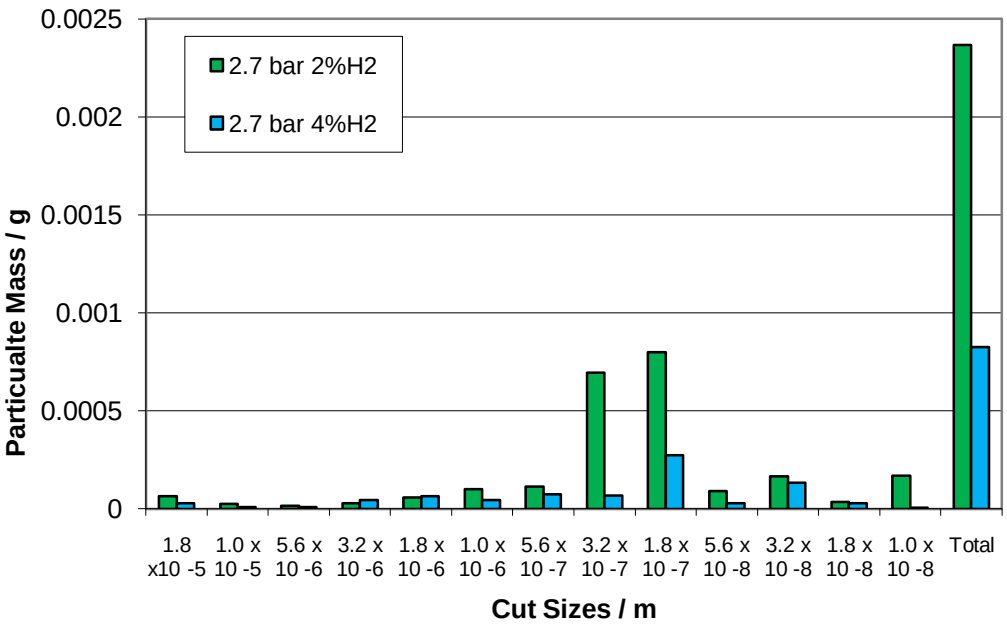

Figure 77 Particulate matter size distribution at 2.7 bar BMEP and 5% EGR

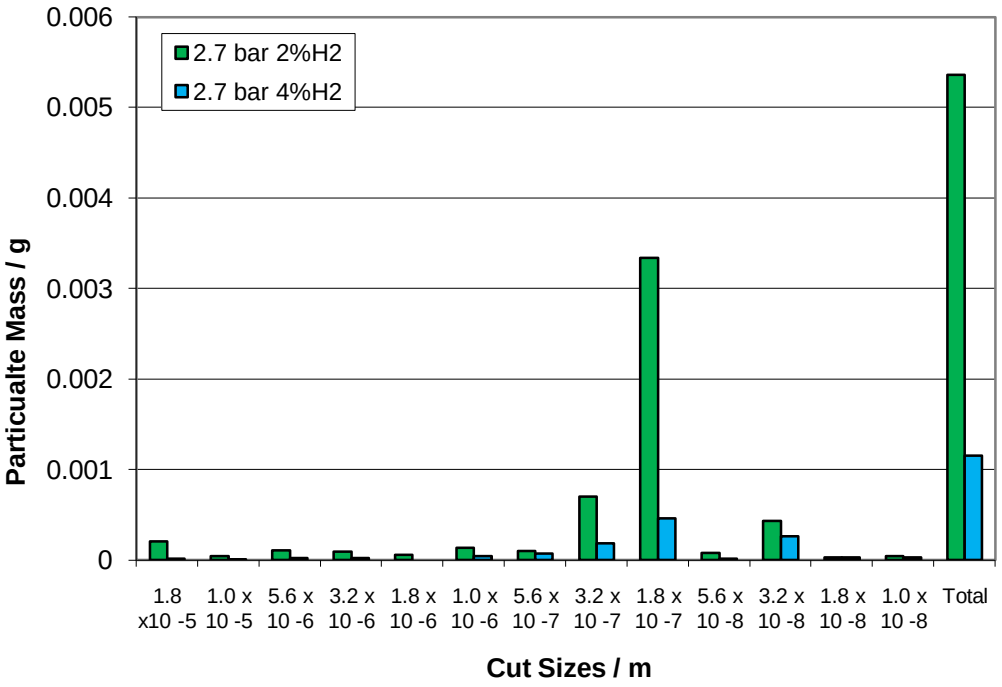

Figure 78 Particulate matter size distribution at 2.7 bar BMEP and 10% EGR

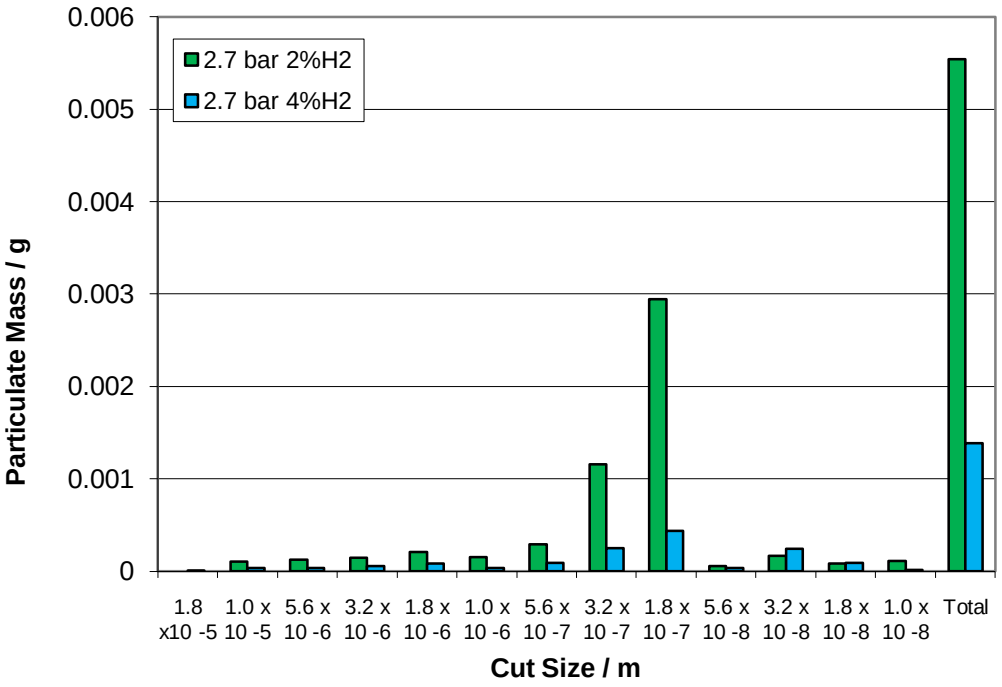

Figure 79 Particulate matter size distribution at 2.7 bar BMEP and 15% EGR

The one exception to this is the case of 5% EGR, shown in Figure 77. The decrease in the 5% EGR case is clearly illustrated by Figure 80. Here the dip at 5% EGR is clearly shown between the 0 and 10% EGR cases. In this case there is a reduction of total mass of 44% in the 2% vol. hydrogen test, from a mass of 4.405 mg to 2.365 mg collected over a 30 minute period, and 55% reduction in the 4% vol. hydrogen test, from a mass of 1.84 mg to 0.825 mg, again collected over a 30 minute period. This trend goes against what is expected, which would be a general increase in total mass with EGR, as the NO_X decreases. However, the NO_X is not decreasing at this specific point, as shown in Figure 81. Clearly, at this specific operating point there is an anomaly in the chemical kinetics which means the particulate matter and the NO_X are behaving contrary to expectation. Possibly this operating point increases late oxidation, or even reduces the incomplete combustion of the

diesel fuel. Further investigation is needed to establish the precise mechanisms of combustion at this point.

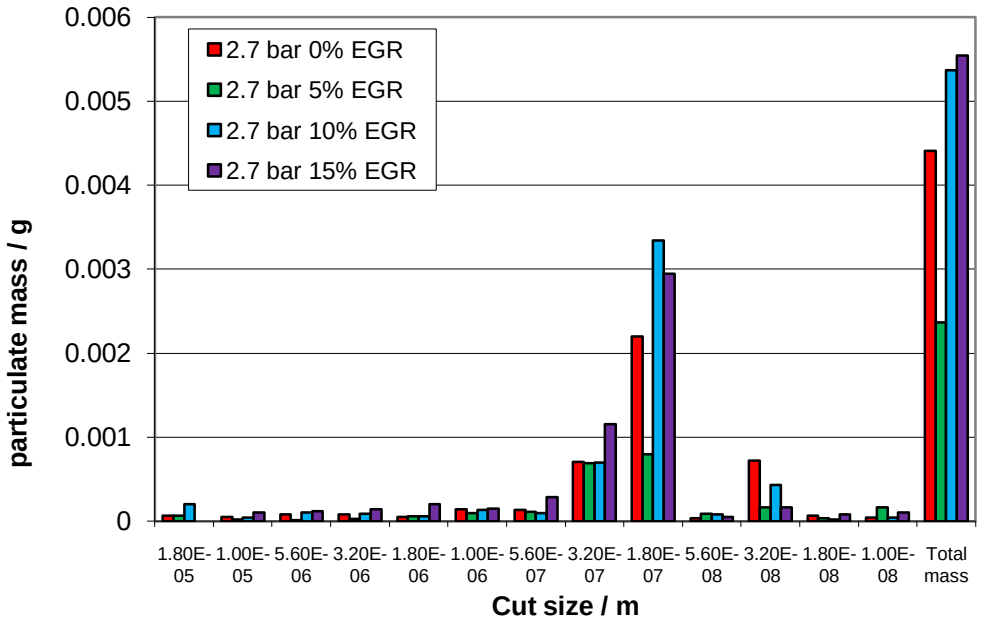

Figure 80 Particulate matter size distribution at 2.7 bar BMEP and 2% vol. hydrogen

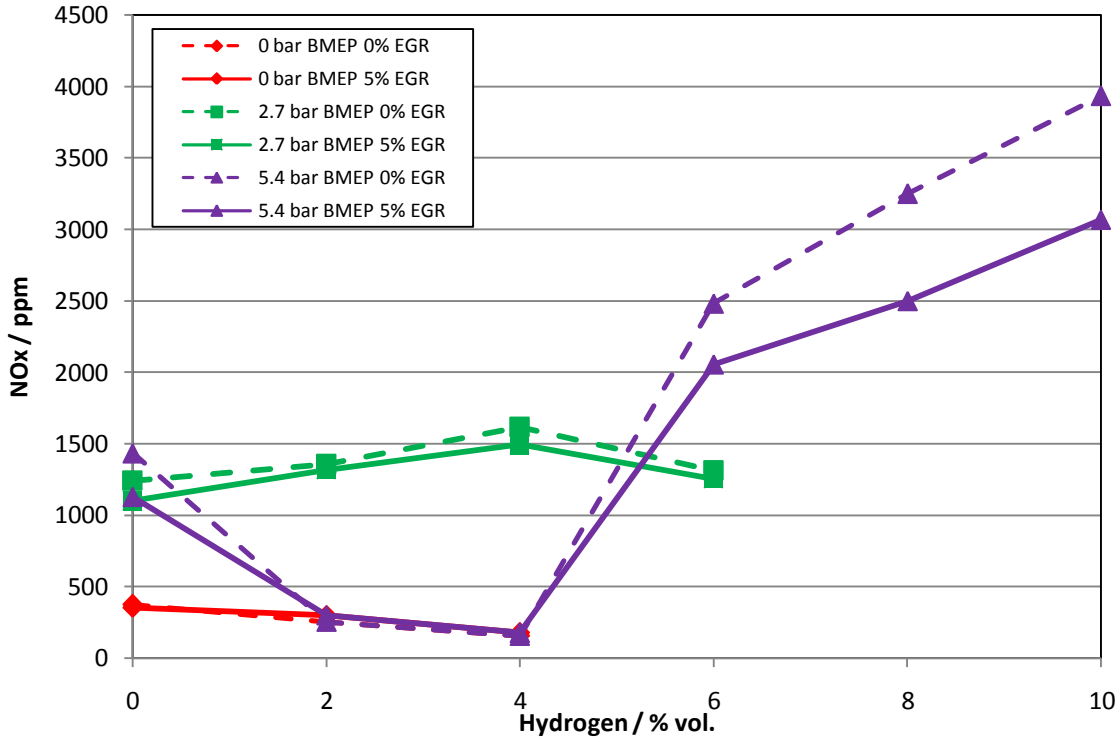

Figure 81 Nitrogen Oxide emissions at 1500rpm and 5% EGR

5.6 Optimum Hydrogen and EGR Strategy

The ultimate aim of this investigation was to determine if there was an advantage in terms of the emissions by using combined hydrogen and EGR addition. Since, as has been shown in the previous sections, the carbon monoxide emissions and filter smoke number always decrease with hydrogen addition, the total unburnt hydrocarbons and nitrogen oxides emissions are used as the emissions to determine the optimum operating strategy.

It should be pointed out here that the injection strategy has not been investigated since finding the most appropriate base point. With further investigation, this area may also improve the emissions of a combined diesel/hydrogen combustion engine. In particular, the use of multiple

injections to smooth the pressure curve will probably decrease the formation of NO_X as the maximum pressure, and therefore temperature, is reduced.

Using the information displayed in Figure 82, the operating point with the lowest THC emissions would be achieved using 10% EGR and 4%vol. hydrogen at 1500rpm and no load. The THC emissions are significantly reduced with hydrogen addition compared with the 0% vol. level which is pure diesel. The operating point for the lowest NO_X emissions would be using 4% vol. hydrogen and 30% EGR. This is a special case, because hydrogen addition at zero load can cause misfire, so the NO_X formation is reduced.

Given the information above, the recommended operating point based purely on the emissions would be 4% vol. hydrogen addition and 30% EGR, which would be the best compromise between NO_X reduction and THC reduction. However, this may not in reality be the most practical operating point to run, since the engine does misfire at this level.

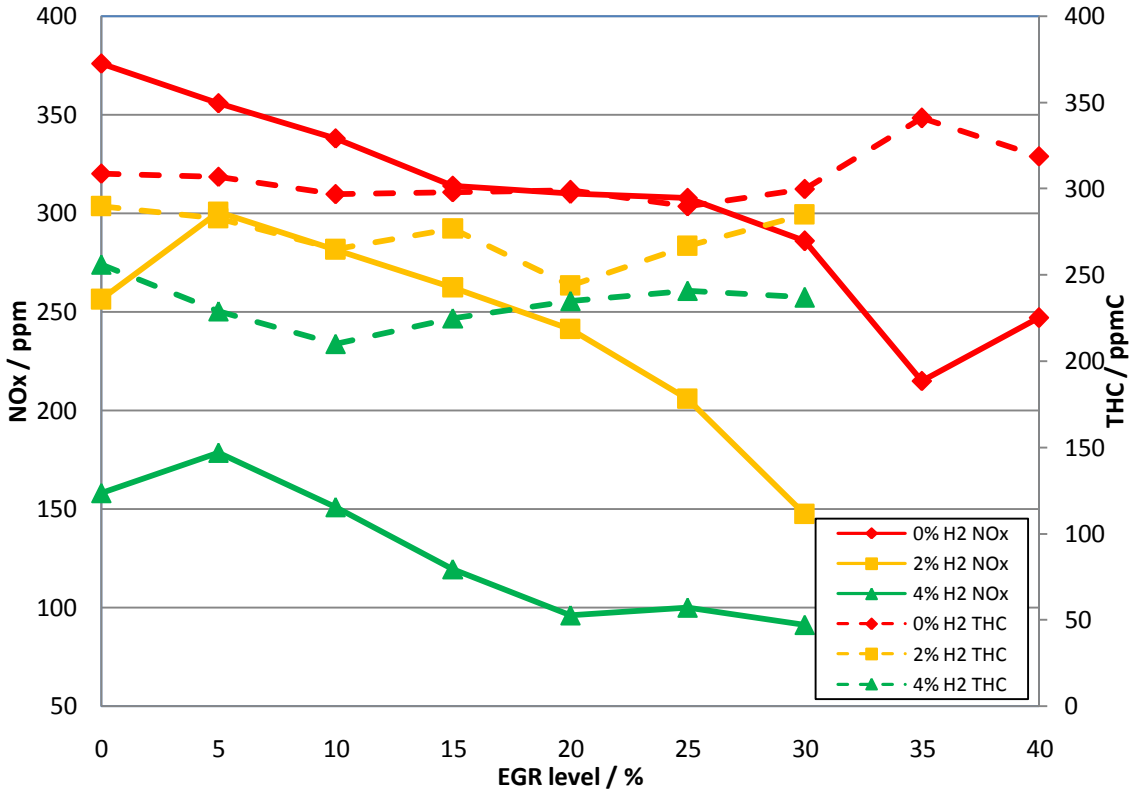

Figure 82 NO_X and THC emissions at 1500rpm and 0bar BMEP

The lowest recorded THC emissions at 1500rpm and 2.7 bar BMEP is with 6% vol. hydrogen addition and 0% EGR, as is shown in Figure 83. The addition of 6% vol. hydrogen can be seen to have significantly reduced the THC emissions even from the 4% vol. hydrogen level case. The lowest achievable NO_X emissions occur at 4% vol. hydrogen addition and 40% EGR, although this is almost identical to the 0% vol. hydrogen level.

The lowest combined emissions of NO_X and THC has to be a compromise in this case. Therefore, the recommended operating point would be 4% vol. hydrogen and 25% EGR. This point shows significant reduction in the NO_X emissions, but nothing like the best possible emissions of THC.

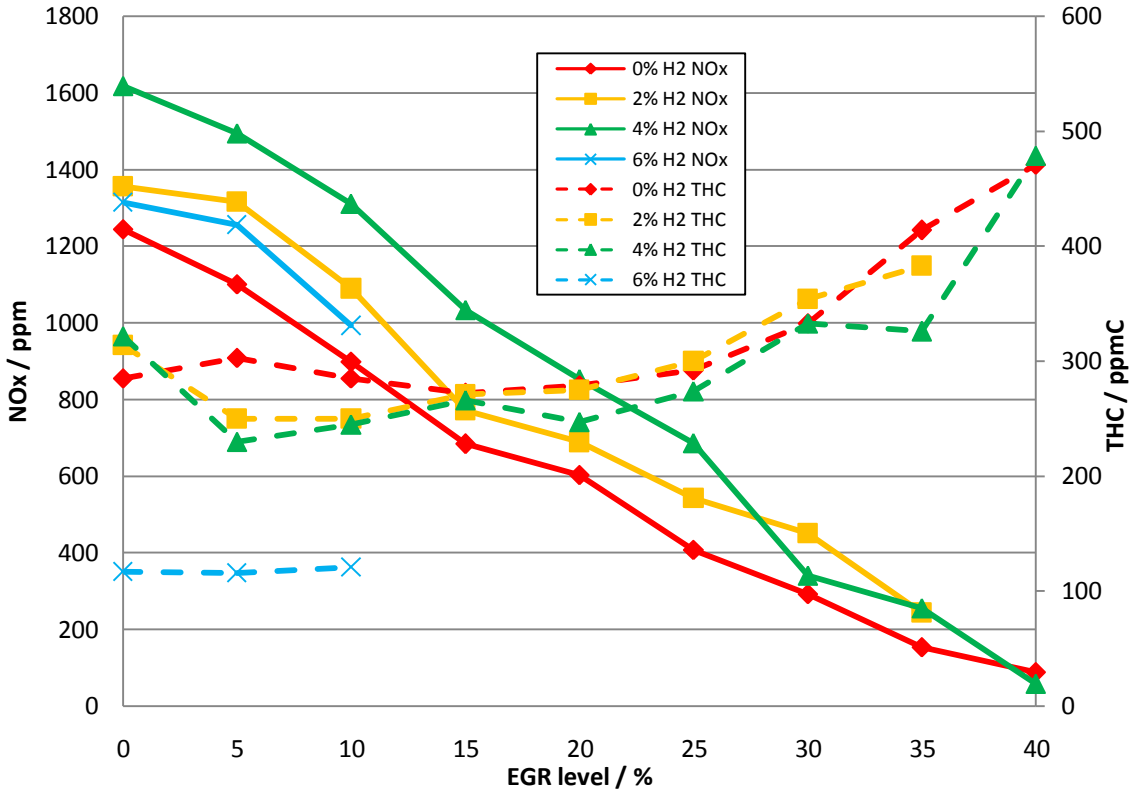

Figure 83 NO_X and THC emissions at 1500rpm and 2.7 bar BMEP

At 1500rpm and 5.4 bar BMEP, the lowest recorded THC emissions are at 6% vol. hydrogen addition and 5% EGR, as shown in Figure 84. The addition of EGR with high levels of hydrogen has little effect on the THC emissions at 5.4 bar BMEP. The lowest NO_X emissions are again at 4% vol. hydrogen and 30% EGR. At this point the THC emissions are actually higher than at the base point of pure diesel without EGR, making a compromise harder to find.

Given the problem of the NO_X versus THC trade off, the recommended operating point for 1500rpm and 5.4 bar BMEP is using 4% vol. hydrogen, and 20% EGR. This allows for a significant reduction in the NO_X formation from the base level, without there being a rise in the THC emissions from the corresponding 0% vol. hydrogen point.

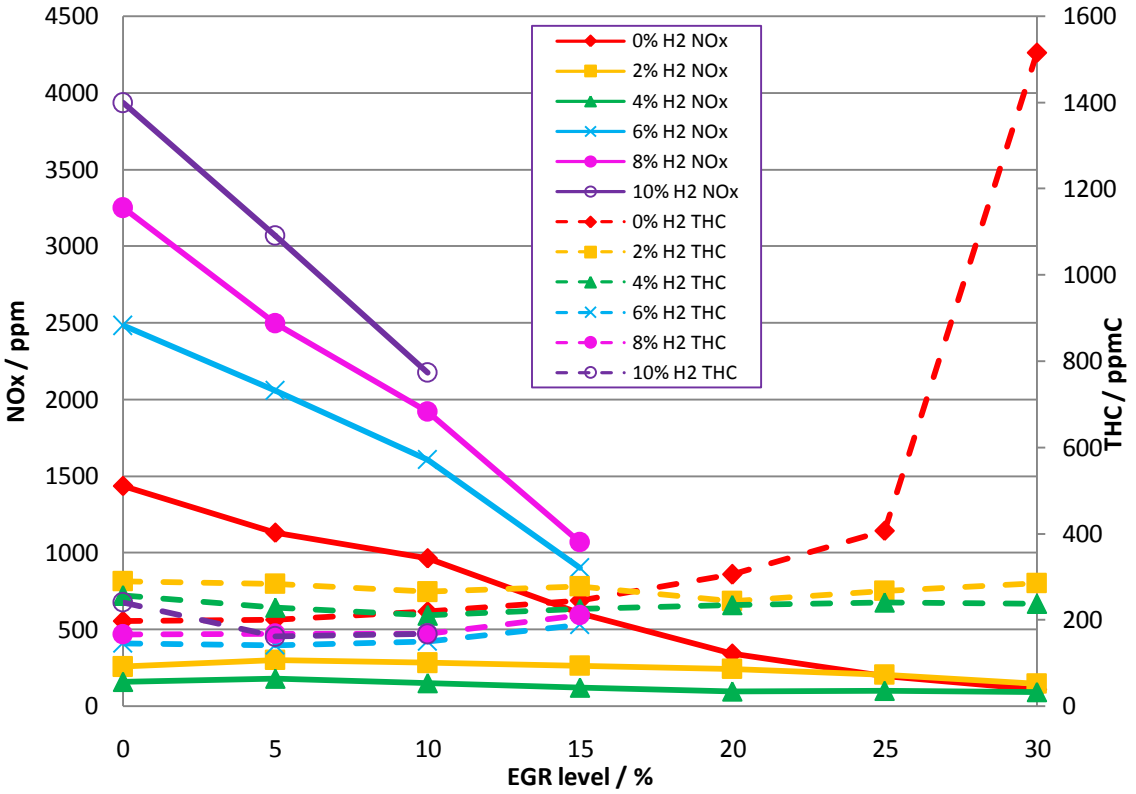

Figure 84 NO_X and THC emissions for 1500rpm and 5.4 bar BMEP

As is the case at 1500 rpm and 0 bar BMEP, at 2500 rpm there is a reduction in both NO_X and THC emissions with 4% vol. hydrogen addition and high levels of EGR. This can be seen in Figure 85. As was discussed in the case of 1500 rpm, this is mainly due to the high levels of misfire.

If the operating point was recommended based purely on the emissions, the best point for 2500 rpm and 0 bar BMEP would be 4% vol. hydrogen and 35% EGR. This is not the best operating point for the engine, however, due to the high in-cylinder pressure rise rate.

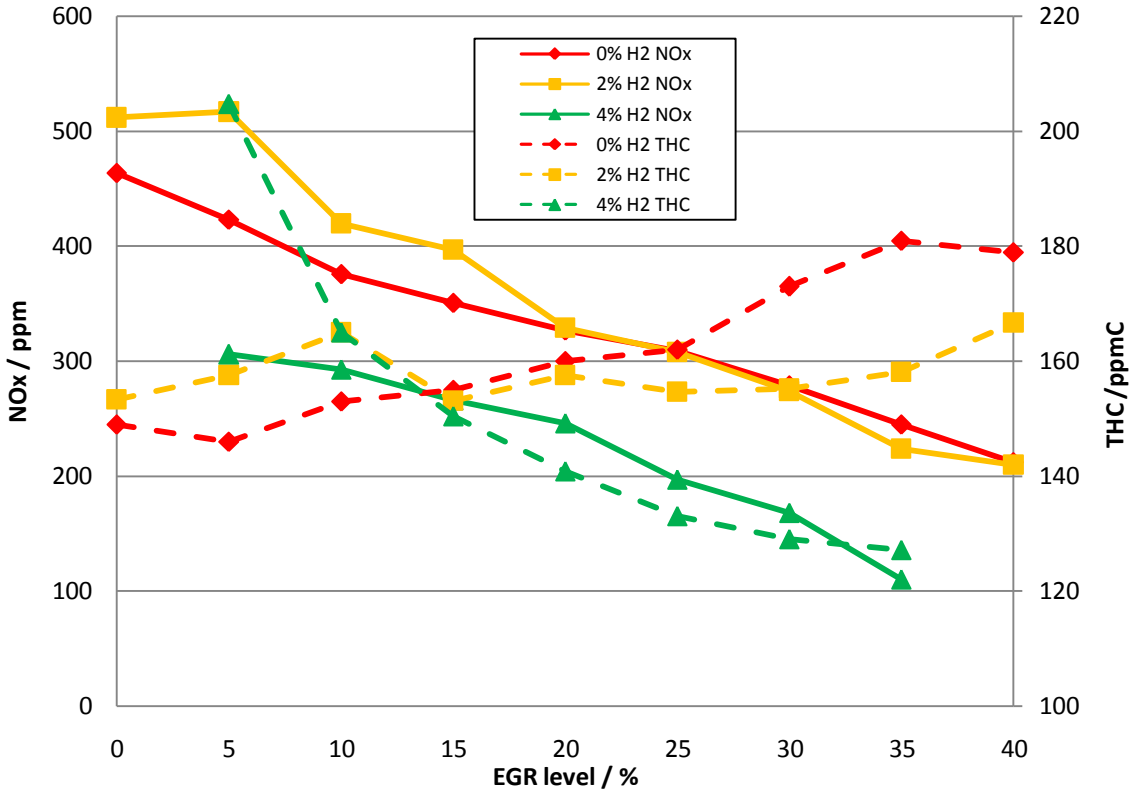

Figure 85 NO_X and THC emissions at 2500rpm and 0 bar BMEP

The lowest THC emissions recorded at 2500rpm and 2.7 bar BMEP was found to be at 4% vol. hydrogen and 15% EGR, as shown in Figure 86. The lowest NO_X emissions were found to be at 6% vol. hydrogen and 35% EGR. The reduction of NO_X with high levels of EGR addition means that the adverse effect of hydrogen addition can be almost completely negated.

The recommended operating point for 2500rpm and 2.7 bar BMEP is 4% vol. hydrogen and 40% EGR. Although this is not the lowest point of either the THC emissions or the NO_X emissions, this point shows significant decreases in both sets of emissions.

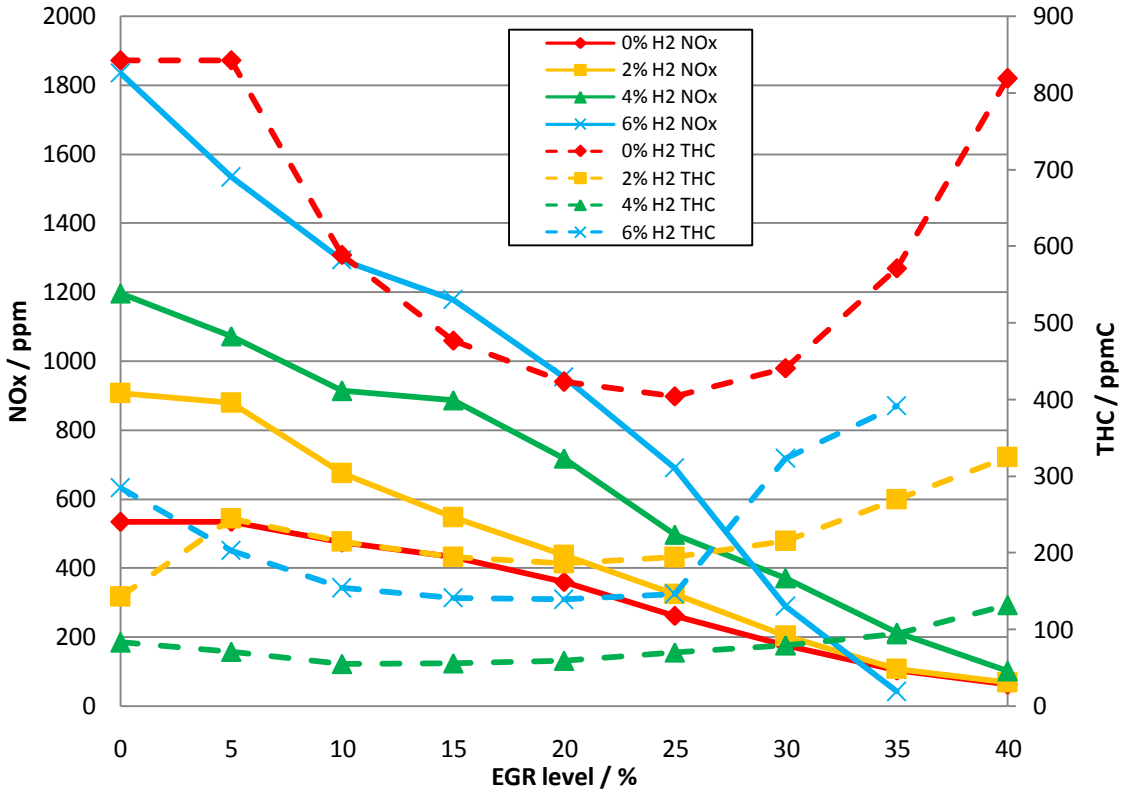

Figure 86 NO_x and THC emissions at 2500rpm and 2.7 bar BMEP

Finally, the lowest emissions of THC for 2500rpm and 5.4 bar BMEP were found from Figure 87 to be at 4% vol. hydrogen and 10% EGR. The lowest NO_X emissions were at 0% vol. hydrogen and 15% EGR. The high speed, high load combustion meant that the adverse effect on the NO_X emissions was most pronounced at this engine operating point.

The recommended operating strategy for 2500rpm and 5.4 bar BMEP is using 4% vol. hydrogen and around 12% EGR. This reduces the NO_X emissions from the base point of 0% vol. hydrogen and 0% EGR, and does not increase the THC.

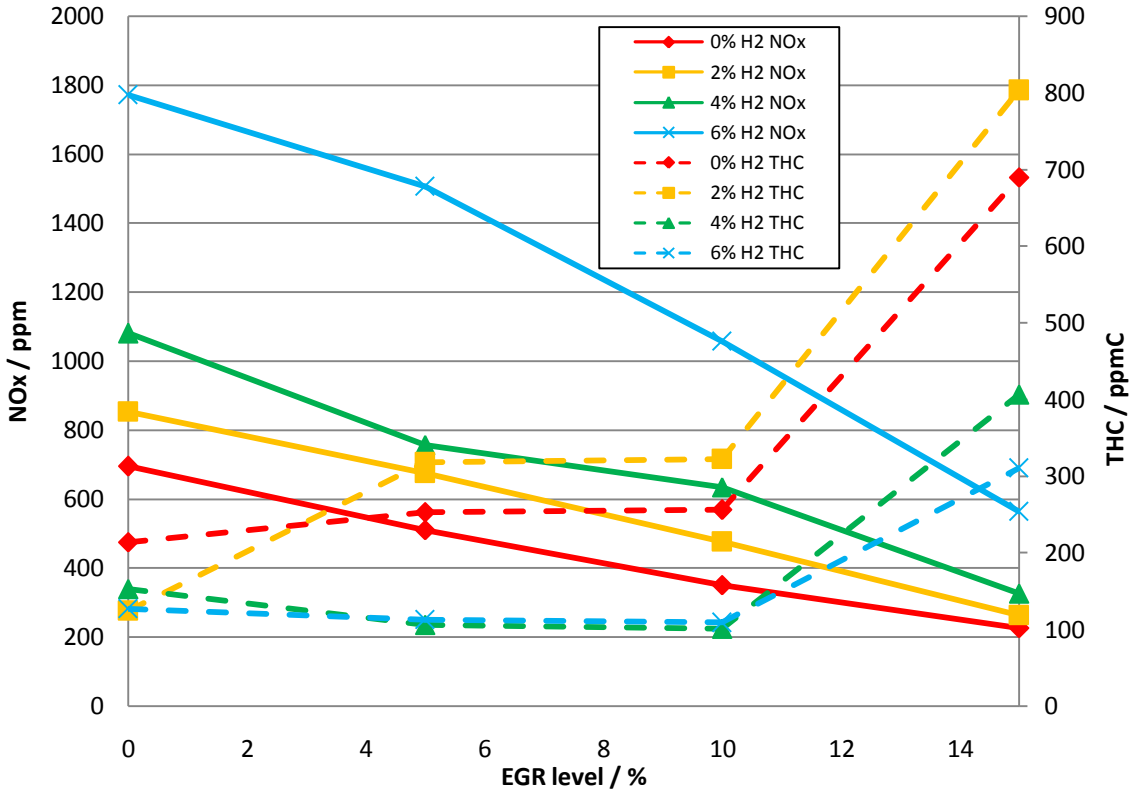

Figure 87 NO_X and THC emissions at 2500rpm and 5.4 bar BMEP

In order to appropriately map an engine for hydrogen and EGR addition, data from a larger number of operating points would be required. However, based on the information captured it seems clear that at idle or low load it would be most appropriate to run low or zero levels of hydrogen addition. In order to combat the production of NO_X, medium to high levels of EGR are required.

At medium load, hydrogen levels of around 4% vol. will significantly reduce the THC emissions. As the speed increases it is necessary to increase the EGR levels in order to control the NO_X emissions.

At high load, hydrogen levels of around 4-6 % vol. again have been shown to significantly reduce the THC emissions. Due to the adverse effects of EGR

at high loads and speed, the EGR levels should be decreased with speed at high loads.

Suggested engine maps for the combined addition of EGR and hydrogen are shown in Figure 88 and Figure 89. These maps are based on the data collected, and would need much better tuning before being applied to an engine, but give an idea of the necessary levels required to control the legislated emissions. The maps only cover the range of speeds and loads investigated. In order to extend the maps more work would be necessary due to the complex chemical kinetics and the non-linear behaviour of hydrogen with temperature and pressure.

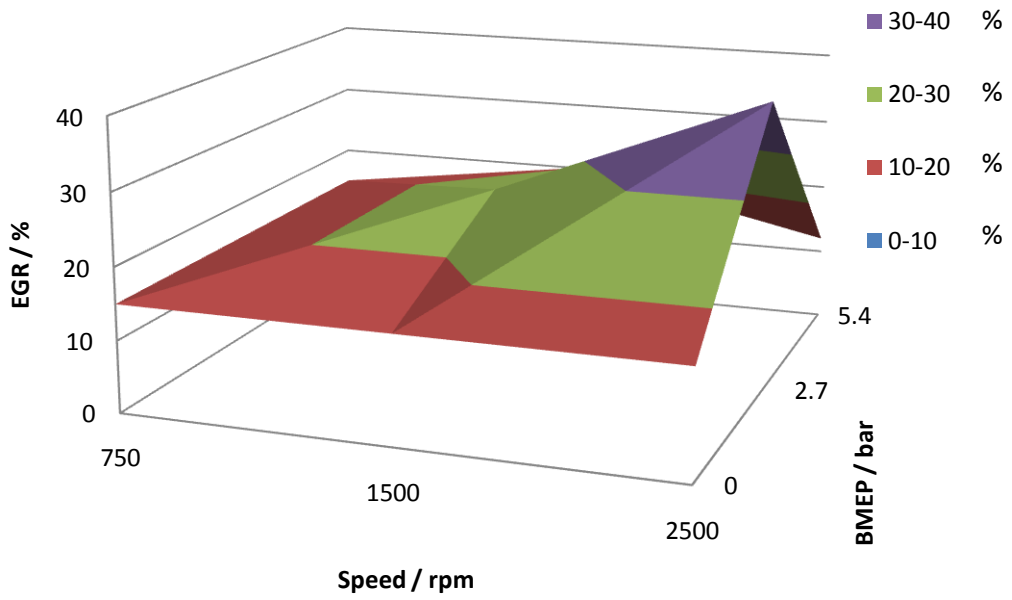

Figure 88 Suggested EGR map

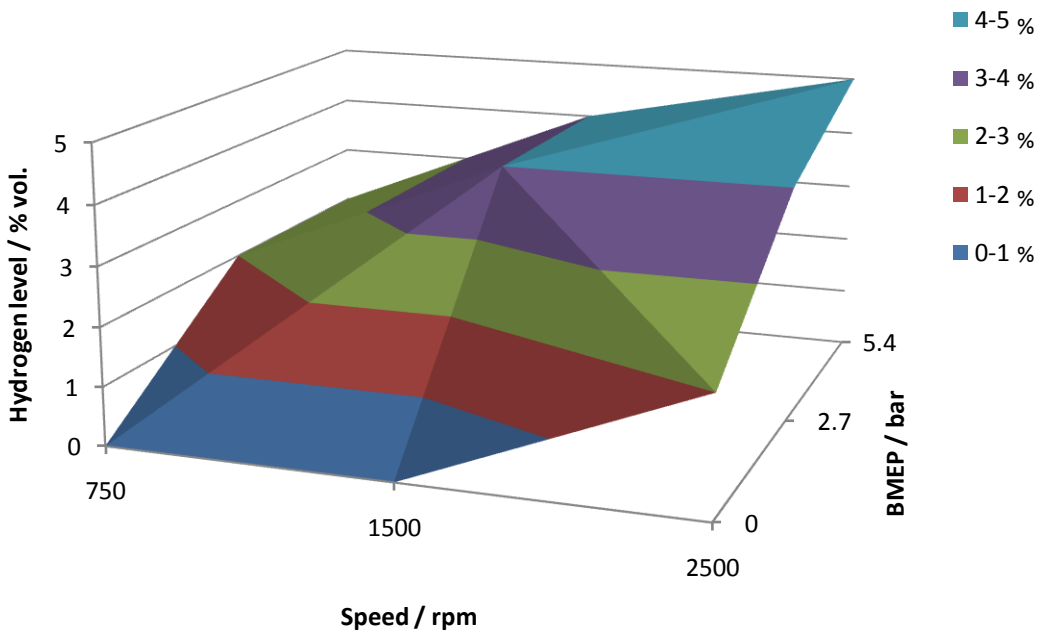

Figure 89 Suggested hydrogen addition map

5.7 Summary

This chapter has covered the investigation of the effects of hydrogen addition on the exhaust gas emissions and particulate matter size distribution using the nano-MOUDI. The results were also presented.

CHAPTER 6

GAS CHROMATOGRAPHY – MASS SPECTROMETRY

6 CHAPTER 6 GAS CHROMATOGRAPHY – MASS SPECTROMETRY

6.1 Introduction

Given the known adverse health effects of some of the chemical compounds emitted from diesel exhaust pipes, speciation of the THC allows for an assessment of the emissions under specific operating conditions. The aim of this part of the investigation was to determine any differences in the THC speciation with the addition of EGR or hydrogen, as well as when changing the fuel injection pressure. In the previous chapter, it was shown that hydrogen addition decreased the THC emitted however; this would not be an advantage if the proportion of carcinogens increased. To this end, a comparison of the hydrocarbon species under various conditions has been conducted.

6.2 Experimental Set-up

As described in Chapter 3, the set-up consisted of a HP 5890 gas chromatograph (GC) coupled to a TRIO-1 mass spectrometer. The column used was a (5%-Phenyl)-methylpolysiloxane (DB-5) stationary phase column, of 30 m length, 0.25 mm internal diameter and a 0.25 μm film thickness. The carrier gas used was helium, supplied from a compressed gas cylinder. It was necessary to calibrate the GC-MS set-up for either the low molecular mass measurements, or high molecular mass measurements.

6.2.1 Low molecular mass set-up

For the low molecular mass experiments, the 6-way gas injection port was used to inset the sample. A 5 mL hypodermic syringe was used to measure and transfer the gas sample from the gas collection bubble to the GC. The helium pressure was held at 10 psi by the pressure regulator. The temperature map used is given in Table 8. This temperature program allowed for good separation, while taking less than 52 minutes. The mass spectrometer was set to scan from 40 to 150 atomic mass units (amu) at 0.52 seconds per scan. This meant that any air 'noise' was eliminated, allowing for a cleaner chromatogram to be captured.

6.2.2 High molecular mass set-up

In order to conduct the high molecular mass experiments particulates were captured from the exhaust gas stream on filter substrates. Prior to testing it was necessary to remove the captured chemicals from the filter substrates to allow them to be transferred to the GC. This was done using 2 mL of acetone to dissolve the chemicals. The split/splitless injection port was used, and a sample of 5 μL was measured and injected using a hypodermic syringe. The temperature map used is given in Table 8. Again, this allows for good separation, whilst minimising the time taken for the test. The mass spectrometer was set to scan from 100 to 300 amu at 0.52 seconds per scan.

Low molecular mass program	High molecular mass program
Initial temperature – 30 ^{O}C for 10 minutes	Initial temperature – 40 ^{O}C for 8 minutes
Ramp – 8 ^{O}C per minute up to 250 ^{O}C	Ramp – 40 ^{O}C per minute up to 100 ^{O}C
Hold 250 ^{O}C for 10 minutes	Ramp – 10 ^{O}C per minute up to 300 ^{O}C
	Hold 300 ^{O}C for 8 minutes

Table 8 Temperature programs for the GC

6.3 Chemical Investigation

Due to the known adverse health effects of certain hydrocarbons, this investigation focused on a number of chemicals which can cause most damage.

6.3.1 Low molecular mass chemicals

The full list of the identified low molecular mass chemicals is given in Table 9 with their retention times (under the specified conditions).

Chemical name	Retention time / minutes
Nonane	10.5
4-methyl-2-propyl-1-pentanol	12.5
1,2,3-trimethyl-benzene	13.8
2,4-nonadiene	14.6
Decane	15.2
2,2-dimethyl-heptane	17.2
Undecane	17.9
Dodecane	20.1
2,7-dimethyl-octanol	22.1
Tridecane	23.2
Pentyl-ethylene oxide	23.8
Tetradecane	25.5

Table 9 Low molecular mass chemicals

As can be seen from the chemicals listed and the diesel chromatogram shown in Figure 90, most of the low molecular mass compounds indentified are remnants of unburnt fuel, plus a few oxidised components of incomplete combustion. Details of the chemical are given in the following sections [USEPA].

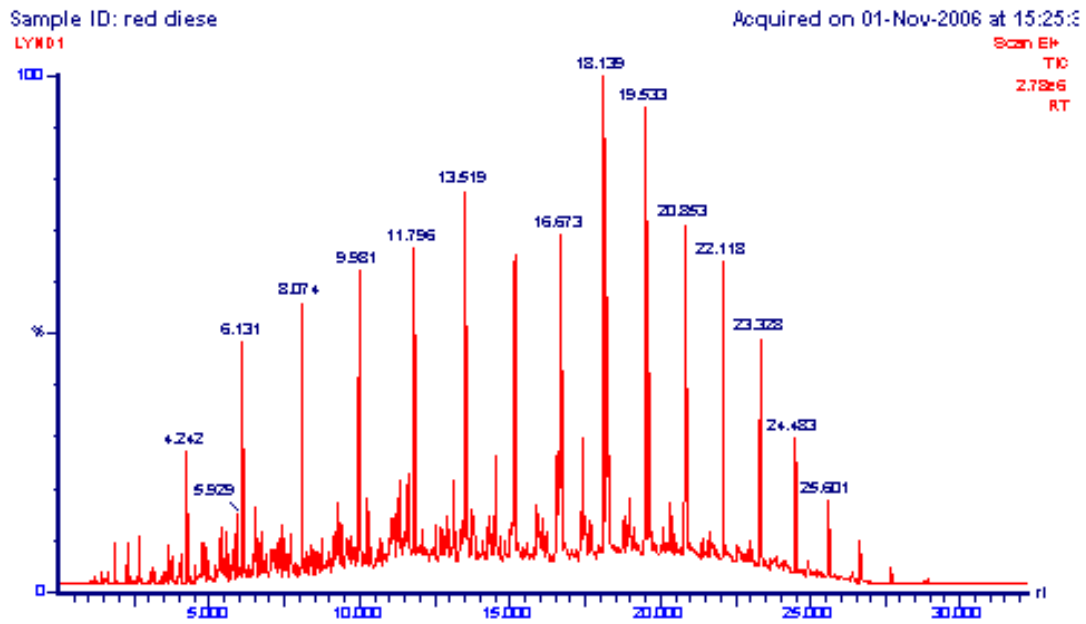

Figure 90 Diesel Fuel chromatogram

6.3.1.1 Alkanes

The alkanes listed above (nonane, decane, 2,2-dimethyl-heptane, undecane, dodecane, tridecane and tetradecane) are all components of the diesel fuel. The diesel chromatogram, shown in Figure 90, shows the various components of the fuel used. Alkanes are not normally harmful to health (hexane is the only exception to this), however, these emissions still indicate wasted fuel. The structure of alkanes are shown in Figure 91.

Figure 91 Chemical structure of alkanes

6.3.1.2 Alcohols

There are two alcohols which were identified in the exhaust emissions: 4-methyl-2-propyl-1-pentanol and 2,7-dimethyl-octanol. Alcohols are based on alkanes, with a hydroxyl functional group. Where ethanol has limited toxicity for humans, other alcohols are not so easily metabolised. Depending on the structure and the break down point, alcohols can form formaldehyde in the gut. This causes severe liver damage, blindness or death in extreme cases. Alcohols themselves can cause respiratory failure. The structure of methanol, the most basic alcohol, is shown in Figure 92.

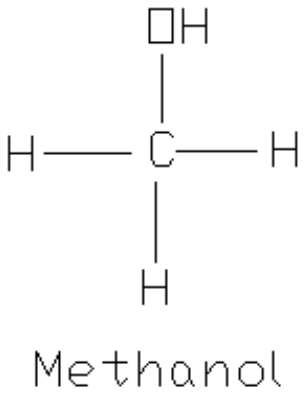

Figure 92 Chemical structure of methanol

6.3.1.3 1,2,3-trimethyl-benzene

Trimethyl-benzene is an aromatic compound with 3 methyl groups. It is known to cause severe skin irritation when even low concentrations are handled. If left it causes burns. By inhalation trimethyl-benzene causes respiratory difficulties. The chemical structure of trimethyl-benzene is shown in Figure 93.

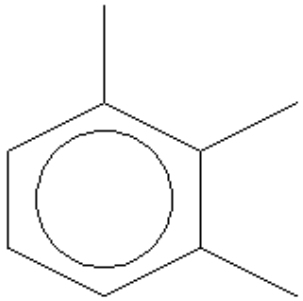

1,2,3-trimethyl-benzene

Figure 93 Chemical structure of trimethyl-benzene

6.3.1.4 2,4-nonadiene

Nonadiene is a straight chain hydrocarbon with 2 double bonds, as shown in Figure 94. It is an irritant, but has no other known adverse health effects.

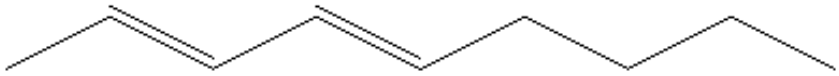

2,4-nonadiene

Figure 94 Chemical structure of 2,4-nonadiene

6.3.1.5 Pentyl-ethylene oxide

Ethylene oxide is an important industrial chemical, used for sterilizing medical supplies and food. However, it is toxic by inhalation, causing headaches and dizziness. Continued exposure can cause seizures and eventually coma. It also affects the respiratory system, and cause a build up

of fluid in the lungs hours after the exposure. Chronic exposure increases the risk of cataracts and possibly liver cancer. By dermal contact, ethylene oxide is a severe irritant. Ethylene oxide can cause miscarriage, or mutations of the unborn foetus. As such it is classified as carcinogenic to humans by the International Agency for Research on Cancer (IARC). The structure of pentyl-ethylene oxide is shown in Figure 95.

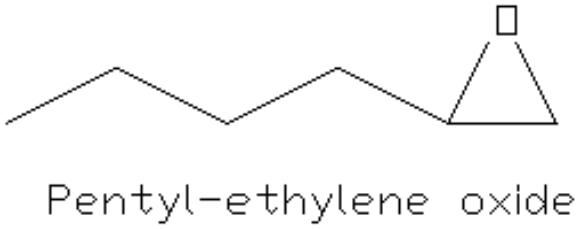

Figure 95 Chemical structure of pentyl-ethylene oxide

6.3.2 High molecular mass chemicals

The high molecular mass chemicals which were examined are listed in Table 10. Each of the chemicals listed were chosen based on their harmful properties, as detailed below [USEPA].

Chemical name	Retention time / minutes
Pentanone	2.6 and 5.4
Toluene	3.5, 4.4, 5.5 and 5.9
Xylene	6.2
Dimethyl-aniline	8.1 and 8.8
Napthalene	8.4
Heptanoic Acid	8.8 and 9.3
Benz[a]anthracene-7,12-dione	10.0 and 16.8
Fluorene	10.2
Anthracene	11.2
Fluoranthrene	13.0
Pyrene	13.4

Table 10 High molecular mass chemicals

6.3.2.1 Pentanone

Pentanone is a member of the ketone family, which has a carbonyl functional group. A schematic of pentanone is shown in Figure 96. Although pentanone is one of the main components of the high molecular mass exhaust, it is not listed at a hazardous substance, and has no known ill health effects.

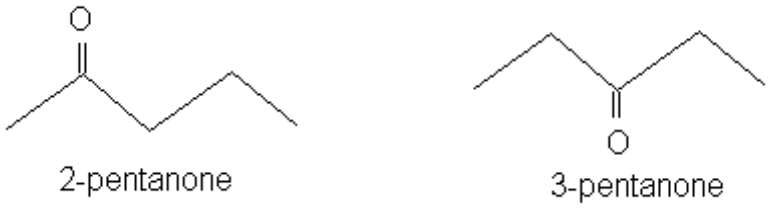

Figure 96 Chemical structure of pentanone

6.3.2.2 Toluene

Toluene, also known as methyl-benzene, is an aromatic hydrocarbon. This means that it contains a benzene ring. A schematic of toluene is shown in Figure 97. In small doses toluene has no ill health effects. In concentrations greater than 100 ppm, however, symptoms can include tiredness, dizziness, headaches, loss of coordination or hearing, euphoria, insomnia, nausea, eye and nose irritation, rapid delay of reaction time, unconsciousness, and death at levels of 4,000 ppm.

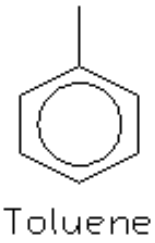

Figure 97 Chemical structure of toluene

6.3.2.3 Xylene

Xylene is an aromatic compound with two methyl groups, as shown in Figure 98. According to the US Environmental Protection Agency (USEPA), the health effects of xylene can include dizziness, lack of muscle control, headaches, confusion, nausea, skin, eyes and throat irritations. Xylene is not a known carcinogen.

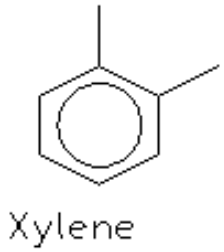

Figure 98 Chemical structure of xylene

6.3.2.4 Napthalene

Napthalene is a polycyclic aromatic hydrocarbon (PAH), as shown in Figure 99. Acute exposure to naphthalene via inhalation, ingestion or dermal contact is reported to cause damage to the liver, haemolytic anaemia and neurological damage. Cataracts may also result from ingestion or inhalation. Chronic exposure causes retinal damage and cataracts. Napthalene is classed as a possible human carcinogen by the USEPA.

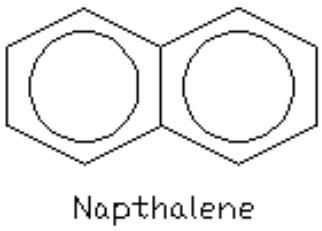

Figure 99 Chemical structure of napthalene

6.3.2.5 Heptanoic Acid

Heptanoic acid, also known as enanthic acid, is harmful by inhalation, ingestion and through skin contact. This acid is highly corrosive, and causes

burns on contact. By inhalation, sever damage can be inflicted on the mucous membranes.

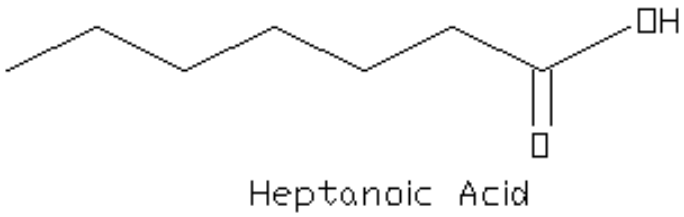

Figure 100 Chemical structure of heptanoic acid

6.3.2.6 Benz[a]anthracene-7,12-dione

Benzo[a]anthracene-7,12-dione is a PAH and a possible human carcinogen. It is also a known mutagen, and causes damage to aquatic organisms. It is expected to cause long term damage to the environment.

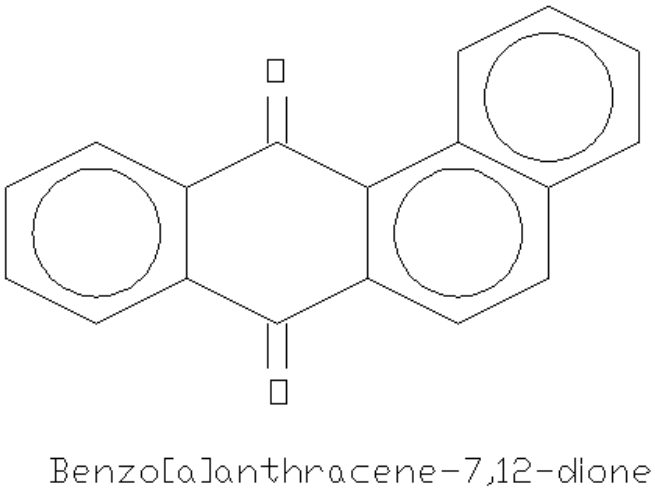

Figure 101 Chemical structure of benzo[a]anthracene-7,12-dione

6.3.2.7 Fluorene

Fluorene is another PAH, and as such has similar health effects as others. Fluorene is known to damage skin and the immune system.

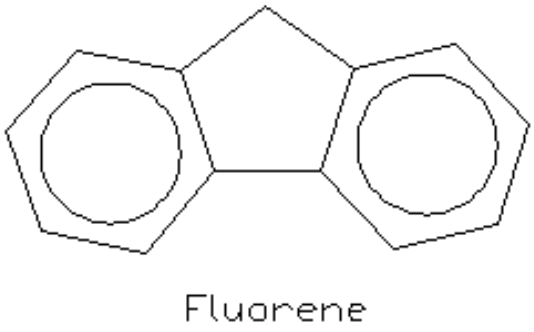

Figure 102 Chemical structure of fluorene

6.3.2.8 Anthracene

Anthracene is one of the more harmful PAHs, without being classed as a carcinogen in humans (It is carcinogenic in rodents). It can cause damage to eyes, nose, throat and skin through inhalation or dermal contact. By ingestion multiple organs are affected, including the liver, lungs, mammary glands and the stomach.

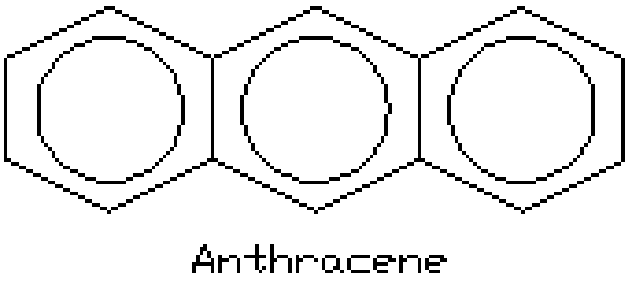

Figure 103 Chemical structure of anthracene

6.3.2.9Fluoranthrene

Fluoranthrene is a PAH, and a component in creosote. It can cause irritation to skin and eyes. If not washed off immediately, or when in contact with sunlight, fluoranthrene causes burns. When inhaled fluoranthrene causes dizziness, nausea, respiratory difficulties and possible collapse.

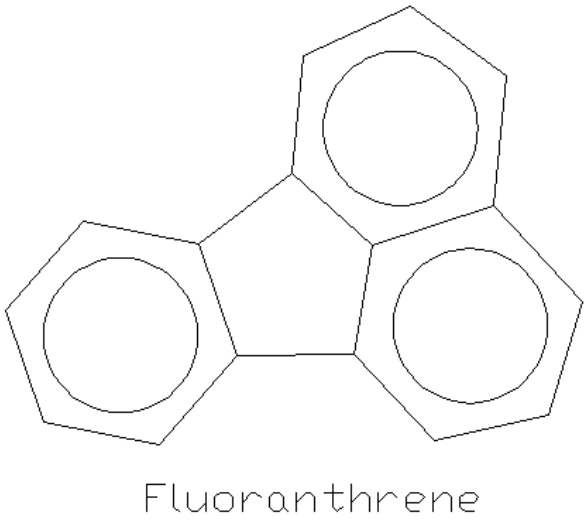

Figure 104 Chemical structure of fluoranthrene

6.3.2.10 Pyrene

Pyrene is the smallest peri-fused polycyclic aromatic hydrocarbon. It is a product of incomplete combustion of any organic material. Pyrene can cause irritation to eyes and skin, but is not known to affect any other organs.

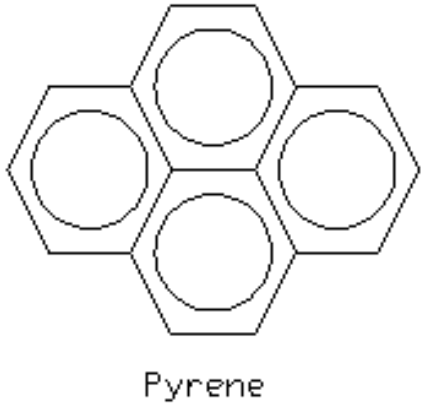

Figure 105 Chemical structure of pyrene

6.4 Experimental Test Matrix

This experimental work looked at the effects of hydrogen addition, EGR level and injection pressure on the chemical composition of the total unburnt hydrocarbons. To this end, the hydrogen addition levels were 0 % vol., 2 % vol. and 4 % vol. The EGR was varied between 0 and 15% in 5% steps. This was all carried out at the base point of 2.7 bar BMEP, 1500 rpm, 800 bar injection pressure and with a single injection at 9 CAD BTDC.

To investigate the effect of the injection pressure on the chemical composition of the THC 6 further tests were carried out at each of 400 bar and 1200 bar injection pressure. The hydrogen addition levels were again 0 % vol., 2 % vol. and 4 % vol., but the EGR levels used were only 0 and 10%.

6.5 Results and Discussion

For the purposes of the results and discussion section, each of the tests has been labelled 1-24, as shown in Table 11. The different chemical compounds are labelled A- V, as shown in Table 12.

Test label	EGR level / %	Hydrogen level / % vol.	Injection Pressure / bar
1	0	0	800
2	5	0	800
3	10	0	800
4	15	0	800
5	0	2	800
6	5	2	800
7	10	2	800
8	15	2	800
9	0	4	800
10	5	4	800
11	10	4	800
12	15	4	800
13	0	0	1200
14	10	0	1200
15	0	2	1200
16	10	2	1200
17	0	4	1200
18	10	4	1200
19	0	0	400
20	10	0	400
21	0	2	400
22	10	2	400
23	0	4	400
24	10	4	400

Table 11 Labels for each operating condition for the tests

Chemical label	Chemical name
A	Nonane
B	4-methyl-2-propyl-1-pentanol
C	1,2,3-trimethyl-benzene
D	2,4-nonadiene
E	Decane
F	2,2-dimethyl-heptane
G	Undecane
H	Dodecane
I	2,7-dimethyl-octanol
J	Tridecane
K	Pentyl-ethylene oxide
L	Tetradecane
M	Pentanone
N	Toluene
O	Xylene
P	Napthalene
Q	Heptanoic Acid
R	Benz[a]anthracene-7,12-dione
S	Fluorene
T	Anthracene
U	Fluoranthrene
V	Pyrene

Table 12 Chemical labels

6.5.1 Low molecular mass

The results of the low molecular mass gas chromatography-mass spectrometry tests are shown in Table 13. It should be noted here that the chromatograms are purely qualitative results. For the quantitative results

the THC measurements discussed in the previous chapters should be used. A typical low molecular mass chromatogram is shown in Figure 106.

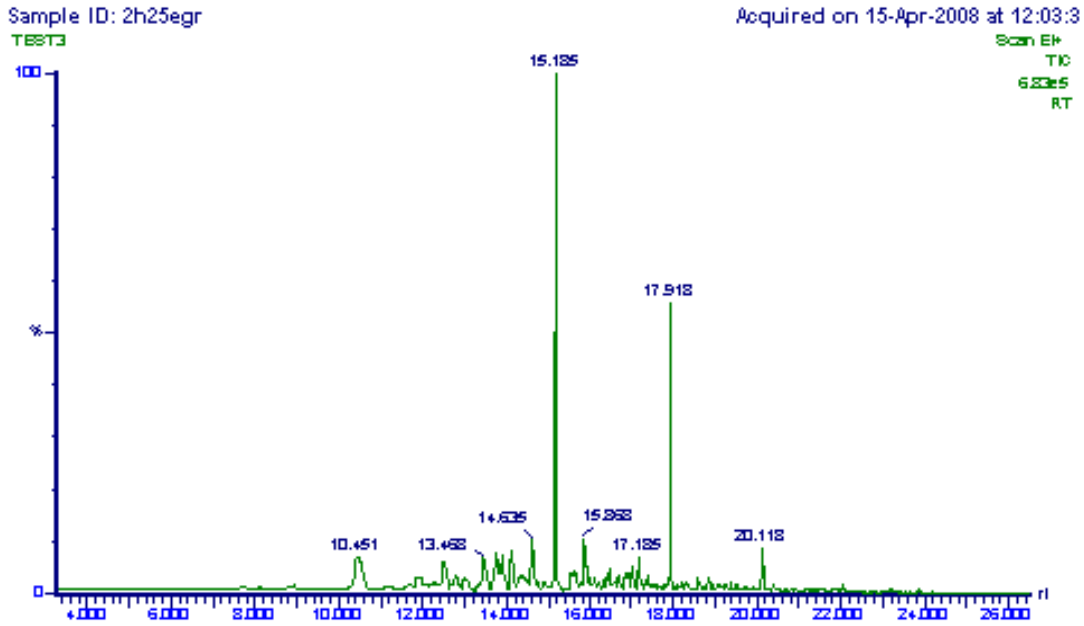

Figure 106 Low molecular mass chromatogram

	A	B	C	D	E	F	G	H	I	J	K	L
1	X			X	X		X	X				
2	X	X		X	X		X	X				
3		X		X	X		X	X				
4				X	X		X	X	X			
5			X		X		X	X	X		X	
6	X			X	X		X	X				
7			X		X		X	X	X			
8				X	X		X	X	X			
9					X		X	X	X			
10	X	X		X	X		X	X				
11				X	X		X	X	X			
12					X		X	X	X			
13					X		X	X	X			
14					X		X	X	X	X		
15					X		X	X	X		X	
16					X		X	X	X	X		
17					X		X	X	X	X		
18					X		X	X	X	X		
19					X		X	X	X	X		
20					X		X	X	X		X	
21					X	X	X	X	X	X		X
22					X	X	X	X	X	X		
23						X	X	X	X	X		
24						X	X	X	X	X		

Table 13 Results of the low molecular mass gas chromatography-mass spectrometry tests

6.5.1.1 Effects of EGR

Generally, as the EGR level increases, so do the molecular masses of the compounds identified. As can be seen from Table 13, there is a significant

overlap of compounds identified at all EGR levels. Once again, the 'anomaly' of the 5% EGR condition can be seen in that nonane is always seen at this point. Otherwise nonane is only identified in the 0% EGR, 0% vol. H_2 case.

The increased combustion of shorter chain molecules suggests that the addition of EGR helps with the vaporisation of these molecules, allowing them to burn. Although with the addition of EGR the maximum in-cylinder pressure, and therefore temperature increase, is decreased, the higher initial temperatures can account for this improved vaporisation.

6.5.1.2 Effects of Hydrogen

The effect of hydrogen addition at 800 bar injection pressure is minimal. As can be seen from Table 13, comparing like for like conditions increasing hydrogen addition either results in the loss of one compound, or the exchange of one compound for its neighbour. This is definitely a good result. Since it has already been shown that addition of hydrogen in this manor decreases the emissions of THC and smoke, the purpose of this investigation was to determine whether or not hydrogen addition increased the production of toxins. Since the results for the cases with hydrogen are similar, or identical, to the cases without, it must be concluded that the only disadvantage of hydrogen addition is the slight increase in NO_X production, as discussed in the previous chapter.

6.5.1.3 Effects of Injection Pressure

As can be seen from Table 13, when the injection pressure was increased to 1200 bar, the range of compounds identified was smaller. This is due to the higher injection pressure producing better atomisation of the fuel, and in

particular the lower molecular mass fraction of the fuel. The smallest compound identified at the 1200 bar injection pressure case is decane, whereas at 800 bar, nonane is one of the unburnt fuel fractions.

Decreasing the injection pressure, as seen in Table 13, results in an increase in the higher molecular mass fraction of the fuel to be identified as unburnt hydrocarbons. As the injection pressure is decreased, the fuel atomisation will deteriorate. This will be more apparent with the longer chain molecules with higher viscosities and evaporation points, resulting in these molecules not burning properly. The combination of low injection pressure and increased ignition delay due to the addition of 2% vol. hydrogen has resulted in the only case of tetradecane being identified.

6.5.1.4 Low molecular mass summary

The important point to note here is that the two harmful compounds in the low molecular mass range – 1,2,3-trimethyl-benzene and pentyl-ethylene oxide – are only identified under certain conditions. Given this fact, it is possible to avoid their production by careful set-up of the engine operating conditions. Pentyl-ethylene oxide is only produced at 3 specific operating points: 0% EGR, 2%vol. H_2 and 800 bar injection pressure, 0% EGR, 2% vol. H_2 and 1200 bar injection pressure and 10% EGR, 0% vol. H_2 and 400 bar injection pressure. This being the case it would be advisable to avoid all of these operating points. 1,2,3-trimethyl-benzene is only found at 2 operating points: 0% and 10% EGR, 2% vol. H_2 and 800 bar. These, too, should be avoided.

6.5.2 High molecular mass

The results of the high molecular mass gas chromatography-mass spectrometry tests are shown in Table 14. As for the low molecular mass case, the results presented here are purely qualitative. The quantitative results have been presented in the previous chapter.

Contrary to the clear chromatograms collected for the low molecular mass tests, the high molecular mass cases were less clear, as seen in Figure 107. The intensity is so much lower than that seen in the low molecular mass cases that in many cases the 'noise' interferes with the accurate identification of the compounds.

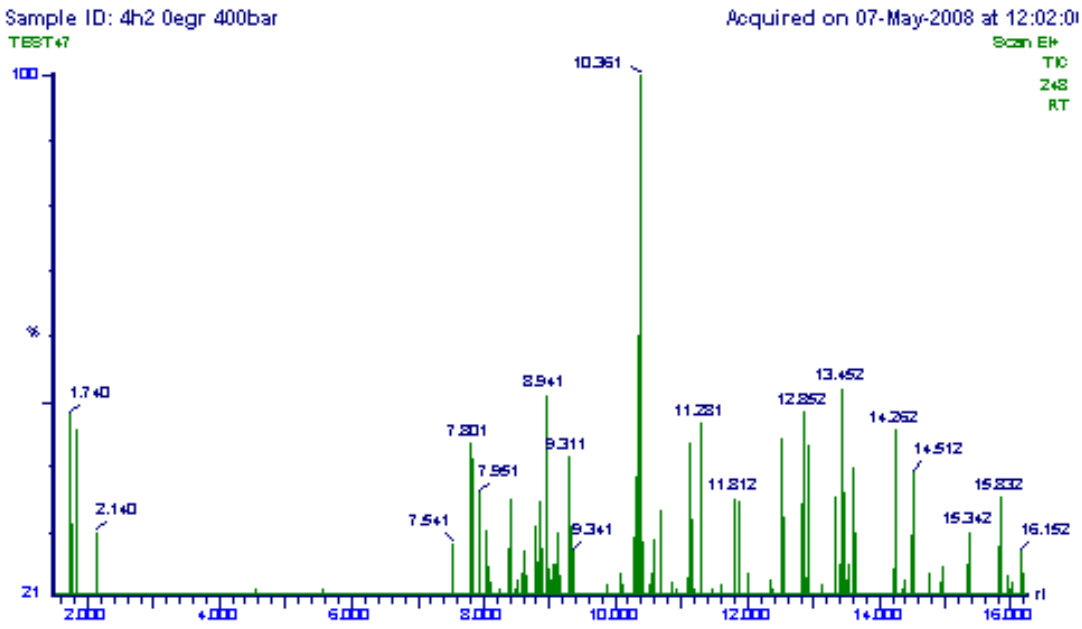

Figure 107 High molecular mass chromatogram

	M	N	O	P	Q	R	S	T	U	V
1	X	X	X		X					X
2		X	X				X			X
3		X	X				X			X
4		X	X				X			X
5	X	X	X				X	X		X
6			X		X				X	X
7			X	X			X	X		X
8	X	X	X	X						
9	X	X	X			X	X	X		X
10		X	X							X
11	X	X	X	X						
12			X		X		X			
13	X	X	X			X	X			X
14	X	X	X	X			X			X
15	X	X	X	X				X		X
16	X	X	X	X	X			X		X
17	X	X	X	X				X		X
18	X	X	X	X	X			X		
19	X	X	X	X			X	X		X
20	X	X	X				X	X		
21	X	X	X	X	X		X	X		X
22	X	X	X	X				X		X
23	X			X	X		X	X		X
24	X	X	X		X		X			X

Table 14 Results of the high molecular mass gas chromatography-mass spectrometry tests

6.5.2.1 Effects of EGR

As is known increasing levels of EGR increase the THC and smoke emissions. This however, does not directly translate into a greater number

of compounds being identified. In fact, the combination of EGR and hydrogen actually decreases the compounds produced, as can be seen from Table 14. In the instances without hydrogen, the identified compounds are very similar over the entire range of EGR levels. Although EGR may produce higher concentrations of THC and smoke, there is no noticeable effect on the high molecular mass compounds identified.

In terms of which compounds have been identified, all of the high molecular mass compounds were chosen based on their effects on human health, so ideally it would be best if none of the compounds were identified. Only napthalene is a known carcinogen however, and the cases where this compound was identified are numerous. At the optimum injection pressure, napthalene was only identified at high levels of EGR in combination with hydrogen addition. It would therefore be advisable to avoid these operating conditions.

6.5.2.2 Effects of Hydrogen

As was stated in the previous section, the combination of hydrogen and EGR has actually decreased the number of compound identified. Since the aim of this investigation was designed to ascertain that hydrogen addition does not increase the formation of harmful hydrocarbon emissions, the similarity between the results with and without hydrogen leads to the conclusion that this is an effective way to control THC and smoke emissions.

The carcinogenic compound napthalene is produced at various hydrogen levels, and seems to be more dependent on the injection pressure and the EGR level used. The effects of the injection pressure and EGR level vary depending on how they are combined. Combinations of high EGR and

hydrogen at 800 bar produced napthalene. At 1200 bar the addition of EGR or hydrogen resulted in napthalene production. Conversely, at 400 bar the addition of hydrogen produced napthalene, and only the combination of 10% EGR and 2% vol. hydrogen produced napthalene.

6.5.2.3 Effects of Injection Pressure

It can be seen in Table 14 that the effect of increasing the injection pressure had minimal effect on the compounds identified. This was not the case in the low molecular mass case, where increasing the injection pressure, and therefore the fuel atomisation, increased the complete combustion of the fuel. As was stated earlier, the only carcinogen which was tested for was napthalene. With the 1200 bar injection pressure tests, the combination of EGR or hydrogen addition both produced napthalene. In fact the only 1200 bar test which did not produce napthalene was the 0% EGR and 0% vol. hydrogen addition. It would therefore be advisable to avoid very high pressure injections at this operating point for the health effects.

As was the case in the low molecular mass case, decreasing the injection pressure meant that the fuel was not atomised properly and therefore resulted in incomplete combustion. This meant a higher number of compounds being identified, both from unburnt fractions of the fuel and products of incomplete combustion. Unlike the cases with the optimum injection pressure or the high injection pressure, the combination of 400 bar and 0% EGR always produced napthalene. The combination of 10% EGR and 2% vol. hydrogen also produced napthalene at this operating condition. This being the case, it is recommended that low injection pressures should be avoided.

6.5.2.4 High molecular mass summary

As has been discussed in the previous few sections, the only carcinogen tested for was napthalene. There are a number of operating conditions which produce this compound, and are therefore not optimum. Injection pressures both higher and lower than the optimum pressure for this engine resulted in the production of napthalene. Combinations of high EGR levels and hydrogen addition at the optimum injection pressure also resulted in napthalene production.

Given all of the above, if hydrogen addition is going to be used it will be important to determine the optimum injection strategy for the proposed engine. At this injection strategy, combined high levels of EGR and hydrogen would not be recommended given the behaviour in this engine.

6.6 Summary

This chapter has examined the effects of EGR level, hydrogen addition and injection pressure on the hydrocarbon species emitted. It was found that the hydrogen did not have any adverse effects. However, an incorrect injection strategy or high levels of EGR can increase the levels of the carcinogen napthalene produced.

CHAPTER 7

CONCLUSIONS AND FURTHER WORK

7 CHAPTER 7 CONCLUSIONS AND FURTHER WORK

7.1 Introduction

A Ford "Puma" 2.0L high-speed direct injection diesel engine was commissioned and modified to investigate the effects of combined diesel/hydrogen combustion. The engine was equipped with a high-pressure common rail injection system, an Exhaust Gas Recirculation (EGR) cooler and a Variable Geometry Turbocharger (VGT). The modifications made to the engine amounted to an induction point for the hydrogen being added to the air intake pipe upstream of the turbocharger and the EGR mixer, but downstream of the air filter. This point was chosen in order to ensure that the hydrogen had fully mixed with the air prior to entering the intake manifold. During the course of this investigation various benefits and drawbacks of combined hydrogen/diesel combustion were identified. The ability to control hydrogen combustion will determine whether or not this proves to be a viable option for exhaust gas emissions control.

7.2 Conclusions

7.2.1 Closed loop control to reduce emissions

The aim of this part of the project was to determine whether or not it would be possible to set-up a closed loop control, based on in-cylinder pressure data, to relate to the exhaust gas emission and therefore control the emissions. The most important conclusions from the closed loop control investigation results can be summarised as follows:

- The position of 50% mass fraction burned (MFB50) has the largest effect on exhaust emissions and fuel consumptions; and there are clear correlations between MFB50 and exhaust emissions, and specific fuel consumption.

- Amongst the other parameters examined, the position of the maximum rate of pressure rise has also been identified as a key parameter effecting exhaust emissions and fuel consumption.

- Results shown in Figure 27 also indicate that the motoring pressure may be used to infer levels of the in-cylinder residuals or EGR.

Further work will be needed to examine if the same conclusions will be applicable to different operating conditions, in particular, at very high EGR levels.

7.2.2 Properties of Combined Diesel/Hydrogen Combustion

The hydrogen addition investigation can be summarised as follows. Hydrogen addition affects the combustion in two ways. While stable combustion can be maintained, hydrogen increases the ignition delay. This results in higher maximum in-cylinder pressures and noisier combustion. The increased ignition delay leads to a great proportion of the fuel being burnt during the premixed phase. At high levels of hydrogen addition there is little or no diffusion flame combustion.

The onset of unstable combustion varies with speed and load, but is very noticeable. When the combustion becomes unstable, the ignition delay decreases, as does the maximum in-cylinder pressure. This unstable

combustion leads to a switch from premixed combustion to incomplete diffusion flame combustion.

7.2.3 Effects of Hydrogen Addition on Emissions

Hydrogen addition to diesel engines could be used in the future to meet ever stricter engine carbon emission regulations. Regarding the other emissions and the combustion characteristics, the effects of hydrogen follow the trends expected for engines operating in the conventional diesel combustion regime (not low temperature combustion (LTC) process). Hydrogen addition, like any method of reducing smoke, THC or the particulate matter, results in increased emissions of nitrogen oxides.

The main advantages of hydrogen can be summarised as a general reduction in the mass of particulate matter produced, a reduction in NO_X when used in conjunction with EGR, particularly high levels of EGR and hydrogen, and a reduction in smoke and THC except at the 0% EGR operating point. Combined with EGR, hydrogen can result in a reduction of both PM and NO_X compared to the base level operation without EGR and hydrogen.

Conversely, the disadvantages of using hydrogen are an increase in NO_X with increasing hydrogen level, increasing ignition delay with increasing hydrogen, increasing maximum cylinder pressure and increasing maximum rate of cylinder pressure rise.

Finally, 'anomalies' such as this observed in the present study for the case of 5% EGR combined with hydrogen at medium engine load (i.e. reduced PM compared to the 0% EGR case) indicate the necessity of further understanding of the diesel combustion with EGR and hydrogen. Further

investigation may suggest a method for significantly reducing NO_X and THC, smoke and particulate matter.

7.2.4 Particulate Matter Size Distribution

The effects of hydrogen addition on the particulate matter size distribution is

- A shift towards nucleation mode particulates, rather than accumulation mode.
- A change is composition, where the lack of soot in the PM is clear.

Conversely, the addition of EGR results in

- A shift towards larger accumulation mode particulates, or even course mode.
- Higher soot content in the exhaust gas emissions.

The combination of hydrogen and EGR meant that the adverse effects of EGR addition, that is the higher smoke and total unburnt hydrocarbon emissions, while limiting the increase of nitrogen oxide emissions, which are promoted by hydrogen combustion.

7.2.5 Chemical Composition of Diesel/Hydrogen Exhaust

The aim of this investigation was to determine whether or not the addition of hydrogen had an adverse effect on the speciation of the THC emitted. The effects of EGR level and fuel injection pressure were also investigated. It was found that at the optimum injection pressure, hydrogen addition did not

have an adverse effect on the compounds produced. It will be very important to optimise the injection strategy to avoid the disadvantages of the incorrect strategy combined with high levels of EGR.

7.3 Recommendations for further projects

Further work to develop appropriate injection and boost strategies is required in order to overcome the problem of high NO_X emissions. It may be useful to investigate the decreased ignition delay at the no load case. A better understanding of the chemical kinetics during hydrogen combustion is needed.

Also there is the move from accumulation mode PM production towards the nucleation mode as hydrogen levels increase. This has the advantage of reducing the total particulate matter mass, but may prove to increase the damage that particulates can cause to health. A detailed study of the penetration capabilities and health effects of the particulate matter of combined diesel/hydrogen combustion would be required.

In order to fully utilise the advantages of hydrogen addition a full engine calibration and optimisation would have to be carried out. With multiple injection used to smooth out the in-cylinder pressure rise rate, the noisy nature of the combined diesel/hydrogen combustion could be avoided. This may also prove to minimise the NO_X emissions by reducing the volume of diesel burnt during the premixed phase of combustion, and therefore limiting the high in-cylinder pressures and temperatures.

7.4 Overview

Given the present level of emissions standards, where the required levels of total unburnt hydrocarbons and nitrogen oxide emissions can be reached by aggressive engine strategies at the expense of fuel consumption, hydrogen addition would not be recommended. However, as the emissions standards become ever more stringent, then combined diesel/hydrogen combustion could be used to minimise the total unburnt hydrocarbons, meaning that hydrocarbon after-treatment would not be required. If this solution were applied, a nitrogen oxides after-treatment system would be needed, but the difficulties of running both NOX and THC after-treatment would be avoided.

While hydrogen addition reduces the products of incomplete combustion, there is also a significant reduction in carbon dioxide emissions, due to the lower carbon introduction to the cylinder. In the current climate of carbon reduction, and with the potential of carbon dioxide becoming a legislated emission, the obvious solution is to move to non-carbon based fuels, such as hydrogen.

REFERENCES

REFERENCES

Atkins, R.C. and Carey, F.A., *Organic Chemistry, 3rd Edition: A Brief Course*, McGraw Hill, 2002, Chapter 13

Aufdenblatten, S., Schänzlin, K., Bertola, A., Mohr, M., Przybilla, K. and Lutz, T., 2002, *Charakterisierung der Partikelemission von moderner Verbrennungsmotoren*, Jahrgang, vol. 63, pp. 962-974.

AVL Internal Data Sheet: 415S Smoke Meter http://www.avl.com/wo/webobsession.servlet.go/encoded/YXBwPWJjbXMmcGFnZT12aWV3Jm1hc2s9ZG93bmxvYWQmbm9kZXRpdGxlaWQ9NjYxOTkmbm9lbmNv_0AZGU9UERG.pdf [21/07/2008]

Beatrice, C., Belardini, P., Bertoli, C., Lisbona, M.G. and Sebastiano, G.M.R., 2002, *Diesel Combustion Control in Common Rail Engines by New Injection Strategies*, Int. J. Engine Res. Volume 3, No. 1, p23-36

Bosch, 1999, *Diesel-engine Management*, Second Edition, SAE International

Brusstar, M., Stuhldreher, M., Swain, D. and Pidgeon, W., 2002, *High Efficiency and Low Emissions From a Port-Injected Engine with Neat Alcohol Fuels*, SAE paper 2002-01-2743

Burtscher, H., 2001, *Literature Study on Tailpipe Particulate Emissions Measurement for Diesel Engines*, Particle Measurement Programme.

Chang, M., Kim, S. and Sioutas, C., 1999, *Experimental studies on particle impaction and bounce: effects of substrate design and material*, Atmospheric Environment, vol. 33, pp. 2313-2322.

Chasteen, T.G., *Split/Splitless Gas Chromatography Injection*, http://www.shsu.edu/~chemistry/primers/pdf/GC.pdf, [Accessed 21/09/08]

Chen, K., Karim, G.A. and Watson, H.C., 2003, *Experimental and analytical examination of the development of inhomogeneities and auto ignition during rapid compression of hydrogen-oxygen-argon mixtures*, Transactions of the ASME, 458, Vol. 125.

Clark, R. H., Wedlock, D. J. and Cherrillo, R. A., 2005, *Future Fuels and Lubricant Base Oils from Shell Gas to Liquid (GTL) Technology*, SAE paper 2005-01-2191

Danielsen, P.H., Risom, L., Wallin, H., Autrup, H., Vogel, U., Loft, S. and Moller, P., 2008, *DNA damage in rats after a single oral exposure to diesel exhaust particles*, Mutation Research, vol. 637, pp. 49-55.

European Emissions Standards, www.ec.gc.ca/transport/publications/trucks/truck4.htm [Accessed 28/10/05]

Ford M.C., *Description of the PUMA 2.0 Engine*, 2001

Garvie, D., Reid, J. and Robertson, A., 1976, *Core Chemistry*, Oxford University Press

Grob, R.L., 1995, *Modern Practice of Gas Chromatography, Third Edition,* John Wiley and sons, Canada

Heywood, J.B., 1988, *Internal Combustion Engine Fundamentals*, McGraw-Hill Book Company.

Horiba 7170DEGR Users Manual [2003]

International Energy Agency, 2004, *Biofuels for Transport, an International Perspective*, Chirat, France

Jaecker-Voirol, A., Delfort, B. and Montagne, X., 2005, *Glycerol Derivatives for Diesel Fuel Reformulation*, SAE paper 2005-01-2203

James, A.T. and Martin, A.J.P.,1952, *Gas-liquid Partition Chromatography: the Separation and Micro-estimation of Volatile Fatty Acids from Formic Acid to Dodecanoic Acid*, Biochemistry Journal, 50:679-690

Kajitani, S., Chen, Z., Oguma, M. and Konno, M., 2002, *A Study of Low-Compression-Ratio Dimethyl Ether Diesel Engines*, Int. J. Engine Res., Volume 3, No. 1, p1-11

Kamimoto, T., Nakajima, T. and Kawashima, Y., 2004, *Temporal Measurements of Mass Concentration of Soot Aggregates in Diesel Exhaust by a Two-Wavelength Extinction Method*, Int. J. Engine Res. Volume 5, No. 5, p453-465

Kittelson, D.B., 1998, *Engines and nanoparticles: a review*, J. Aerosol Sci, vol. 29, pp. 575-588.

Knottenbelt, C., 2002, *Mossgass "Gas-To-Liquid" Diesel Fuels – an Environmentally Friendly Option*, Catalysis Today, Volume 71, p437-445

Ladommatos, N., Abdelhalim, S. and Zhao, H., 2000, *The Effects of Exhaust Gas Recirculation on Diesel Combustion and Emissions*, Int. J. Engine Res. Volume 1, No. 1, p107-126

Lee, CS, Lee, KH and Kim, DS, 2003, *Experimental and numerical study on the combustion characteristics of partially premixed charge compression ignition engine with dual fuel*, Fuel, vol. 82, pp. 553-560.

Majewski, W.A., NOX Adsorbers, www.dieselnet.com/tech/cat_nox-trap.htmp, [Accessed 10/09/2008]

McTaggart-Cowan, G. P., Rogak, S. N., Hill, P. G., Bushe, W. K. and Munshi, S. R., 2004, *Effects of Operating Condition on Particulate Matter and Nitrogen Oxides Emissions from a Heavy-Duty Direct Injection Natural Gas Engine Using Cooled Exhaust Gas Recirculation*, Int. J. Engine Res. Volume 5, No 6, p499-511

McTaggart-Cowan, G., Bushe, W. K., Hill, P.G. and Munshi, S. R.,2004, *NO_X Reduction from a Heavy-Duty Diesel Engine with Direct Injection of Natural Gas and Cooled Exhaust Gas Recirculation*, Int. J. Engine Res. Volume 5, No. 2, p175-191

MOUDI – Micro-Orifice Uniform-Deposit Impactor Models 100 and 110, MSP Corporation 1999

Muraro, W., Shiraiwa, N. M., Monte, M., Figueiredo, F. A. B., De Almedia, A., Moura, T. M. and Sanchez, C. G., 2005, *Evalution of Engine Running with Gas of Low Power Heat Rate from Biomass (Rice Husk) Produced by Gasifier*, SAE paper 2005-01-2185

Nabi, N., Akhter, S. and Shahadat, Z., 2006, *Improvement of Engine Emissions with Conventional Diesel Fuel and Biodiesel-Diesel Blends*, Bioresource Technology, Volume 97, (available online from 17/05/05), p372-378

Nag, P., Song, K-H., Litzinger, T. A. and Haworth, D. C., 2001, *A Chemical Kinetic Modelling Study of the Mechanism of Soot Reduction by Oxygenated Additives in Diesel Engines*, Int. J. Engine. Res., Volume 2, No 3, p163-175

Nakakita, K., Akihama, K., Weissman, W. and Farrell, J. T., 2005, *Effect of the Hydrocarbon Molecular Structure in Diesel Fuel on the In-Cylinder Soot Formation and Exhaust Emissions*, Int. J. Engine Res., Volume 6, p187-205

Non-Thermal Plasma (NTP) Exhaust After-treatment, http://www.psa-peugeot-citroen.com/document/presse_dossier/psa-delphi_2001_11_281017849837.rtf [Accessed 01/11/05]

Oh, S-M. and Chung, K-H., 2006, *Identification of mammalian cell genotoxins in respirable diesel exhaust particles by bioassay-directed chemical analysis,* Toxicology Letters, vol. 161, pp. 226-235.

Power Transmission and Technology Manual, www.engineeredge.com/power_transmission/air_intake.htm [Accessed 19/10/05]

Quadrupole Set up, http://www.chem.vt.edu/chem-ed/ms/quadrupo.html, [Accessed 20/07/08]

Rakopoulos, C.D., Scott, M.A., Kyritsis, D.C., and Giakoumis, E.G., 2008, *Availability analysis of hydrogen/natural gas blends combustion in internal combustion engines*, Energy, vol. 33, pp. 248-255.

Sample injection with 6 port valve, http://www.vici.com/support/app/app11j.php, [Accessed 21/09/08]

Saravanan, N., Ngarajan, G., Kalaiselvan, K.M. and Dhanasekaran, C., 2008, *An experimental investigation on hydrogen as a duel fuel for diesel engine system with exhaust gas recirculation technique*, Renewable Energy, vol. 33, pp. 422-427.

Sasaki, H., Sekiyama, S. and Nakashima, K., 2002, *A New Combustion System of a Heat-Insulated Natural Gas Engine with a Pre-Chamber Having a Throat Valve*, Int. J. Engine Res., Volume 3, No. 4, p197-208

Schaberg, P., Botha, J., Schnell, M., Hermann, H-O., Pelz, N and Maly, R., 2005, *Emissions Performance of GTL Diesel Fuel and Blends with Optimized Engine Calibrations,* SAE paper 2005-01-2187

Schenck, C.,1983, *Instruction manual eddy-current* dynamometer, Type W130

Schwarzenbach, R. P., Gschwend, P. M. and Imboden, D. M., 2003, *Environmental Organic Chemistry: Second Edition*, John Wiley and Sons, Inc., p32-34

Scientific Committee on Food, 2002, *Opinion on the Scientific Committee on Food on the Risk to human health of Polycyclic Aromatic Hydrocarbons in Food*, SCF/CS/CNTM/PAH/29/Final.

Senthil Kumar, M., Ramesh, A. and Nagalingam, B., 2003, *Use of hydrogen to enhance the performance of a vegetable oil fuelled compression ignition engine,* International Journal of Hydrogen Energy, vol. 28, pp. 1143-1154.

Sethi, V. P. and Salariya, K. S., 2004, *Exhaust Analysis and Performance of a Single-Cylinder Diesel Engine Run on Dual Fuels*, IE (I) Journal – MC, Volume 85, p1-7

Shudo, T. and Yamada, H., 2006, *Hydrogen as an ignition controlling agent for HCCI combustion engine by suppressing the low temperature oxidation*, International Journal of Hydrogen Energy, vol. 32, pp. 3066-3072.

Stone, R., *Introduction to Internal Combustion Engines*, Second Edition, MacMillan Press Ltd, ISBN 0-333-55084-6 Pbk, Basingstoke, Hampshire, 1992

Thermocouple Application Note, Pico Tech Website, http://www.picotech.com/applications/thermocouple.html, [Accessed 20/09/08]

Tilagone, R., Venturi, S. and Monnier, G., 2005, *Natural Gas – an Environmentally Friendly Fuel for Urban Vehicles: the SMART Demonstrator Approach*, SAE paper 2005-01-2186

Tissera, C.A., Swartz, M. M., Talti, E., Vellaisamy, R., Clark, N. N., Thompson, G. J. and Atkinson, R. J., 2005, *NO_X Decomposition in Natural Gas, Diesel and Gasoline Engines for Selective NO_X Recirculation*, SAE paper 2005-01-2144

Trapel, E., Mayer, C., Schulz, C. and Roth, P., 2005, *Effects of Biodiesel Injection in a DI Diesel Engine on Gaseous and Particulate Emissions*, SAE paper 2005-01-2204

Tsolakis, A and Megaritis, A, 2004, *Exhaust Gas Fuel Reforming for Diesel Engines – A Way to Reduce Smoke and NO_x Emissions Simultaneously*, SAE paper No. 2004-01-1844.

Tsolakis, A and Megaritis, A, 2005a, *Partially premixed charge compression ignition engine with on-board H2 production by exhaust gas fuel reforming of diesel and biodiesel*, International Journal of Hydrogen Energy, vol. 30, pp. 731-745.

Tsolakis, A., Hernandez, J.J., Megaritis, A. and Crampton, M., 2005b, *Dual fuel diesel engine operation using H2. Effect on particulate emissions*, Energy and Fuels, vol. 19, pp. 418-425.

Tsolakis, A., Megaritis, A., Yap, D. and Abu-Jrai, A., 2005c, *Combustion characteristics and exhaust gas emissions of a diesel engine supplied with reformed EGR*, SAE paper No. 2005-01-2087.

Twigg, M.V., 2006, *Progress and future challenges in controlling automotive exhaust gas emissions,* Applied Catalysis B : Environmental 70:2-15

USA Emissions Standards, www.dieselnet.com/standards/us/light.html [Accessed 28/10/05]

USEPA, Health Effects Notebook for Hazardous Air Pollutants, http://www.epa.gov/ttnatw01/hlthef/hapindex.html , [31/07/08]

Verhaeven, E. Pelkmans, L., Govaerts, L., Lamers, R. and Theunissen, F., 2005, *Results from Demonstration and Evaluation Projects of Biodiesel from Rapeseed and Used Frying Oil on Light Duty and Heavy Duty Vehicles*, SAE paper 2005-01-2201

Wannatong, K., Akarapanyavit, N., Siengsanorh, S. and Chanchaona, S., 2007, *Combustion and Knock Characteristics of Natural Gas Diesel Dual Fuel Engine*, JSAE 20077147

Watson, H., Khan, M. A., Liew, G. and Baker, P., 2005, *Opportunities for Making LPG a Clean and Low Greenhouse Emission Fuel*, SAE paper 2005-01-2217

Xiaoming, L., Yunshan, G., Sijin, W. and Xiukun, H., 2005*, An Experimental Investigation on Combustion and Emissions Characteristics of Turbocharged DI Engines Fuelled with Blends of Biodiesel*, SAE paper 2005-01-2199

Yamane, K., Yuuki, R., Kawasaki, K., Asakawa, T., Numao, H. and Komori, M., 2005, *Characteristics of DPF for Diesel Engine Fueled with Biodiesel Fuel – Second Report: Exhaust Gas Emission Characteristics at Self-Regulation of DPF*, SAE paper 2005-01-2198

Yap, D., Karlovsky, J., Megaritis, A., Wyszynski, M.L. and Xu, H., 2005, *An investigation into propane homogeneous charge compression ignition (HCCI) engine operation with residual gas trapping*, Fuel, 84, p 2372-2379

Zhao H., Peng Z., Ladommatos N., 2003, *Understanding of controlled autoignition combustion in a four-stroke gasoline engine,* Inst Mech Eng Part D J Automot Eng, 215:1297–310

Zhao, H. and Ladommatos, N., 2001, *Engine Combustion Instrumentation and Diagnostics*, SAE

Zumdahl, S.S., 1995, *Chemical Principles*, Second Edition, D.C. Heath and Company, ISBN 0-669-39321-5, Lexington, MA

APPENDIX A

ENGINE SPECIFICATION

APPENDIX A

Engine Specification

Base Engine Data

Number of Cylinders	4
Cylinder Bore	86 mm
Crankshaft stroke	86 mm
Swept Volume	1998.23 cc
Compression Ratio	18.2:1
Maximum Cylinder Pressure	150 bar
Piston Design	Central bowl in piston
Nominal Bowl Volume	21.7 cc
Oil Type	15W40
Water Temperature	70 ^{o}C
Maximum Turbine Speed	180 000 rpm
Idle Engine Speed	750 ± 5 rpm
Maximum No Load Speed	4800 ± 50 rpm

Fuel Injection system

Common rail Fuel injection system

Fuel Injection Pump	B2 Level HP Pump with 6bar ILP: Lucas part C4 1882528***, C41882529A**
High Pressure Fuel Rail	RAIL ASSY-15 workhorse type 30cc rail (one outlet blanked off), with 1600bar
High Pressure Pipe	Pump to rail: Lucas part RRR264B 1-of Rail to injectors: Lucas part RRR466A 1-off, RRR467A 3 of
Venturi Assembly	ILP compatible type, with pressure regulator: Lucas part 4506-4243D
Injectors	VCO 760cc/min @100bar 6 holes × 154° Cone Angle Lucas part C06054321B C06054320C
ICU	B1 level, software to be C5A16H09

APPENDIX B

DIESEL FUEL SPECIFICATION

APPENDIX B

Diesel Fuel Specification

TEST	METHOD	SPECIFICAT	RESULT
Appearance	Visual	Report	Slight
Colour	Visual	Report	Red
Water & Sediment, %(V/V)	Visual	Report	Nil
Flash Point, ^{o}C	IP 34	55 min	71
Carbon Residue on 10%	IP 14	0.30 max	0.20
Ash Content, % (m/m)	IP4	0.01 max	<0.005
Water Content (mg/kg)	ASTM D1744	200 max	61
Particulates (mg/kg)	DIN 51419	24 max	13
Cu Corrosion, 3h @ 50^{o}C	IP154	1 max	1
Oxidation Stability, (g/m^{3})	ASTM D2274	25 max	14
Sulphur, % (m/m)	IP336	0.20 max	0.19
CFPP, ^{o}C	IP 309	-15 max	-11
Density @ 15 ^{o}C, (kg/m^{3})	ASTM D4052	820-860	853.8
Cetane Number	ASTM D613	49 min	49.1
Cetane Index	ISO 4264	46 min	47.3
Distillation	IP123		-
Initial Boiling Point ^{o}C			169.0
10% Vol Rec @ ^{o}C			213.5
50% Vol Rec @ ^{o}C			279.0
90% Vol Rec @ ^{o}C			343.0
Final Boiling Point ^{o}C			371.5
% (V/V) Rec @ 250^{o}C		65 max	30.0
% (V/V) Rec @ 350^{o}C		85 min	92.5

% (V/V) Rec @ 370°C		95 min	97
Carbon % (m/m)	ASTM D5291		86.2
Hydrogen % (V/V)	ASTM D5291		13.4
Aromatics % (V/V)	IP 156		25.1
Olefines % (V/V)	IP 156		2.5
Saturates % (V/V)	IP 156		72.4

APPENDIX C
PREVIOUS PUBLICATIONS

APPENDIX C

Previous Publications by this Author

McWilliam, L. and Zhao, H., 2007, *Analysis of In-cylinder Pressure and Heat Release Characteristics and Their Correlation with Exhaust Emissions and Fuel Consumption in a HSDI Diesel Engine,* Produced For Siemens

McWilliam, L, Megaritis, T. and Zhao, H., 2008, *Experimental investigation of the effects of combined hydrogen and diesel combustion on the emissions of a HSDI Diesel engine,* SAE 2008-01-1787

McWilliam, L. and Megaritis, T., 2008, *Experimental investigation of the effect of combined hydrogen and diesel combustion on the particulate size distribution from a HSDI diesel engine,* International Journal of Vehicle Design